

ISSN : 21 65-4069(Online)

ISSN : 21 65-4050(Print)



IJARAI

International Journal of
Advanced Research in Artificial Intelligence

Volume 5 Issue 10

www.ijarai.thesai.org

A Publication of
The Science and Information Organization

Editorial Preface

From the Desk of Managing Editor...

Artificial Intelligence is hardly a new idea. Human likenesses, with the ability to act as human, dates back to Geek mythology with Pygmalion's ivory statue or the bronze robot of Hephaestus. However, with innovations in the technological world, AI is undergoing a renaissance that is giving way to new channels of creativity.

The study and pursuit of creating artificial intelligence is more than designing a system that can beat grand masters at chess or win endless rounds of Jeopardy!. Instead, the journey of discovery has more real-life applications than could be expected. While it may seem like it is out of a science fiction novel, work in the field of AI can be used to perfect face recognition software or be used to design a fully functioning neural network.

At the International Journal of Advanced Research in Artificial Intelligence, we strive to disseminate proposals for new ways of looking at problems related to AI. This includes being able to provide demonstrations of effectiveness in this field. We also look for papers that have real-life applications complete with descriptions of scenarios, solutions, and in-depth evaluations of the techniques being utilized.

Our mission is to be one of the most respected publications in the field and engage in the ubiquitous spread of knowledge with effectiveness to a wide audience. It is why all of articles are open access and available view at any time.

IJARAI strives to include articles of both research and innovative applications of AI from all over the world. It is our goal to bring together researchers, professors, and students to share ideas, problems, and solution relating to artificial intelligence and application with its convergence strategies. We would like to express our gratitude to all authors, whose research results have been published in our journal, as well as our referees for their in-depth evaluations.

We hope that this journal will inspire and educate. For those who may be enticed to submit papers, thank you for sharing your wisdom.

Editor-in-Chief

IJARAI

Volume 5 Issue 10 October 2016

ISSN: 2165-4069(Online)

ISSN: 2165-4050(Print)

©2013 The Science and Information (SAI) Organization

Editorial Board

Peter Sapaty - Editor-in-Chief

National Academy of Sciences of Ukraine

Domains of Research: Artificial Intelligence

Alaa F. Sheta

Electronics Research Institute (ERI)

Domain of Research: Evolutionary Computation, System Identification, Automation and Control, Artificial Neural Networks, Fuzzy Logic, Image Processing, Software Reliability, Software Cost Estimation, Swarm Intelligence, Robotics

Antonio Dourado

University of Coimbra

Domain of Research: Computational Intelligence, Signal Processing, data mining for medical and industrial applications, and intelligent control.

David M W Powers

Flinders University

Domain of Research: Language Learning, Cognitive Science and Evolutionary Robotics, Unsupervised Learning, Evaluation, Human Factors, Natural Language Learning, Computational Psycholinguistics, Cognitive Neuroscience, Brain Computer Interface, Sensor Fusion, Model Fusion, Ensembles and Stacking, Self-organization of Ontologies, Sensory-Motor Perception and Reactivity, Feature Selection, Dimension Reduction, Information Retrieval, Information Visualization, Embodied Conversational Agents

Liming Luke Chen

University of Ulster

Domain of Research: Semantic and knowledge technologies, Artificial Intelligence

T. V. Prasad

Lingaya's University

Domain of Research: Bioinformatics, Natural Language Processing, Image Processing, Robotics, Knowledge Representation

Wichian Sittiprapaporn

Maharakham University

Domain of Research: Cognitive Neuroscience; Cognitive Science

Yaxin Bi

University of Ulster

Domains of Research: Ensemble Learning/Machine Learning, Multiple Classification Systems, Evidence Theory, Text Analytics and Sentiment Analysis

Reviewer Board Members

- **Abdul Wahid Ansari**
Assistant Professor
- **Ahmed Nabih Zaki Rashed**
Menoufia University
- **Akram Belghith**
University Of California, San Diego
- **Alaa Sheta**
Computers and Systems Department,
Electronics Research Institute (ERI)
- **Albert S**
Kongu Engineering College
- **Alexane Bouënard**
Sensopia
- **Amir HAJJAM EL HASSANI**
Université de Technologie de Belfort-
Monbéliard
- **Amitava Biswas**
Cisco Systems
- **Anshuman Sahu**
Hitachi America Ltd.
- **Antonio Dourado**
University of Coimbra
- **Appasami Govindasamy**
- **ASIM TOKGOZ**
Marmara University
- **Athanasios Koutras**
- **Babatunde Opeoluwa Akinkunmi**
University of Ibadan
- **Bae Bossoufi**
University of Liege
- **BASANT VERMA**
RAJEEV GANDHI MEMORIAL COLLEGE,
HYDERABAD
- **Basem ElHalawany**
Benha University
- **Basim Almayahi**
UOK
- **Bestoun Ahmed**
College of Engineering, Salahaddin
University - Hawler (SUH)
- **Bhanu Prasad Pinnamaneni**
Rajalakshmi Engineering College; Matrix
Vision GmbH
- **Chee Hon Lew**
- **Chien-Peng Ho**
Information and Communications
Research Laboratories, Industrial
Technology Research Institute of Taiwan
- **Chun-Kit (Ben) Ngan**
The Pennsylvania State University
- **Daniel Hunyadi**
"Lucian Blaga" University of Sibiu
- **David M W Powers**
Flinders University
- **Dimitris Chrysostomou**
Production and Management Engineering
/ Democritus University of Thrace
- **Ehsan Mohebi**
Federation University Australia
- **El Sayed Mahmoud**
Sheridan College Institute of Technology
and Advanced Learning
- **Fabio Mercorio**
University of Milan-Bicocca
- **Francesco Perrotta**
University of Macerata
- **Frank Ibikunle**
Botswana Int'l University of Science &
Technology (BIUST), Botswana
- **Gerard Dumancas**
Oklahoma Baptist University
- **Goraksh Garje**
Pune Vidyarthi Griha's College of
Engineering and Technology, Pune
- **Grigoras Gheorghe**
"Gheorghe Asachi" Technical University of
Iasi, Romania
- **Guandong Xu**
Victoria University
- **Haibo Yu**
Shanghai Jiao Tong University
- **Harco Leslie Henic SPITS WARNARS**
Bina Nusantara University
- **Hela Mahersia**
- **Ibrahim Adeyanju**
Ladoke Akintola University of Technology,
Ogbomoso, Nigeria
- **Imed JABRI**

- **Imran Chaudhry**
National University of Sciences & Technology, Islamabad
- **ISMAIL YUSUF**
Lamintang Education & Training (LET) Centre
- **Jabar Yousif**
Faculty of computing and Information Technology, Sohar University, Oman
- **Jacek M. Czerniak**
Casimir the Great University in Bydgoszcz
- **Jatinderkumar Saini**
Narmada College of Computer Application, Bharuch
- **José Santos Reyes**
University of A Coruña (Spain)
- **Kamran Kowsari**
The George Washington University
- **KARTHIK MURUGESAN**
- **Krasimir Yordzhev**
South-West University, Faculty of Mathematics and Natural Sciences, Blagoevgrad, Bulgaria
- **Krishna Prasad Miyapuram**
University of Trento
- **Le Li**
University of Waterloo
- **Leon Abdillah**
Bina Darma University
- **Liming Chen**
De Montfort University
- **Ljubomir Jerinic**
University of Novi Sad, Faculty of Sciences, Department of Mathematics and Computer Science
- **M. Reza Mashinchi**
Research Fellow
- **madjid khalilian**
- **Malack Oteri**
jkuat
- **Marek Reformat**
University of Alberta
- **Md. Zia Ur Rahman**
Narasaraopeta Engg. College, Narasaraopeta
- **Mehdi Bahrami**
University of California, Merced
- **Mehdi Neshat**
- **Mohamed Najeh LAKHOUA**
ESTI, University of Carthage
- **Mohammad Haghghat**
University of Miami
- **Mohd Ashraf Ahmad**
Universiti Malaysia Pahang
- **Nagy Darwish**
Department of Computer and Information Sciences, Institute of Statistical Studies and Researches, Cairo University
- **Nestor Velasco-Bermeo**
UPFIM, Mexican Society of Artificial Intelligence
- **Nidhi Arora**
M.C.A. Institute, Ganpat University
- **Olawande Daramola**
Covenant University
- **Omaima Al-Allaf**
Asesstant Professor
- **Parminder Kang**
De Montfort University, Leicester, UK
- **PRASUN CHAKRABARTI**
Sir Padampat Singhanian University
- **Purwanto Purwanto**
Faculty of Computer Science, Dian Nuswantoro University
- **Qifeng Qiao**
University of Virginia
- **raja boddu**
LENORA COLLEGE OF ENGINEERING
- **Rajesh Kumar**
National University of Singapore
- **Rashad Al-Jawfi**
Ibb university
- **RAVINA CHANGALA**
- **Reza Fazel-Rezai**
Electrical Engineering Department, University of North Dakota
- **Said Ghoniemy**
Taif University
- **Said Jadid Abdulkadir**
- **Secui Calin**
University of Oradea
- **Selem Charfi**
HD Technology
- **Shahab Shamshirband**
University of Malaya

- **Shaidah Jusoh**
- **Shriniwas Chavan**
MSS's Arts, Commerce and Science
College
- **Sim-Hui Tee**
Multimedia University
- **Simon Ewedafe**
The University of the West Indies
- **SUKUMAR SETHILKUMAR**
Universiti Sains Malaysia
- **T C.Manjunath**
HKBK College of Engg
- **T V Narayana rao Rao**
SNIST
- **T. V. Prasad**
Lingaya's University
- **Tran Sang**
IT Faculty - Vinh University – Vietnam
- **Urmila Shrawankar**
GHRCE, Nagpur, India
- **V Deepa**
M. Kumarasamy College of Engineering
(Autonomous)
- **Vijay Semwal**
- **Visara Urovi**
University of Applied Sciences of Western
Switzerland
- **Vishal Goyal**
- **Vitus Lam**
The University of Hong Kong
- **Voon Ching Khoo**
- **VUDA SREENIVASARAO**
PROFESSOR AND DEAN, St.Mary's
Integrated Campus,Hyderabad
- **Wali Mashwani**
Kohat University of Science & Technology
(KUST)
- **Wei Zhong**
University of south Carolina Upstate
- **Wichian Sittiprapaporn**
Mahasarakham University
- **Yanping Huang**
- **Yaxin Bi**
University of Ulster
- **Yuval Cohen**
Tel-Aviv Afeka College of Engineering
- **Zhao Zhang**
Deptment of EE, City University of Hong
Kong
- **Zhigang Yin**
Institute of Linguistics, Chinese Academy of
Social Sciences
- **Zhihan Lv**
Chinese Academy of Science
- **Zne-Jung Lee**
Dept. of Information management, Huafan
University

CONTENTS

Paper 1: Image Retrieval Method Utilizing Texture Information Derived from Discrete Wavelet Transformation Together with Color Information

Authors: Kohei Arai, Cahya Ragmad

PAGE 1 – 6

Paper 2: Pattern of Success Vs. Pattern of Failure: Adaptive Authentication Through Kolmogorov–Smirnov (K-S) Statistics

Authors: Gahangir Hossain, Pradeep Palaniswamy, Rajab Chaloo

PAGE 7 – 13

Paper 3: Error Analysis of Line of Sight Estimation using Purkinje Images for Eye-based Human-Computer Interaction: HCI

Authors: Kohei Arai

PAGE 14 – 23

Paper 4: Method for Vigor Diagnosis of Tea Trees based on Nitrogen Content in Tealeaves Relating to NDVI

Authors: Kohei Arai

PAGE 24 – 30

Paper 5: Flowcharting the Meaning of Logic Formulas

Authors: Sabah Al-Fedaghi

PAGE 31 – 36

Paper 6: Pursuit Reinforcement Competitive Learning: PRCL based Online Clustering with Learning Automata

Authors: Kohei Arai

PAGE 37 – 45

Image Retrieval Method Utilizing Texture Information Derived from Discrete Wavelet Transformation Together with Color Information

Kohei Arai¹

¹ Graduate School of Science and Engineering
Saga University
Saga City, Japan

Cahya Ragmad²

² State Polytechnics of Malang,
East Java, 65145 Indonesia

Abstract—Image retrieval method utilizing texture information which is derived from Discrete Wavelet Transformation: DWT together with color information is proposed. One of the specific features of the texture information extracted from portions of image is based on Dyadic wavelet transformation with forming texture feature vector by using energy derived from Gabor transform on 7 by 7 pixel neighbor of significant points. Using the Wang's dataset, the proposed method is evaluated with retrieval success rate (precision and recall) as well as Euclidian distance between the image in concern (Query image) and the other images in the database of interest and is compared to the other method. As the result through the experiments, it is found that the DWT derived texture information is significantly effective in comparison to the color information.

Keywords—Wavelet; DWT; local feature; Color; Texture; CBIR

I. INTRODUCTION

Henning Müller, et al. presented the paper which is entitled "Benchmarking image retrieval applications" [1]. In their paper, almost all the methods for image retrievals are tested and compared. One of the conclusions is Content Based Image Retrieval: CBIR is the most effective. Brahmi et al. mentioned the two drawbacks in the keyword annotation image retrieval. First, images are not always annotated and the manual annotation expensive also time consuming. Second, human annotation is not objective the same image may be annotated differently by different observers [2]. CBIR based image retrievals is based on the similarity of feature vector of color, texture, shape and other image content between a query image in concern and the images in a database of interest. Also, CBIR based image retrievals is objectively in comparison to the conventional image retrieval methods [3].

Although color and texture information is significant for image retrieval in particular, color and texture are different by portion by portion of whole image [4]. Therefore, local properties of color and texture information have to be used for image retrievals are commonly used to describe the image content in image.

There are so many methods for extraction of texture information from the local images. The proposed method uses 2D Discrete Wavelet Transform: DWT with Haar base

function, combined with the two high sub-band frequencies to make significant points and edge, for choosing any part of image by threshold the high coefficient value. Although, the image size of frequency components derived from the conventional DWT is decimated with the factor of 2 by 2, a Dyadic wavelet transformation maintains the image size of frequency component which represent texture information. Therefore, this paper proposes a method for texture information extraction based on the Dyadic wavelet transformation.

This paper is organized as follows: In the following section, Discrete Wavelet Transform: DWT is briefly described. Then, color and texture information is explained followed by the proposed method for image retrieval. After that, similarity and performance measure is discussed. Then the texture information extraction method with Dyadic wavelet transformation is proposed followed by experimental results. Finally, conclusion is given together with some discussions.

II. PROPOSED METHOD

A. Discrete Wavelet Transform

One of the specific features of the DWT is time and frequency analysis [5]. Namely, not only frequency component analysis, but also frequency component analysis at the time in concern is available for the DWT. Although the well-known Fourier analysis allows only frequency component analysis, the DWT makes frequency component analysis at the time in concern. The DWT represents an image as a sum of wavelet functions at different locations (shift) and scales [6].

The DWT is based on a base function (mother wavelet function). If the base function is bi-orthogonal function, then the original image before the DWT can be reconstructed through Inverse DWT: IDWT. Any decomposition of an 2D image into wavelet involves four sub-band elements representing LL (Approximation), HL (Vertical Detail), LH (Horizontal Detail), and HH (Detail), respectively as shown in Fig.1.

The DWT works as a filter bank and the functions of the filter bank are explained as follows,

On a one dimensional signal $x[n]$. $x[n]$ is input signal that contains high frequencies and low frequencies. $h[k]$ and $g[k]$ is channel filter bank involving sub-sampling as shown in Fig.2. $c[n]$ is called averages contains low frequencies signal. $d[n]$ is called wavelet coefficients contain high frequencies signal. $c[n]$ and $d[n]$ be sub sampled (decimated by 2: $\downarrow 2$) the next process for further decomposition is iterated on the low signal $c[n]$.

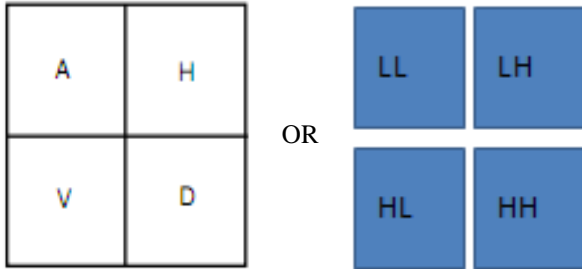


Fig. 1. Level 1 of 2D DWT

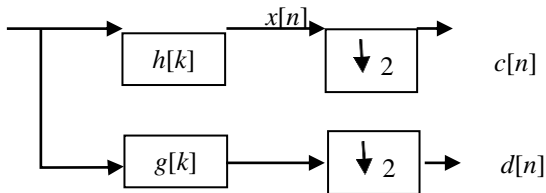


Fig. 2. Two channel filter bank

B. Example 1D Haar wavelet decomposition

Let the $x[n]$ as an input $x[n]= X_0, X_1, X_2, \dots X_{N-1}$ contains N elements the output is $N/2$ elements of averages and is stored in $c[n]$. Also, it assumed to be containing $N/2$ elements wavelet coefficients values and is stored in $d[n]$. The Haar equation to calculate an average AV_i in equation (1) and a wavelet coefficient WC_i in equation (2) from pair data odd and even element in the input data are:

$$AV_i = \frac{X_i + X_{i+1}}{2} \quad (1)$$

$$WC_i = \frac{X_i - X_{i+1}}{2} \quad (2)$$

C. Wavelet Multi-Resolution Analysis

One dimensional wavelet transformation is expressed with the following equation.

$$F = C_n f \quad (3)$$

where F, f denotes wavelet frequency component and radar echo signal as a function of time. C_n denotes wavelet transformation matrix which is expressed as a bi-orthogonal function based on base functions. C_n can be determined with a reference to the appendix. Therefore,

$$C_n C_n^T = I \quad (4)$$

Then, f is converted to the followings,

$$F_1 = (L_1, H_1),$$

$$F_2 = C_n L_1 = (L_2, H_2),$$

$$F_3 = C_n L_2 = (L_3, H_3),$$

...

$$F_m = C_n L_m^{-1} = (L_m, H_m) \quad (5)$$

Also f is reconstructed as follows,

$$C_n^{-1} F_m = C_n^{-1} (L_m, H_m) = L_m^{-1}, \dots, C_n^{-1} F_2 = L_1, C_n^{-1} F_1 = f \quad (6)$$

The suffix of 1 to m is called "level". Level m implies that wavelet transformation is applied m times. Multi-resolution Analysis: MRA ensure that the original signal can be reconstructed with the wavelet coefficients or frequency components of the level m . The frequency components derived from MRA are corresponding to the level m . Therefore, MRA does work as a filter bank.

There are some base functions such as Haar, Daubechies¹, etc. In order to conduct a preliminary experiment, Haar base function is selected for showing an effectiveness of the DWT for texture information extractions.

D. Texture

Texture is pattern, tracery, crease patten, etc. with intensities and colors. Texture contains repeating pattern of local variations in image intensity also an area that can be perceived as being spatially homogeneous. Texture provides important characteristics for surface and object identification. Texture information can be extracted from the original image and are typical features that can be used for image retrievals [7]. The texture is characterized with the statistical distribution such as probability density functions, co-occurrence matrices, etc. of the image intensity. It also may extracted by using energy of Gabor filter on 7 by 7 pixel neighbor of significant points.

E. Color

Color is visual perceptual property corresponding in human to the category called red (600 nm of wavelength), green (550 nm), blue (450 nm), black, yellow, etc. Color is produced by spectra of light that absorbed or reflected then received by the human eye and processed by the human brain. To extract the color feature, the first order statistical moments and the second order statistical moments in the Hue, Saturation, and Intensity: HSI color space on neighbor of significant points with size 3 by 3 pixels is used. HSI color space is similar to human perception color system so we used it to extract the color feature.

The first order statistical moment is as follows,

$$\mu = \frac{1}{MN} \sum_{i=1}^M \sum_{j=1}^N p(i, j) \quad (7)$$

where:

¹ Daubechies base function is defined as $\{\alpha_k\}$ satisfying the following conditions,

$$\phi(x) = \sum_k \alpha_k \sqrt{2} \phi(2x - k)$$

$$\beta_k = (-1)^k \alpha_{1-k}$$

$$\varphi(x) = \sum_k \beta_k \sqrt{2} \phi(2x - k)$$

P = Pixel value
 MN = Size of significant points and its neighbor.
 The second order statistical moment is as follows,

$$\sigma = \sqrt{\frac{1}{MN} \sum_{i=1}^M \sum_{j=1}^N (p(i,j) - \mu)^2} \quad (8)$$

where:

P = pixel value
 MN = Size of significant points and its neighbor

F. Propose Method for Image Retrieval

The procedure proposed here is as follows,

- 1) Read Query image and Convert from RGB image to gray image and HSI image.
- 2) Decomposition using wavelet transformation.
- 3) Make absolute for every wavelet coefficient,
 $WC_{new} = |WC_{old}|$.
- 4) Combine Vertical Detail and Horizontal Detail,
 $CV_d H_d(i,j) = \text{Max}(V_d(i,j), H_d(i,j))$.
- 5) Choose significant points on $CV_d H_d(i,j)$ by threshold the high value.
- 6) Choose points on HSI image and it neighbor (3 by 3 pixel) base on coordinate significant points on $CV_d H_d(i,j)$ then Forming color feature vector by using The first order statistical moment and the second order statistical moment.
- 7) Forming texture feature vector by using Gabor transform on 7 by 7 pixel neighbor of significant points.
- 8) Implement "MinMax" normalization on all feature vector with range [0 1].
- 9) Measure the distance between feature vector image query and feature vector image by using Euclidean distance.
- 10) Showing image with X top ranking from the dataset.

G. Similarity

The similarity is measured by using Euclidean distance between features of the query image in concern and the images in the dataset of interest. The retrieved result is not a single image but a list of image ranked with their similarity. The feature representation is image feature refer to the characteristics which are described with the contents of an image.

$$\begin{aligned} FQ &= (Q_1, Q_2, \dots, Q_n) \\ FD &= (D_1, D_2, \dots, D_n) \\ \text{dis}(FQ, FD) &= \sqrt{\sum_{j=1}^n (Q_j - D_j)^2} \end{aligned} \quad (9)$$

where:

FQ = Feature vector of query image.
 FD = Feature vector of image in data set
 n = The number element of feature vector

If the Euclidean distance between features of the query image in concern and the images in the dataset of interest is short, then it is to be considered as similar features. For example, a distance of 0 have meaning an exact match with

the query and 1 mean totally different. Base on the rank of that the measured similarity, the retrieval results are to be displayed.

H. Performance Measure

There is two-step approach to retrieve the relevant image from the dataset of interest. First, CBIR method extracts a feature vector for every portion of the image in concern and put the feature into the feature dataset. Second, the user provides a query image and a feature vector of the query image is extracted. Then the feature vector of query image is compared to the feature vectors of the portion of images in the database of interest for finding the feature vector which shows a shortest distance between two feature vectors.

The performance of CBIR system of the aforementioned method is evaluated for showing image with X top ranking from the dataset. It is a common way to evaluate the performance of the CBIR system based on the well-known precision and recall evaluations. Precision measures the retrieval accuracies. It is a ratio between the number of relevant images retrieved and the total number of images retrieved. Recall measures the ability of retrieving all relevant images in the dataset. It is a ratio between the number of relevant images retrieved and the whole relevant images in the dataset.

The performance of the CBIR system is calculated as follows,

$$\text{Precision} = \frac{NRRI}{XR} \quad (10)$$

where:

$NRRI$ = Number of relevant retrieved images

XR = X Top ranking of retrieved images

$$\text{Recall} = \frac{NRRI}{TR} \quad (11)$$

where:

TR = Total number of relevant images in dataset

III. EXPERIMENTS

A. Performance Measure

The Wang's dataset [8] is used for the experiments. The retrieved results are compared with the standard system SIMPLICITY, FIRM and also color salient points by using the same dataset [8] [9] [10]. The proposed method is developed with MATLAB tool for the evaluation of performance matrices.

Fig.3 shows the query image and relevant image as a result of the proposed method and system. The relevant image results for "Bus", "Dinosaur", "Elephant", "Flower", and "Horse" as a query image are #6, #10, #7, #8 and #7, respectively. It seems that "Horse" and "Elephant" are very similar due to the fact that the backgrounds of these images are resembled.

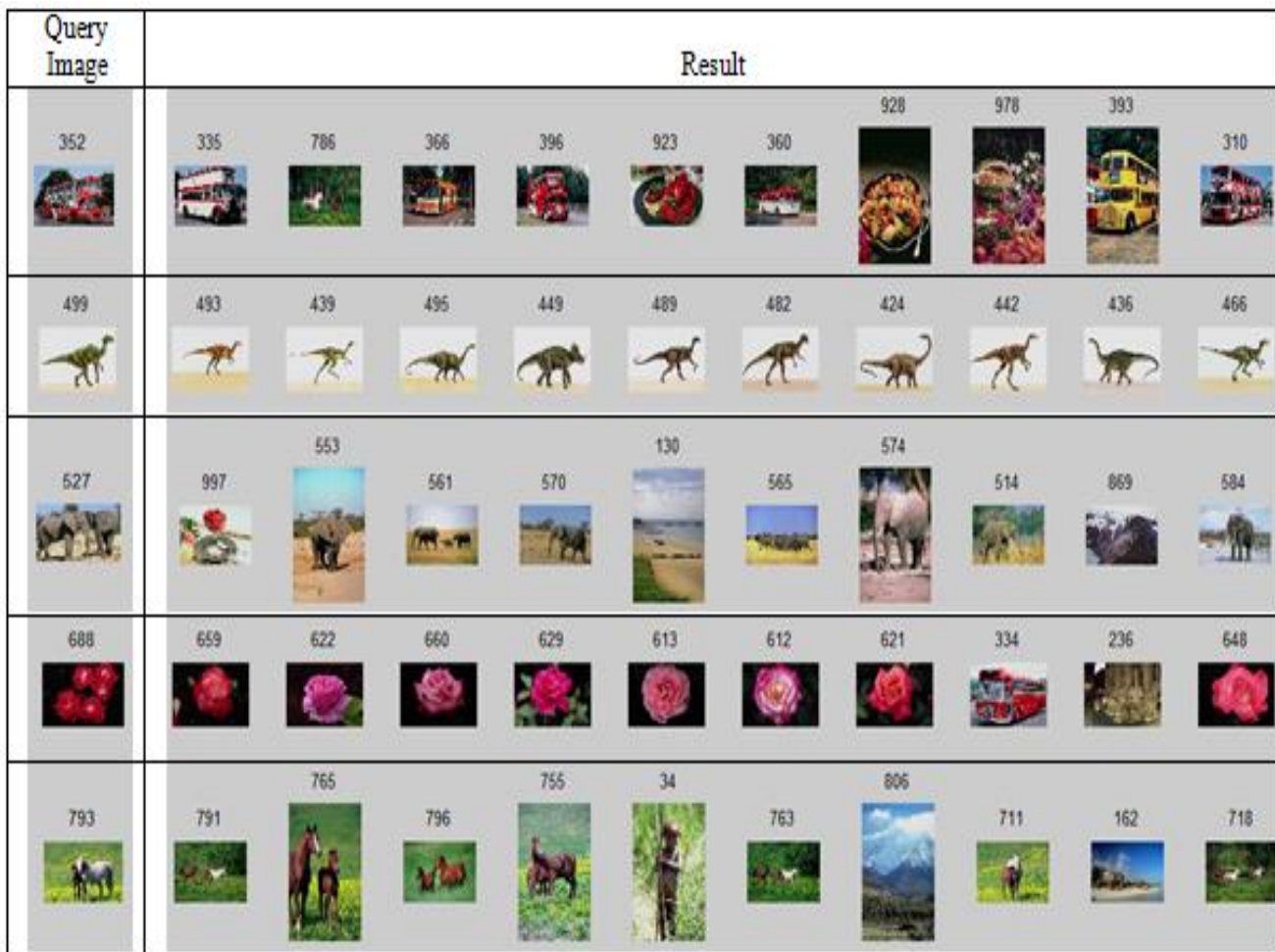


Fig. 3. Example results for the bus, dinosaur, elephant, flower and horses query

In the Table 1, the comparison of the averaged precision results between the proposed method and other method show that the proposed method is superior to the other conventional methods for most of the cases. The proposed method achieved the improvements of 12%, 17%, 11%, in comparison to the Firm, Simplicity, and Color Salient Points, respectively.

TABLE I. AVERAGE PRECISION RESULTS

Category	Firm	Simplicity	Color salient points	Proposed method
Bus	0.60	0.36	0.52	0.68
Dinosaur	0.95	0.95	0.95	0.94
Elephant	0.25	0.38	0.40	0.60
Flower	0.65	0.42	0.60	0.75
Horses	0.65	0.72	0.70	0.71
Average	0.62	0.57	0.63	0.74

B. Dyadic Wavelet Utilized Method

Another example of image database which includes 24 of species of planktons is shown in Fig. 4. In the figure, there are 24 of color images. Process flow of the proposed image retrievals is shown in Fig. 5. In this case, Dyadic wavelet transformation is used for texture information extraction. Although the conventional DWT makes a down-sampling

(from 1 to 1/4), the input and output image size are same for the Dyadic wavelet transformation. Therefore, much texture information can be extracted with Dyadic wavelet transformation rather than the conventional DWT.



Fig. 4. Another example of image database which includes 24 of species of planktons

Dyadic wavelet transformation can be expressed as follows,

$$C_n[i] = \sum_k h[k] C_{n-1}[i + k2^{n-1}] \quad (12)$$

$$d_n[i] = \sum_k g[k] C_{n-1}[i + k2^{n-1}] \quad (13)$$

where C_n d_n denotes low and high frequency components, respectively. Inverse Dyadic wavelet transformation is represented as follows,

$$C_{n-1}[i] = \frac{1}{2} \left(\sum_k h[k] C_n[i - k2^{n-1}] + \sum_k g[k] d_n[i - k2^{n-1}] \right)$$

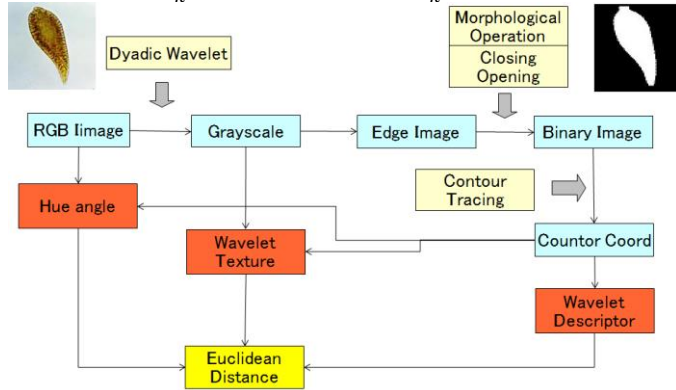


Fig. 5. Process flow of the proposed image retrievals

On the other hand, color information is represented with the following Hue angle, Saturation and Intensity: HSI.

Hue angle:

$$H = \begin{cases} 60 \frac{G-B}{MAX-MIN} + 0 (if MAX = R) \\ 60 \frac{B-R}{MAX-MIN} + 120 (if MAX = G) \\ 60 \frac{R-G}{MAX-MIN} + 240 (if MAX = B) \end{cases} \quad (14)$$

Saturation:

$$S = MAX - MIN \quad (15)$$

Intensity:

$$I = MAX \quad (16)$$

If the image number 3 in the Fig.4 is query image, then the Euclidian distance between the query image and the image of interest calculated. Table 2 shows the distance for the cases of which only texture information is taken into account ($D(t)$) and only hue information is used ($D(h)$). The difference is quite obvious that the distance between the query image and the other image of interest for using texture derived from Dyadic wavelet transformation is much longer than that for hue information. Also, it is quite obvious that the extracted texture information with Dyadic wavelet transformation is greater than that with the conventional DWT due to the fact that much detail frequency components are maintained for Dyadic wavelet transformation rather than that for the conventional DWT. Therefore, it may concluded that the followings,

- 1) Texture information is greater than color information,
- 2) Texture information can be extracted with Dyadic wavelet transformation much effectively than the conventional DWT
- 3) Forming texture feature vector by using energy derived from Gabor transform on 7 by 7 pixel neighbor of significant points is also effective for texture information extractions.

TABLE II. EUCLIDIAN DISTANCE BETWEEN THE QUERY IMAGE AND THE IMAGE OF INTEREST

Plankton	D(t)	D(h)
a.catenella1cell	0.751	0.428
a.catenella4cell	0.143	2.842
c.antiqua	0.0	0.0
c.antiqua2	1.561	1.096
c.antiqua3	1.926	0.053
c.furca	6.563	0.710
c.marina	1.802	0.060
c.polykrikoides2cell	1.915	0.256
c.polykrikoides8cell	0.560	0.121
d.fortii	6.611	0.506
g.catenatum1cell	1.069	0.013
g.catenatum5cell	3.543	0.073
g.instriatum	0.490	0.468
g.mikimotoi	0.785	1.461
g.polygramma	2.124	0.115
g.sanguineum	4.948	0.211
h.akashiwo	1.295	0.186
h.circularisquama	1.455	0.022
m.rubrum	2.396	0.576
n.scintillans4	1.037	1.3676
n.scintillans5	2.764	0.6447
p.dentatum	3.882	0.401
p.dentatum2	4.732	0.114
p.signoides	3.476	0.132

IV. CONCLUSION

Image retrieval method utilizing texture information which is derived from Discrete Wavelet Transformation: DWT together with color information is proposed. One of the specific features of the texture information extracted from portions of image is based on Dyadic wavelet transformation with forming texture feature vector by using energy derived from Gabor transform on 7 by 7 pixel neighbor of significant points. Using the Wang's dataset, the proposed method is evaluated with retrieval success rate (precision and recall) as well as Euclidian distance between the image in concern (Query image) and the other images in the database of interest and is compared to the other method. As the result through the experiments, it is found that the DWT derived texture information is significantly effective in comparison to the color information.

Through the experiments with the Wang's image dataset, it is found that the proposed method is superior to the other conventional methods for most of the cases. The proposed method achieved the improvements of 12%, 17%, 11%, in comparison to the Firm, Simplicity, and Color Salient Points, respectively. Also, it is found that texture information is greater than color information. Furthermore, it is found that texture information can be extracted with Dyadic wavelet transformation much effectively than the conventional DWT. Moreover, it may concluded that the forming texture feature vector by using energy derived from Gabor transform on 7 by 7 pixel neighbor of significant points is also effective for texture information extractions.

Further investigations are required for utilization of relational information, shape information, and so on. Also, it is desirable to conduct a research on image retrieval based on deep learning.

REFERENCES

AUTHORS PROFILE

- [1] Henning M'uller, Antoine Geissbuhler, et al. "Benchmarking Image Retrieval Applications". San Francisco, CA : In The Seventh International Conference, September 2004. pp. 334–337.
- [2] Kherfi, M., Brahmi, D. and Ziou D. "Combining Visual Features with Semantics for a More Effective Image Retrieval". : in ICPR '04, vol. 2, 2004. pp. 961–964.
- [3] H. Yu, M. Li, H.-J. Zhang and Feng, J. "Color texture moments for content-based image retrieval". : In International Conference on Image Processing, 2002. pp. 24–28.
- [4] N. Sebe, Q. Tian, E. Loupias, M. Lew and T. Huang. "Evaluation of salient point techniques". s.l. : In International Conference, 2004.
- [5] Stephane Mallet. "Wavelets for a Vision". : Proceeding to the IEEE, Vol. 84, 1996. pp. 604-685.
- [6] I.Daubechies. "Ten lecturer on wavelet". Philadelphia, PA:Society for Industrial and Applied Mathematics Analysis, vol. 23, Nov. 1992. pp. 1544–1576.
- [7] Kohei Arai and Y.Yamada. "Image retrieval method based on hue information and wavelet description based shape information as well as texture information of the objects extracted with dyadic wavelet transformation". s.l. : 11th Asian Symposium on Visualization, NIIGATA, JAPAN, 2011.
- [8] <http://wang.ist.psu.edu>.
- [9] Hiremath P.S and Jagadeesh Pujari. "Content Based Image Retrieval using Color Boosted Salient Points and Shape features of an image". : International Journal of Image Processing (IJIP) Vol.2, Issue 1, January-February 2008. pp. 10-17.
- [10] J. Li, J.Z. Wang, and G. Wiederhold. "IRM: Integrated Region Matching for Image Retrieval". : in Proc. of the 8th ACM Int. Conf. on Multimedia, Oct. 2000. pp. 147-156.

Kohei Arai, He received BS, MS and PhD degrees in 1972, 1974 and 1982, respectively. He was with The Institute for Industrial Science and Technology of the University of Tokyo from April 1974 to December 1978 and also was with National Space Development Agency of Japan from January, 1979 to March, 1990. During from 1985 to 1987, he was with Canada Centre for Remote Sensing as a Post Doctoral Fellow of National Science and Engineering Research Council of Canada. He moved to Saga University as a Professor in Department of Information Science on April 1990. He was a councilor for the Aeronautics and Space related to the Technology Committee of the Ministry of Science and Technology during from 1998 to 2000. He was a councilor of Saga University for 2002 and 2003. He also was an executive councilor for the Remote Sensing Society of Japan for 2003 to 2005. He is an Adjunct Professor of University of Arizona, USA since 1998. He also is Vice Chairman of the Commission-A of ICSU/COSPAR since 2008. He received Science and Engineering Award of the year 2014 from the minister of the ministry of Science Education of Japan and also received the Bset Paper Award of the year 2012 of IJACSA from Science and Information Organization: SAI. In 2016, he also received Vikram Sarabhai Medal of ICSU/COSPAR and also received 20 awards. He wrote 34 books and published 520 journal papers. He is Editor-in-Chief of International Journal of Advanced Computer Science and Applications as well as International Journal of Intelligent Systems and Applications. <http://teagis.ip.is.saga-u.ac.jp/>

Cahya Rahmad, He received BS from Brawijaya University indonesia in 1998 and MS degrees from Informatics engineering at Tenth of November Institute of Technology indonesia in 2005. he is a lecturer in The State Polytechnic of Malang Since 2005 also a doctoral student at Saga University Japan Since 2010. His interest research are image processing, data mining and patterns recognition.

Pattern of Success Vs. Pattern of Failure: Adaptive Authentication Through Kolmogorov–Smirnov (K-S) Statistics

Gahangir Hossain

Texas A&M University-Kingsville
Kingsville, TX, USA

Pradeep Palaniswamy

Texas A&M University-Kingsville
Kingsville, TX, USA

Rajab Chaloo

Texas A&M University-Kingsville
Kingsville, TX, USA

Abstract—Smartphones have become a basic necessity in lives of all human beings. Apart from the core functionality of communication, these become a medium for storage of sensitive personal information, financial data and official documents. Hence, there is an inevitable need to emphasize on securing access to such devices considering the nature of data being stored. In addition, accessibility and authentication methods need to be secure, robust, and user-friendly. This paper discusses an adaptive authentication mechanism with a nonparametric classification approach, Kolmogorov–Smirnov (K-S) statistic, which is coupled with the use of lock pattern dynamics as a secure and user-friendly two-factor authentication method. The data used for experimental exploration were collected from a systematically programmed Android device to capture the temporal parameters when individuals drew lock patterns on the touch screen. Each user has his individualistic way of drawing the pattern, which is used as the key for identifying imposters from valid users.

Keywords—Mobile user experience; Biometrics; Smart mobile devices; Mobile identity management; Mobile authentication; Lock patterns; Mean time value

I. INTRODUCTION

The use of mobile smart devices for storing sensitive information and accessing online services has been increasing steadily. Mobile smart devices have become the one smart destination for all kinds of user data starting from social networking data [12] through mails (both personal and official) so on up to financial information. Despite all the information contained in a device and the transactions that can be performed with it, many users choose not to protect their devices, and at the same time they tend to be perpetually logged into some of the services provided by mobile third party applications. Thus, an attack on the mobile device or the loss can lead to undesired consequences such as the intrusion of privacy, the opportunity to impersonate users, and even severe financial loss.

Currently, most of the solutions that are designed for authenticating users into their mobile services are similar to authentication systems in mobiles. They usually use a PIN, a strong password, or some sort of extra external security token device. These techniques become cumbersome when applied to mobile devices and do not always provide a satisfactory user experience. Besides, they are not a sustainable approach for the future of mobile interactions, in which people would

carry only one secure trustable device to perform most operations and would preferably use only one hand to operate such a device.

Pattern locking is another approach used in mobile smart devices with touch screen. Pattern locking refers to the option contained in the Android mobile platform [5] for locking the phone's screen. Pattern locks are graphical passwords that can be used to authenticate a user. Since it is a graphical approach users usually tend to remember the passwords better than a text-based pin. They also have the advantage that they can be easily drawn using a single hand, giving much better user experience when compared to text-based passwords. However the enhanced user experience that comes with using a visualized password has its own setbacks. Unlike text-based passwords that are hidden when being typed pattern locks visible to eyes or video recording devices when they are being drawn. This makes pattern matched authorization more vulnerable to attacks.

As a generic solution to this issue, this paper discusses about enhancing the feature of pattern matched authorization by totaling its design with behavioral biometric features. The time taken by the user to draw the pattern, time taken between subsequent checkpoints in the pattern differs from user to user, this is considered as the behavioral biometric trait. The paper also hypothesizes that adding a biometric trait to lock pattern authorization can enhance the security of this type of graphical passwords by becoming a two-factor authentication mechanism.

II. RELATED LITERATURE

As of now, research has been carried out on different approaches that provide an additional level of security for authenticating users both in mobiles as well as in desktops. There have been approaches where in users day to day activity can be used as a key for authenticating a user. As an example, a Smartphone might ask the user: "Today morning from who did you receive an SMS?" This type of authorization system has been discussed in [10].

Another popular approach of identifying users is using key stroke dynamics. Keystroke dynamics or typing dynamics refers to the automated method of identifying or confirming the identity of an individual based on the manner and the rhythm of typing on a keyboard. Keystroke dynamics is a behavioral biometric. Specifically, most of the

research done on the analysis of keystroke dynamics are for identifying users as they type on a mobile phone. Some can be found in [1], [2], [6], [7], [9] and others. One of these studies, [1], considers the dynamics of typed 4-digit PIN codes, in which the researchers achieved an average Equal Error Rate (ERR) 2 of 8.5%. However, the data for this experiment was collected using a mobile phone Handset interfaced to a PC through the keyboard connection "[1], thus their experiment does not portray real mobile situations neither does it consider typing PIN codes on touch-screens.

One of the mentioned studies, [9], partially considers the use of on-screen keyboards. The approach taken in this study however, has the disadvantage that the system has to be trained with a minimum of 250 keystrokes in order to achieve a low Equal Error Rate of approximately 2% which is not suitable for applications that do not require a lot of typing, neither for detecting short passwords or PIN intrusions.

Imposing the use of alphanumeric passwords on mobile devices creates the problem that users tend to choose simpler, weaker or repetitive passwords [7], since complicated strong passwords are harder to type on smaller on-screen keyboards. Therefore, suggestions for more unobtrusive methods for authentication on mobile smart phones have emerged as an alternative to typed passwords, such as gait biometrics (achieving an EER of 20.1%) [4] [8], or the unique movement users perform when answering or placing a phone call (EER being between 4.5% and 9.5%) [3]. Although these methods seem to be a promising approach towards enhancing the user experience, they require users to take the explicit actions like answering phone calls in order to be effective. Therefore, they are not fully suitable for scenarios when a user needs to interact or look at the phone in order to login to a mobile application or Online service. Besides, these methods only provide a one-factor authentication mechanism.

To the best of our knowledge, only one approach [11] deals with the use of biometric traits over a pattern matching authorization technique. In this approach the author would have compared various anomaly detectors (i.e., Euclidian detector, random forest, etc.) to find and compare the EERs and standard deviations of the techniques.

In our we use the same data set that was used in [11], the data collection is done using Google's platform for mobile devices, Android [5], we use a mobile application to collect data from different individuals on the way they draw lock patterns, their experience while doing so and other contextual factors., test participants were asked to draw three different lock patterns correctly a certain number of times (n=50 trials for each pattern), with each pattern consisting of six dots, as shown in Figure 1. More specifically, during a test session test participants were first shown an animation on how to draw the first lock pattern (see Figure 1(a)), once they had learnt it they were asked to draw that pattern correctly 50 times. They were then shown the second pattern (Figure 1(b)) and were also asked to draw it 50 times, and the same was done for the third pattern (Figure 1(c)). A static approach was used in which all participants drew the same three patterns, i.e., the input was identical for all tests [1]. Analogous to earlier keystroke studies (in which different distinguishing features are used,

such as key holding time and digraphs [9]), two main features were captured for each successful trial: the *finger-in-dot* time, which is the time in milliseconds from the moment the participant's finger touches a dot to the moment the finger is dragged outside the dot area, and the *finger-in-between-dots* time, representing the speed at which the finger moves from one dot to the next. All erroneous trials were disregarded.



(a) 1st Lock pattern (b) 2nd Lock pattern (c) 3rd Lock pattern
Fig. 1. The three lock patterns that participants were asked to draw

After pattern unlocking experiment is designed, the data is collected that contains pattern matching timings for 32 users for three patterns. Each pattern is attempted to be drawn right 50 times. There are 11 temporal parameters (six time_on_dot timings and 5 five time_between_dot timings) that were recorded in this experiment during every single trial.

III. METHOD

The basic purpose of an authentication system is to block the invalid access from the valid access. A commonly used authentication technique separates the invalid pattern from the valid pattern of using response time as modulators with minimum mean squared errors. However, whenever a user's tapped lock pattern becomes similar (but not same) to the acceptable lock pattern, system might allow user to access the system and update the variance of lock pattern. This can be considered as adaptive lock pattern, or adaptive authentication. This adaptation process is explained with a block diagram as figure.

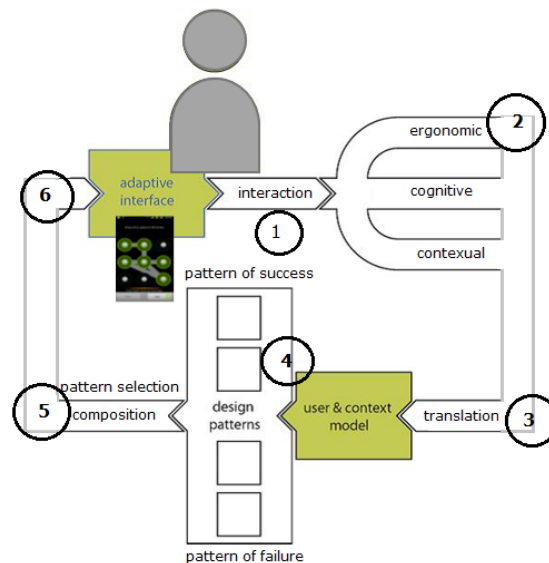


Fig. 2. A schematic representation of adaptive authentication with a pattern of success and a pattern of failure. Circles indicate the steps of the authentication and updating process

Step 1: User type lock pattern

Step 2: ergonomic, cognitive and contextual factors are applied to the patter to modulate it.

Step 3: The modulated signal is translated to the user and context model (personalized profile).

Step 4: Pattern is matched (with K-S test)

Step 5: Pattern is selected and composed to the adaptive model.

A formal model of an adaptive authentication system is shown in figure 3.

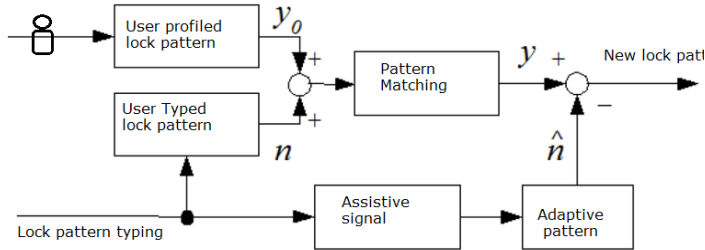


Fig. 3. A formal model of adaptive authentication

Figure 3, the formal model is a schematic representation of the flow of events that take place in pattern based cognitive authentication system. When a new user tries to enter into the system by swiping the lock pattern, if the attempted pattern was drawn right then we capture the 11 temporal parameters (i.e, 6 time_on_dot timings and 5 time_between_dot timings). We also have a pattern model of composed of a matrix [96*11](96-32 users * 3 patterns, 11- temporal parameters) of mean time values. Based on the user and the pattern we choose the corresponding mean time value (i.e., corresponding row) from the pattern model. Next we perform a KS test on both these samples to derive the P and D values. If the P-value is greater than the D-value then the user is an authorized user, else the user is considered as an imposter and is requested to repeat the process. A complete flow diagram of the pattern matching is shown in figure 4.

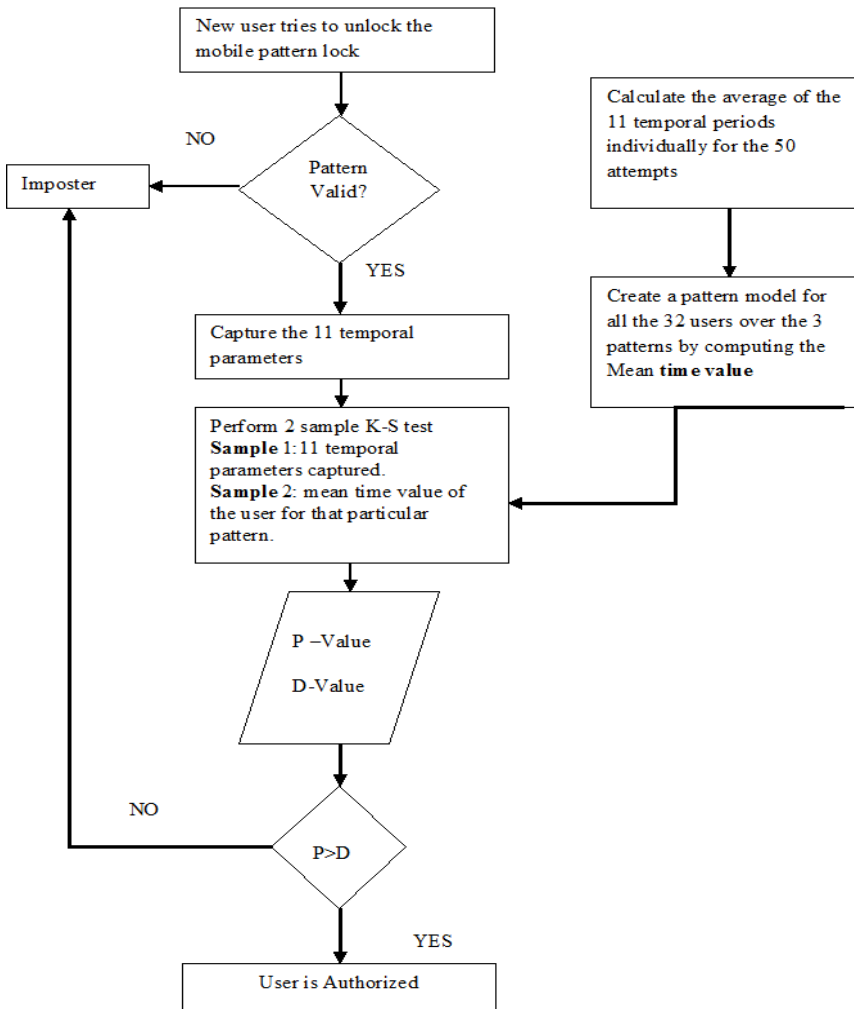


Fig. 4. Adaptive authentication analysis flow diagram

IV. PATTERN OF SUCCESS VS. FAILURE

The proposed design is a logical extension of the technique handled in [11]. Non-parametric tests are performed in-order to determine whether the sequence of moves made by the user to unlock a pattern matches statistically with the pattern recorded on the system. A non-parametric test is one in which there are no pre-requisite on the data that is to be processed, i.e. There is no emphasis that the data must follow a particular distribution.

A. The Kolmogorov–Smirnov Test

The **Kolmogorov–Smirnov** test (commonly known as a K–S test or **KS** test) is a nonparametric test of the equality of continuous, one-dimensional probability distributions that can be used to compare a sample with a reference probability distribution or to compare two independent samples. Since two temporal parameters need to be compared a two sample K-S test is used.

The temporal data for the legitimate user’s (i.e. the user the system is trained to accept) attempts is averaged out and considered as the first sample.

When a user tries to access the system by drawing the unlocking pattern, the temporal values for the attempt are captured and considered as the second sample.

The two samples are compared using K-S test so as to determine whether they belong to the same distribution (i.e. prove whether they are statistically similar). On a contrary, if the samples are statistically dissimilar we can say that the user is an imposter.

A classic example to explain the scenario is the summary of a cricket match, how can one determine whether the pattern of the chase is similar?

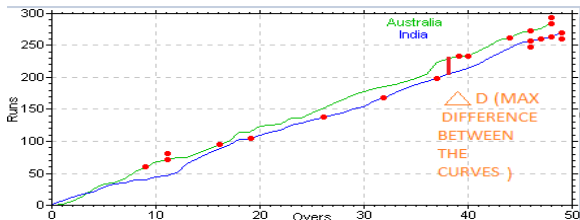


Fig. 5. Example score patterns from a cricket match

The deviation in chase patterns can be captured by analyzing delta D, lesser the value similar the pattern. K-S test follows a similar approach.

The Kolmogorov–Smirnov statistic quantifies a distance between the empirical distribution functions of two samples. K-S test computes the maximum absolute distance between the two cumulative functions. The null distribution of K-S test is calculated under the null hypothesis that the samples are drawn from the same distribution (two-sample case).

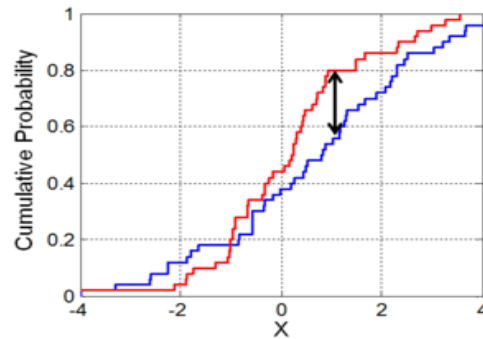


Fig. 6. Example of a K-S test (2 Sample)

Figure 5 portrays the example score pattern (Given in figure 6) in terms of cumulative probability.

B. Kolmogorov–Smirnov (K-S) statistic

The Kolmogorov–Smirnov (K-S) statistic for a two sample test is defined as

$$D_{n,n'} = \sup |F_{1,n}(x) - F_{2,n'}(x)|$$

Where $F_{1,n}$ and $F_{2,n'}$ are the empirical distribution functions of the first and the second sample respectively. Sup is the supremum[12] function. The null hypothesis is given by

$$D_{n,n'} > P_{n,n'}$$

Where $P_{n,n'}$ is given by

$$P_{n,n'} = c(\alpha) \sqrt{\frac{n+n'}{\sqrt{n \cdot n'}}$$

The value of $c(\alpha)$ is given in the table below for each level of α .

TABLE I. RANGE OF SIGNIFICANCE LEVELS

α	0.10	0.05	0.025	0.01	0.005	0.001
$c(\alpha)$	1.22	1.36	1.48	1.63	1.73	1.95

The level α is the "significance level" of the test, the rate of Type I error, the probability of detecting a difference under the assumptions of the null hypothesis (that the two samples are drawn from the same distribution). For our experiment we assume $c(\alpha)$ to be 0.05.

V. METRICS AND COMPUTATION

A. Types of errors

False rejection rate (Type I error): The false rejection rate or FRR is the probability that the system incorrectly rejects access to an authorized person, due to failing to match the biometric input with a template.

False acceptance rate (Type II error): The false acceptance rate or FAR is the measure of the likelihood that the biometric security system will incorrectly accept an access attempt by an

unauthorized user. A system's far typically is stated as the ratio of the number of false acceptances divided by the number of identification attempts.

B. Mean Time Value

Mean time value of a particular user drawing a particular pattern is the average time that the particular user might take to complete drawing the pattern. Mean time value is calculated by simple computing the mean of all the 11 temporal parameters individually for all the 50 attempts made by the user drawing the pattern. Resultant would be a set of 11 normalized temporal parameters.

C. False Acceptance Rate

FAR is computed for each user by selecting the mean time value for a user and then conducting a K-S test against all other user samples obtained (31 other users for their 50 attempts).This is termed as a Set and each set consists of (31*50) K-S tests . 32 Sets are obtained by repeating the procedure for all the 32 users. The resulting data set would contain 992 comparisons (32 *31 users).The number of tests that has failed the null hypothesis is then computed for each user individually in order to compute the FAR value (i.e., more tests failed lesser the false acceptance).

D. False Rejection rate

In order to compute the false rejection rate of a particular user in a particular Patten, Mean time value of that particular user is tested against the 50 samples for the same user. The same procedure is repeated for all 32 users. In case of FRR computation the number of tests that failed the null hypothesis is directly proportional to FRR value.

VI. RESULTS

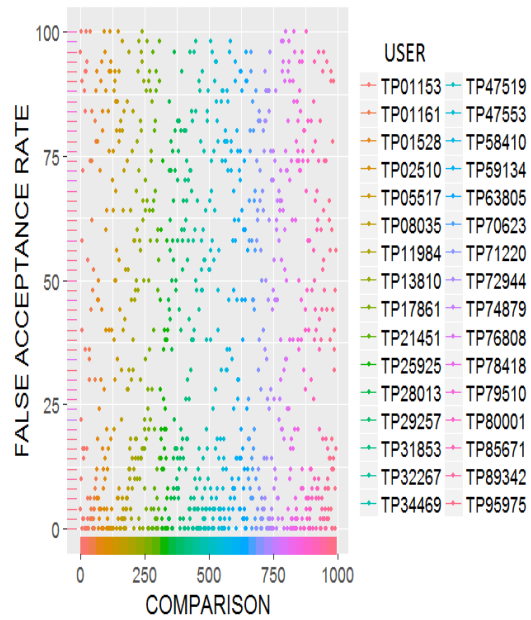
We summarize the results in the tabular column given in Table 2.

TABLE II. OVERALL COMPARISON OF FALSE ACCEPTANCE VS. FALSE REJECTION RATES FOR THE THREE PATTERNS USED

PATTERN	FALSE REJECTION RATE	FALSE ACCEPTANCE RATE
pattern 1	17	38.32258
pattern 2	13.4375	43.14516
pattern 3	14.5625	36.38508

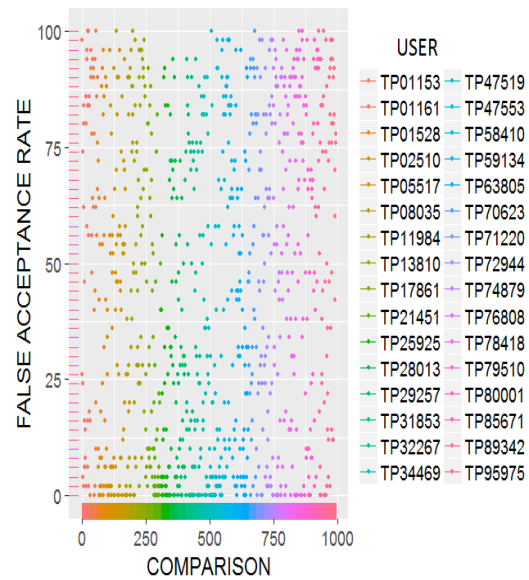
The overall results are pictorially summarized as follows. There are three patterns and for each pattern both FAR and FRR are calculated.

FALSE ACCEPTANCE RATE PATTERN- 1



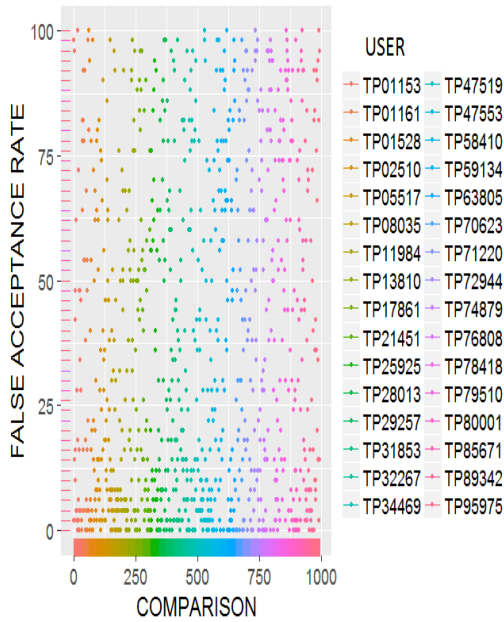
(a) False acceptance rate on pattern 1

FALSE ACCEPTANCE RATE PATTERN- 2



(b) False acceptance rate on pattern 2

FALSE ACCEPTANCE RATE PATTERN- 3



(c) False acceptance rate on pattern 3

Fig. 7. (a) False acceptance rate on pattern 1 (b) False acceptance rate on pattern 2 (c) False acceptance rate on pattern 3

A. Inference

Figures 7 (a) (b) and (c) make it evident that in most Cases the incorrect acceptance rate is lesser than 15. However, there are outliers reaching up to peaks. To be specific, there is 100% fault acceptance rate between users "TP01153" "TP02510" while drawing pattern 1. While having a closer look at this issue it can be observed that when the two users are KS-Tested against each other a D value comparatively smaller to P value is obtained (i.e.: $D = 0.25$, $p\text{-value} = 0.8475$). This has resulted because the timing patterns of these 2 users closely matches with each other. This infers that the users have very similar pattern of drawing. It can be also absorbed that these 2 users have very high false acceptance rates on other 2 patterns as well (Pattern 2 is 74% and pattern3 is 96%).

With respect to false rejection it can be observed that the false rejection rate, it is usually below 20%. However there are few spikes in FRR graph as well. When examined it is evident that user TP11984 has a false rejection rate of 88% on pattern 1. On closer observation it is clear that the user's swipe times undergoes a wide range of oscillations. For example a temporal parameter (time_on_dot1) values range from 65 to 506 mille seconds. These in constancies follow throughout the pattern leading to a very false high false rejection rate (pattern of success). This is shown in figure 8.

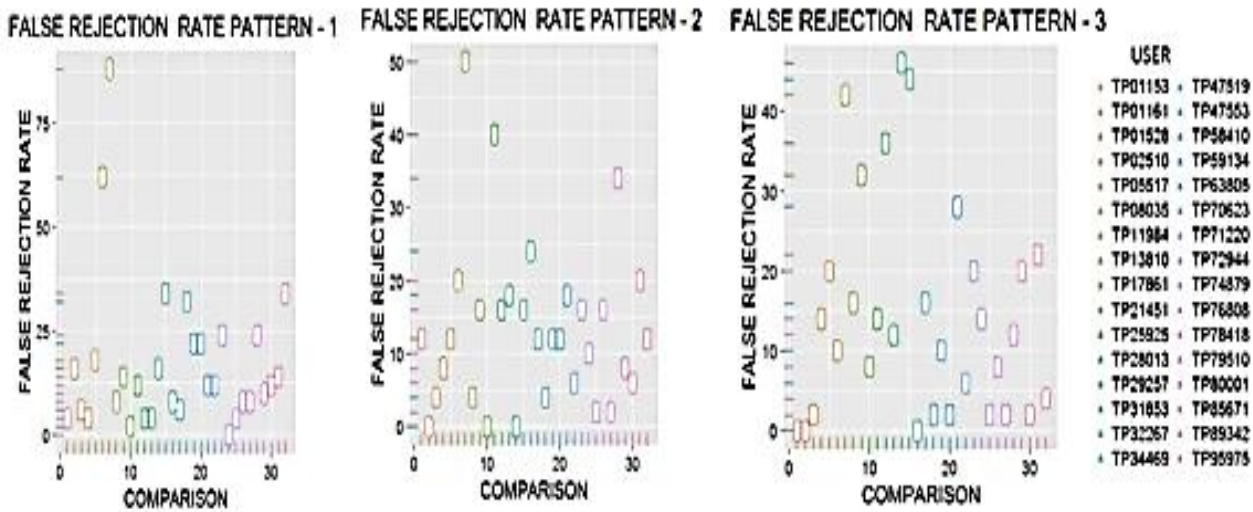


Fig. 8. False rejection rate across the 3 patterns

VII. CONCLUSION

K-S test is a simple but effective nonparametric test that can be used in order to determine whether 2 Radom samples belong to the same distribution. Hence, it is useful pattern of success and pattern of failure identification. As K-S test compares the overall distributions rather than specifically locations or dispersions, the test is a useful adaptive classification tool. Though the failures in results are justified to a certain extent we cannot deny the fact that the proposed method needs improvement, alternative choices for non-parametric tests include multivariate [13] and multidimensional [14] K-S test. Another, improvement that

can be considered is for calculating the mean time value for a particular user against a pattern. In the current approach, we just compute a normal average of all the values, whereas we can do much better than that. The pitfall in calculating the average is that, we will not be able to eliminate the outliers. By eliminating the outliers could improve the result of the computation by a great extent.

Though the two factor authorization mechanism is an effective one there were various inconsistencies those were observed as outliers when calculating the FRR and the FAR value. An effective approach to reduce such inconsistencies can be implemented by reducing the distance between checkpoints. In current scenario there are 6 checkpoints to

obtain the temporal parameters. However, if the distance between check points is decreased the number of temporal parameters will increase, for example if the distance between check points is reduced by 50% the number of temporal parameters will increase by 50%. Increased number of temporal parameters will result in higher precision of results.

REFERENCES

- [1] Clarke, N.L., Furnell, S.: Authenticating mobile phone users using keystroke analysis .Int. J. Inf. Sec. 6(1), 1{14 (2007).
- [2] Clarke, N.L., Karatzouni, S., Furnell, S.: Flexible and transparent user authentication for mobile devices. In: SEC. pp. 1{12 (2009).
- [3] Conti, M., Zachia-Zlatea, I., Crispo, B.: Mind how you answer me!: transparently Authenticating the user of a Smartphone when answering or placing a call. In:Proceedings of the 6th ACM Symposium on Information, Computer and Communications Security. pp. 249-259. ASIACCS '11, ACM, New York, NY, USA (2011).
- [4] Derawi, M.O., Nickel, C., Bours, P., Busch, C.: Unobtrusive user-authentication on mobile phones using biometric gait recognition. In: Proceedings of the 2010 Sixth International Conference on Intelligent Information Hiding and Multimedia Signal Processing. pp. 306{311. IHH-MSP '10, IEEE Computer Society, USA (2010).
- [5] Google: Android: Android - open source project (June 2011), <http://source.android.com/>
- [6] Karatzouni, S., Clarke, N.L.: Keystroke analysis for thumb-based keyboards on mobile devices. In: SEC. pp. 253{263 (2007).
- [7] Nauman, M., Ali, T.: TOKEN: Trustable Keystroke-Based Authentication for Web-Based Applications on Smartphones. In: Bandyopadhyay, S.K., Adi, W., Kim, T.h., Xiao, Y. (eds.) Information Security and Assurance, Communications in Computer and Information Science, vol. 76, pp. 286{297. Springer Berlin (2010).
- [8] Nickel, C., Derawi, M.O., Bours, P., Busch, C.: Scenario test of accelerometer-based biometric gait recognition. In: Security and Communication Networks (IWSCN). 3rd International Workshop, Gjøvik, Norway (2011).
- [9] Zahid, S., Shahzad, M., Khayam, S., Farooq, M.: Keystroke-based user identification on smart phones. In: Kirda, E., Jha, S., Balzarotti, D. (eds.) Recent Advances in Intrusion Detection, Lecture Notes in Computer Science, vol. 5758, pp. 224{243. Springer Berlin / Heidelberg (2009).
- [10] Sourav Kumar DandapatIIT Kharagpur, India,Swadhin Pradhan,UTAustin, USA,Bivas MitraIIT Kharagpur, India,Romit Roy Choudhury,UIUC, USA.,Niloy Ganguly,IIT Kharagpur, India ., ActivPass: Your Daily Activity is Your Password Proceeding CHI '15 Proceedings of the 33rd Annual ACM Conference on Human Factors in Computing Systems Pages 2325-2334 ACM New York, NY, USA ©2015.
- [11] Exploring Touch-screen Biometrics for UserIdentification on Smart Phones Julio Angulo and Erik WastlundKarlstad University,Universitetsgatan 2, 651 88 Karlstad, Swedenjulio.angulo , erik.wastlundg@kau.sehttp://www.kau.se Aviv, A.J., Gibson, K., Mossop, E., Blaze, M., Smith, J.M.: Smudge attacks on smartphone touch screens. In: Proceedings of the 4th USENIX conference on Offensive technologies. pp. 1{7. WOOT'10, USENIX Association, Berkeley, CA, USA(2010).
- [12] The supremum (abbreviated sup;pural suprema) of a subset S of a partially ordered set T is the least element in T that is greater than or equal to all elements of S, if such an element exists. Consequently, the supremum is also referred to as the least upper bound (or LUB) https://en.wikipedia.org/wiki/Infimum_and_supremum. Alpher, , and J. P. N. Fotheringham-Smythe. Frobnication revisited. Journal of Foo, 13(1):234–778, 2003.
- [13] Justel, A.; Peña, D.; Zamar, R. (1997). "A multivariate Kolmogorov–Smirnov test of goodness of fit". *Statistics & Probability Letters* 35 (3): 251–259. doi:10.1016/S0167-7152(97)00020-5.
- [14] Fasano, G., Franceschini, A. (1987). "A multidimensional version of the Kolmogorov–Smirnov test". *Monthly Notices of the Royal Astronomical Society* 225: 155–170. Bibcode:1987MNRAS.225..155F. doi:10.1093/mnras/225.1.155. ISSN 0035-8711.

Error Analysis of Line of Sight Estimation using Purkinje Images for Eye-based Human-Computer Interaction: HCI

Kohei Arai¹

¹ Graduate School of Science and Engineering
Saga University
Saga City, Japan

Abstract—Error analysis of line of sight estimation using Purkinje images for eye-based Human-Computer Interaction: HCI is conducted. Double Purkinje images which are obtained by two points of light sources are used in the proposed method for eye rotation angle estimation. It aimed at the improvement of the eyeball rotation angle accuracy by simply presuming the value of the curvature radius of the cornea. This technique is a cancellation of the time of the calibration that is the problem of past glance presumption. By presuming the size of the radius of curvature of the cornea. As a result, the eyeball rotation angle presumption accuracy of about 0.98deg was obtained 0.57deg and horizontally in the vertical direction without doing the calibration.

Keywords—Computer input just by sight; Computer input by human eyes only; Purkinje image

I. INTRODUCTION

As for the computer input system with human eyes only based on an image-analysis method, many methods have been proposed so far. Matsuda et al. makes the line of sight which connects eyeball rotation center coordinates and a pupil center, and is performing gaze measurement [1]. Eyeball rotation center coordinates are searched for by moving an eyeball in the various directions before gaze measurement. Therefore, since there is no necessity of showing an index, gaze measurement is possible in all places, but preparation takes time and there is a fault of not permitting head movement. Moreover, Ono et al. makes the line of sight which connects cornea center-of-curvature coordinates and a pupil center, and is performing gaze measurement [2].

Cornea center-of-curvature coordinates are the light source of one point, and installing a camera on the optical axis, and are searched for using the general cornea radius-of-curvature value. However, since they assumed models, such as Japanese typical eyeball form, the error remained in the direction estimation of a gaze not a little, and if these methods did not perform a calibration, when there were, they did not become. That is, in order to cancel the gaze estimation error based on the gap of a central fovea to an eyeball center, the refraction in a cornea, and the individual difference concerning the form of a cornea, the calibration which draws a gaze correction coefficient needed to be performed by gazing at two or more indices displayed on the display one by one [3]. Moreover, since it was not what permits a motion of a user, the burden

has been forced upon the user. The former presumes the point of regard on the display at the point of the look obtained from gaze estimation (three dimension measurement) of not only the direction of a gaze but both eyes, and uses the pupil center and the corneal reflex center for gaze estimation. The latter presumes a cornea center of curvature using two Purkinje images, makes a user gaze at the index of three points, presumes an eyeball rotation center, is the method of making a gaze the straight line which connects these, and is verifying accuracy by the experiment using a model eye [4].

There are some methods which allow gaze estimations and its applications for HCI [5]-[35]. In particular, paper 13 describes the method for gaze detection and line of sight estimation. In this paper, an error analysis is made for the previously proposed method. For the method, an expensive stereo camera is not needed, but only a cheap simple eye camera permits a motion of a user, and the method of determining the direction of a look from a pupil center and a cornea center of curvature is proposed without the calibration which forces a user a gaze of three points. By specifically measuring an eyeball cornea curvature radius simply, the degree estimation of eyeball rotation angle which does not need a calibration is performed, details are extracted from a face picture, the posture of a head is detected from those relative spatial relationships, and a motion of a head is permitted. The light source of two points was used for measurement of the cornea curvature radius of an eyeball, and two Purkinje images obtained from the cornea surface were used for it. At this time, it decided to also use together the near infrared light source which a camera has using the near-infrared camera which became budget prices, and to acquire the clear Purkinje image in recent years. When five subjects estimate the direction estimation accuracy of a look for this, a motion of the head of the 30 roll directions and the 15 directions of a pitch is permitted, and since it checked that the direction of a gaze could be presumed without a calibration with the error of 0.57 to 0.98 degrees, it reports here.

The angle estimation method of eyeball rotation angle of using two light sources and one near infrared camera is proposed first, the head angle detection method using the details in a face picture is described, and this paper estimates the validity of the proposed method by the direction estimation experiment of a look by five subjective examiners.

The following section describes the proposed line of sight vector estimation with Purkinje images briefly followed by the proposed error analysis method. Then experimental results are described together with some remarks. Finally, conclusion is described with some discussions and future investigations.

II. PROPOSED METHOD FOR LINE OF SIGHT ESTIMATION

A. Eye model

Fig.1 (a) shows eye shape model while Fig.1 (b) shows the definitions of Purkinje images of the first to the fourth Purkinje images. The size and the curvature of cornea, sclera, retina, and eyeball are different for everybody. Therefore, calibration is required before using computer input just by sight. It is possible to estimate the size and the curvature by using the locations of the first to the fourth Purkinje images. The line of sight is defined as the line starting from the cornea curvature center which is estimated with Purkinje images to pupil center.

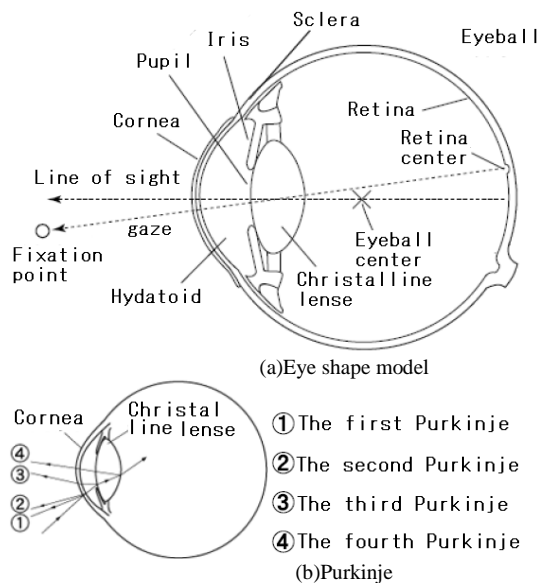


Fig. 1. Eye model and Purkinje images

B. Procedure for estimation of fixation point on display at which user is looking

The procedure for estimation of fixation point on display at which user is looking is as follows,

- 1) Cornea curvature radius is estimated with double Purkinje images
- 2) Pupil center is determined with ellipsoidal approximation of pupil shape
- 3) Cornea curvature center is determined with geometric relations among eyeball, camera, display and light sources
- 4) Line of sight is determined with the cornea curvature center and pupil center
- 5) Fixation point on the display is determined with the line of sight vector

Fig.2 shows the method for estimation of cornea curvature center and radius.

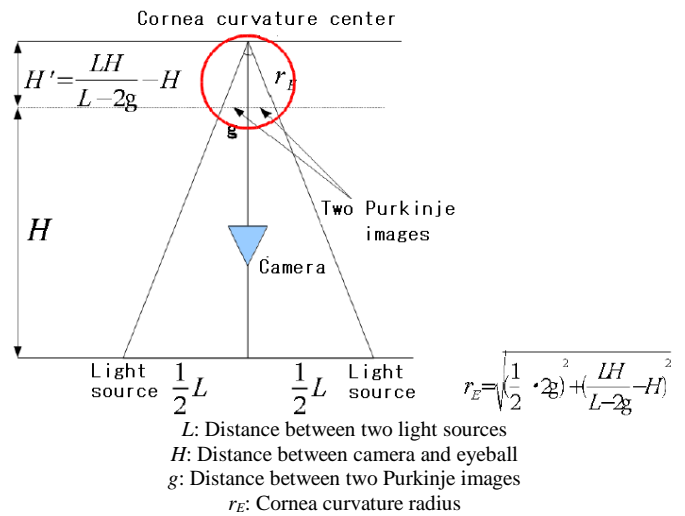


Fig. 2. Method for estimation of cornea curvature center and radius

L and H are given. The distance between two Purkinje images can be measured as follows,

- 1) binarize the acquired NIR image of the eye and its surroundings,
- 2) isolated noise pixels are removed by using morphological filter,
- 3) the distance between the locations of two Purkinje images is measured

This procedure is illustrated in the Fig.3. Thus the cornea curvature radius can be estimated.

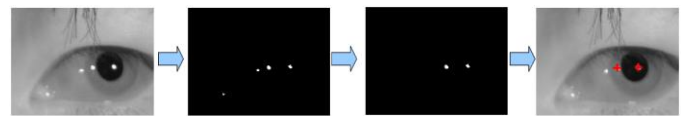


Fig. 3. Procedure of the cornea curvature radius measurement

Through this procedure, the relation between the distance between the eye and the camera and the number of pixels within 10cm of distance interval is shown in Fig.4. Meanwhile, the estimated cornea curvature radius is shown in Fig.5 as a function of the distance from the eye. These can be derived from the following equation representing the cornea curvature radius.

$$r_E = \sqrt{\left(\frac{1}{2} \cdot g\right)^2 + \left(\frac{LH}{L-2g} - H\right)^2} \tag{1}$$

Next, a pupillary zone is extracted using a dark pupil method, ellipse approximation of the pupil form is carried out, and a pupil center is searched for. With a dark pupil method, if an infrared floodlight is installed in the position distant from the lens optic axis of a camera and an eyeball is illuminated, the reflection of light of the pupil portion of the illuminated eyeball will be lost, and the pupil portion of the eyeball picture caught with the camera will use the character to become dark here. Image processing extracts this dark portion.

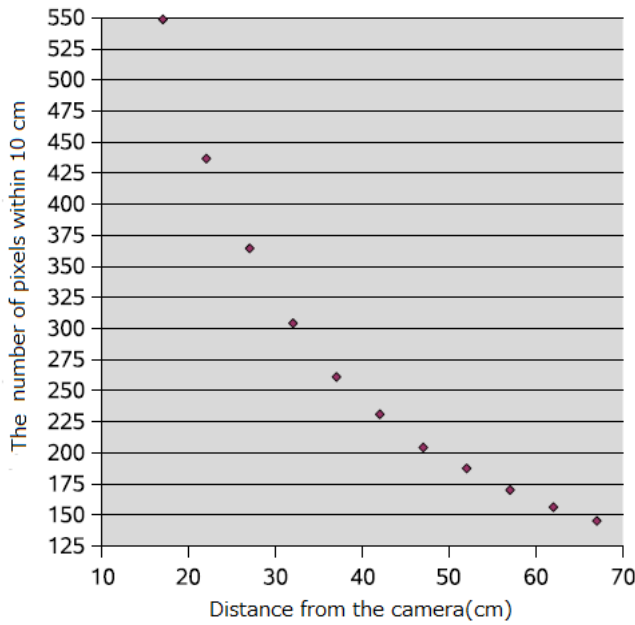


Fig. 4. Relation between the distance between the eye and the camera and the number of pixels within 10cm of distance interval

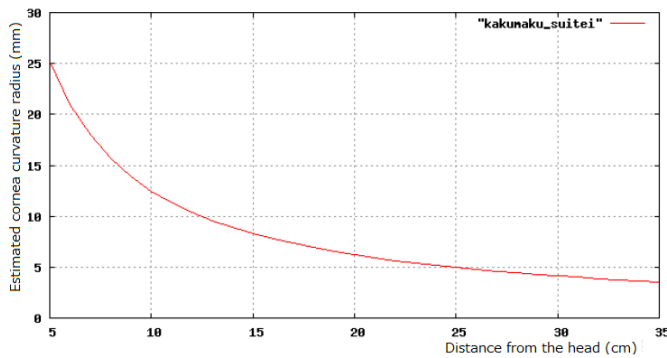


Fig. 5. Relation between the estimated cornea curvature radius and the distance from the eye

Moreover, in the extracted pupillary zone, since reflected lighting and the up-and-down portion of a pupil hide and are missing by the eyelid, the pupil may not be able to be extracted correctly. Therefore, edge is detected from the obtained temporary pupillary zone, and the edge concerned is approximated to an ellipse by a least squares method. However, when it calculates using except a pupil outline, there is a possibility of resembling the mistaken ellipse. Therefore, pupil ellipse approximation using the character of an ellipse was performed.

That is, in Fig.6, straight lines l, m, and n shall be parallel, and l and n shall exist in the equal distance from m. The intersection of an ellipse and a straight line l is set to a and b, the intersection of an ellipse and a straight line n is set to c and d, and the middle point of the intersection of an ellipse and a straight line m is set to o. When the middle point of a line which connects the middle point of a and b and the middle point of c and d is set to o₀, there is character in which o₀ overlaps with o.

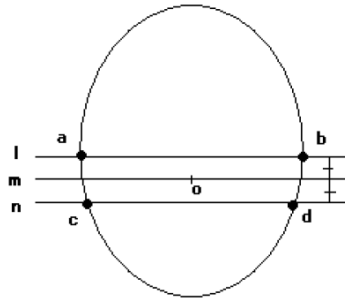
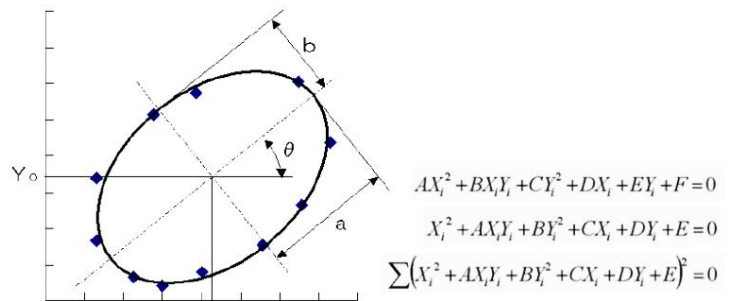


Fig. 6. Elliptic approximation

Least square method for elliptic approximation is illustrated in Fig.7.

$$\left(\frac{(X_i - X_0)\cos\theta + (Y_i - Y_0)\sin\theta}{a}\right)^2 + \left(\frac{-(X_i - X_0)\sin\theta + (Y_i - Y_0)\cos\theta}{b}\right)^2 = 1$$



$$\begin{matrix} \sum X_i^2 Y_i^2 & \sum X_i Y_i^3 & \sum X_i^2 Y_i & \sum X_i Y_i^2 & \sum X_i Y_i & A \\ \sum X_i Y_i^3 & \sum Y_i^4 & \sum X_i Y_i^2 & \sum Y_i^3 & \sum Y_i^2 & B \\ \sum X_i^2 Y_i & \sum X_i Y_i^2 & \sum X_i^2 & \sum X_i Y_i & \sum X_i & C \\ \sum X_i Y_i^2 & \sum Y_i^3 & \sum X_i Y_i & \sum Y_i^2 & \sum Y_i & D \\ \sum X_i Y_i & \sum Y_i^2 & \sum X_i & \sum Y_i & \sum 1 & E \end{matrix} \begin{matrix} A \\ B \\ C \\ D \\ E \end{matrix} = \begin{matrix} -\sum X_i^3 Y_i \\ -\sum X_i^2 Y_i^2 \\ -\sum X_i^3 \\ -\sum X_i^2 Y_i \\ -\sum X_i^2 \end{matrix}$$

$$X_0 = \frac{AD - 2BC}{4B - A^2} \quad Y_0 = \frac{AC - 2D}{4B - A^2} \quad \theta = \frac{\tan^{-1}\left(\frac{A}{1-B}\right)}{2}$$

$$a = \sqrt{(X_0 \cos\theta + Y_0 \sin\theta)^2 - E \cos^2\theta - \{(X_0 \sin\theta - Y_0 \cos\theta)^2 - E \sin^2\theta\} \frac{\sin^2\theta - B \cos^2\theta}{\cos^2\theta - B \sin^2\theta}}$$

$$b = \sqrt{(X_0 \sin\theta - Y_0 \cos\theta)^2 - E \sin^2\theta - \{(X_0 \cos\theta + Y_0 \sin\theta)^2 - E \cos^2\theta\} \frac{\cos^2\theta - B \sin^2\theta}{\sin^2\theta - B \cos^2\theta}}$$

Fig. 7. Least square method for elliptic approximation

N which is in the equal distance about a temporary pupillary zone from the straight line m drawn in the center. The point of hitting o_{i0} (i = 1-N) of the group of the parallel lines is searched for. The point searched for is distributed on a straight line m. When there are few noises enough, the position in which most many points o₀ gathered is equivalent to the position of o. Since the point which is distant from the

position will include the point which is not on the locus of an ellipse, it accepts them. o point a_i which is alike and has sufficiently near o_{i0}; b_i; c_i; Since d_i is a point on an ellipse, ellipse approximation of an exact pupil outline can be performed by using them.

Next, a cornea center of curvature is searched for from the spatial relationship of the acquired cornea curvature radius and the light source of Fig.8, an eyeball, and a camera, and the geometric expression of relations in a Figure. A cornea center of curvature exists here on the bisector which ties a camera, the Purkinje image, and lighting. It asks for a look vector from a pupil center and a cornea center of curvature.

Finally, the point of regard on a display is computed from a look vector. The vector which passes along two points, a cornea center of curvature and a pupil center, is made into a look vector, and the point of regard on a display is computed.

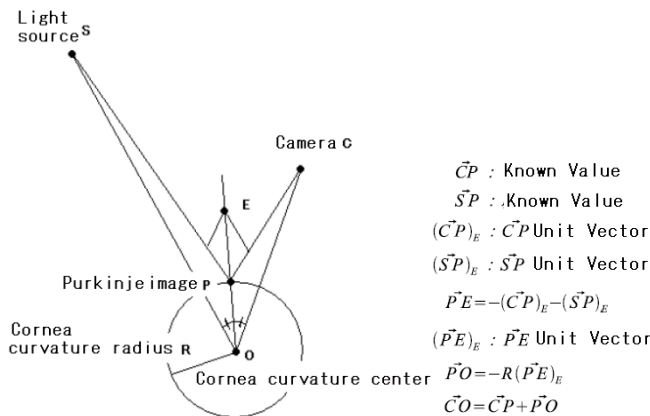
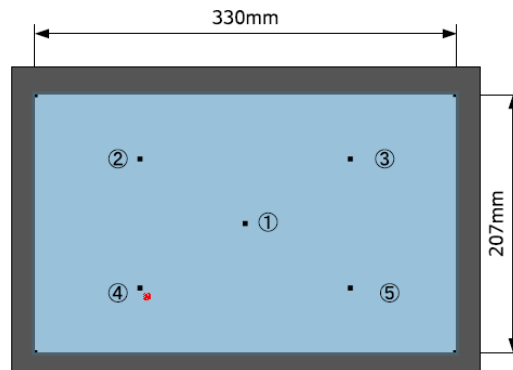


Fig. 8. Geometric relation among light source, camera and eyeball

It is considered as a camera position (0, 0, 0), and is considered as the main coordinates (0, 0z) of the picture picturized with the camera. If a line of sight vector is made into $v = (x_v; y_v; z_v)$, a camera, lighting, and a display assume that it is being fixed and the head is also being fixed, and are z. The distance of the direction of an axis is known. When distance of an eyeball and a display is set to z_h , point-of-regard coordinates $t =$ on a display $(x_t; y_t)$ is,

$$\begin{pmatrix} x_t \\ y_t \end{pmatrix} = \begin{pmatrix} x_v \times \frac{z_h}{z_v} \\ y_v \times \frac{z_h}{z_v} \end{pmatrix} \quad (2)$$

so that the gaze fixed point can be calculated as is shown in Fig.9.



(a) Calibration point locations on the computer screen for evaluation of gaze position estimation accuracy (red point shows the estimated gaze fixed point)



(b) The estimated cornea center and pupil center

Fig. 9. Method for gaze fixed position

During the process, ellipsoidal contour and feature points extraction can be done with the procedure as shown in Fig.10.

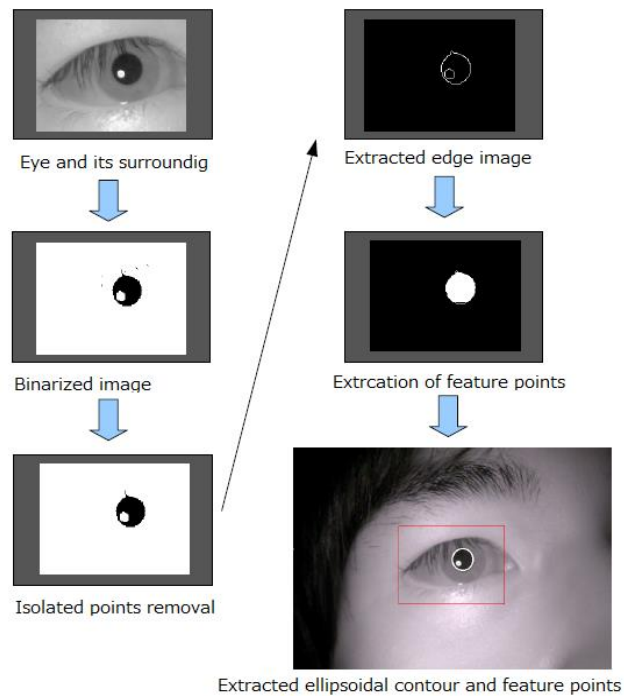


Fig. 10. Procedure for ellipsoidal contour and feature points extraction

III. EXPERIMENT FOR ERROR ANALYSIS

A. Configuration

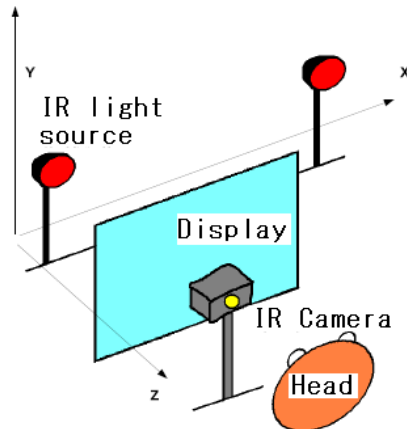
Experimental configuration is setup as shown in Fig.11 (a). Meanwhile, the top view of configuration is shown in Fig.11 (b). The measurement equipment used is as follows,

PC: Dell Computer Optiplex 755 Core 2 Quad 2.66 GHz CPU with 2 MB RAM of main memory

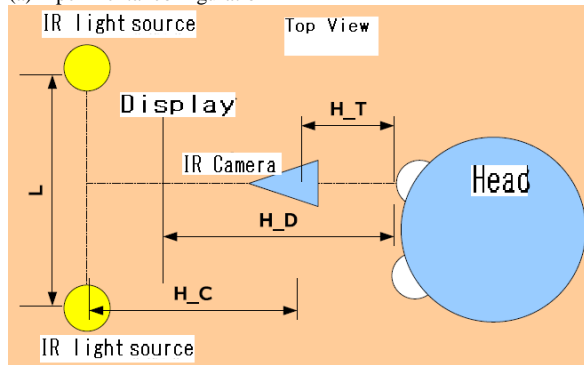
OS: WindowsXP home Service Pack2IR

Camera: (640 by 480 pixels) of DC-NCR 131 type manufactured by NetCowBoy and frame rate: 10 frames-per-second

Infrared floodlight: KMT-7787.



(a)Experimental configuration



(b)Top view of the configuration

Fig. 11. Experimental configuration for error analysis

The parameters of the experimental configuration are as follows,

$L = 1000 \text{ mm}$; $HC = 670 \text{ mm}$; $HT = 150 \text{ mm}$; $HD = 380\text{mm}$

Software development environment is as follows,

Microsoft Visual C++

Microsoft Visual studio.NET2

OpenCV 1.0

Moreover, the picture acquired from the camera on the occasion of look measurement was processed in real time, and performed accuracy verification.

B. Preliminary Experimental Results

The measurement result of a cornea curvature radius is shown in Fig.12. The spike in a Figure is based on incorrect detection of the Purkinje image, and these can be accepted from measurement of a cornea radius. Moreover, two lines in a Figure are the maximum errors of the cornea curvature-radius point estimate considered when movement of $\pm 1.0\text{cm}$ has a head in the display direction. The average of the cornea curvature-radius point estimate except an edge portion is used for the point estimate of the cornea curvature radius used for the actual degree estimation of eyeball rotation angle. The value of a cornea curvature radius was set to $R = 7.92 \text{ mm}$ from this result.

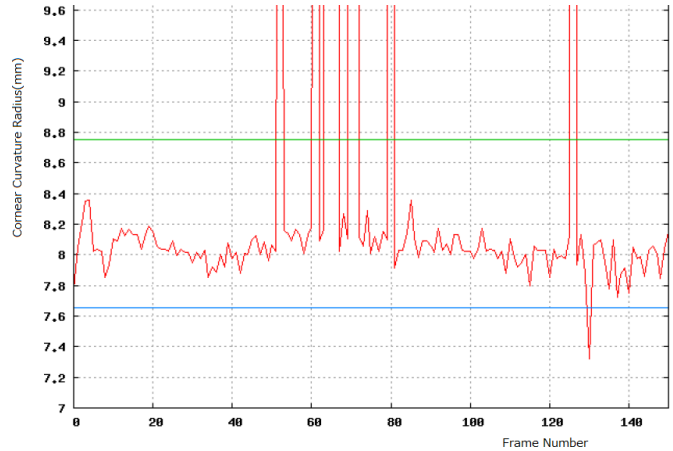


Fig. 12. Result from the preliminary experiment

C. Sensitivity and Stability

How to permit a motion of a head finally is shown. The both ends of eye and a mouth, the middle point between two ends of eye, and the middle point of the both ends of a mouth are detected from a face picture. Template matching is used for pursuit of details at these details extraction using OpenCV. By the middle point of both eyes, and the middle point of a mouth, three square shapes can be constituted and a plane can be defined. The normal direction of this plane is judged to be the posture of a head. Once extracting these details, by using template matching which can pursue most in a short time, it is devising so that the pursuit in real time may be possible. An example of details extraction and pursuit is shown in Fig.13. The distance between the details in a Figure is found and the degree of rotation angle of a head can be presumed in comparison with the position of the details extracted in early stages by OpenCV. The blue line segment of Fig.13 is a head posture (the plane normal direction is shown.). Moreover, a green line segment connects the middle point between the middle points of both eyes, and the middle point of the both ends of a mouth.

The geometric relation between the rotation center of a head and an eyeball rotation center is shown in Fig.14, and can presume an eyeball rotation center position after this. If the method of presuming a look from an eyeball rotation center position is considered to be the same thing as the above-mentioned method, a motion of a head will be permitted and the direction estimation of a look will be

attained. At this time, that the both ends of both eyes and the both ends of a mouth are not occluded are the conditions which presume a head rotation center and an eyeball rotation center, and 30 degrees and about 15 degrees are rotation allowable limits in the roll direction and the direction of a pitch.

As described before, movement in the direction of z is compared with movement to x and a y direction, and has serious influence on eyeball angle detection.

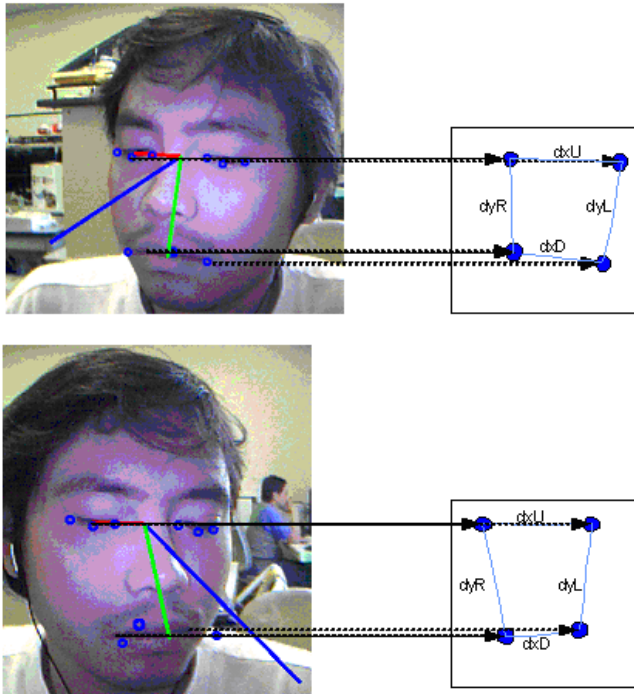


Fig. 13. Method for head pose angle estimation using the extracted feature points from the acquired face image

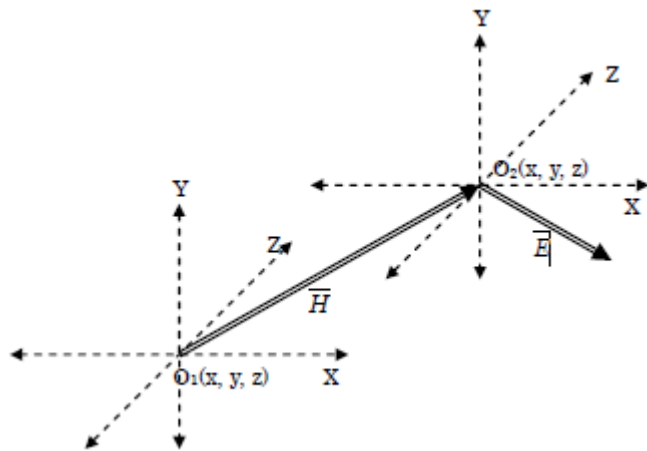


Fig. 14. Geometric relation between the rotation center of a head and an eyeball rotation center

Therefore, I need to get a user to maintain distance with a computer display to some extent (separating beyond the defined distance and twisting like). As also described before, to rotation of x of a head, the parallel translation of a y direction, a roll, a pitch, and the direction of Yaw, it is

detectable. As for parallel translation, it is highly accurate and can presume correctly about 100%. Therefore, the degree of setting head rotation angle and average estimation error by five subjects were checked by experiment here. An experimental result is shown in Fig.15. Since the Yaw rotation of a head is rotation in a head plane, a presumed error is comparatively small. The presumed error of the direction of a pitch was the largest, and it turned out that the presumed error of about 5 times is produced also in rotation of about 1.0 degrees in the pitch rotation to a direction which especially bows. Even if it is relatively stout and rotates about 30 degrees to the pitch rotation to a direction which raises the head, the presumed error is settled in about 1.7 degrees. Moreover, the presumed error over rotation of the head of the roll direction was located in that middle, and when it was ± 30 roll rotations, it has checked fitting in the presumed error of less than 1.7 degrees. Furthermore, one of eyes occlusion roll rotation exceeding 40 degrees, and a presumed error becomes large rapidly. Therefore, ± 30 - $10 \sim +30$ degrees, even if the head rotated ± 30 degrees in a roll, a pitch, and each direction of Yaw, it checked fitting in the presumed error of less than 1.7 degrees to them.

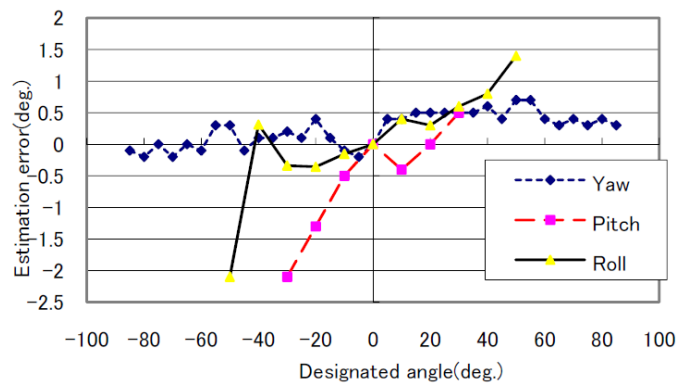


Fig. 15. Head angle estimation error

A cornea curvature radius is presumed using the Purkinje image of two points obtained by using the two-point light source proposed in this paper, the proposed method of eyeball rotation angle estimation which does not need the calibration for individual difference dissolution of cornea curvature are 0.57 degree and y to the direction of x in the state where the head was fixed in simple. It turned out that the degree of eyeball rotation angle can be presumed with the error of about 0.98 degree in a direction. Moreover, since the degree estimation method of head rotation angle using the details of the face proposed in this paper is the presumed error of about 1.7 degrees under restriction of the degree of rotation angle, it assumes that rotation of these heads and rotation of an eyeball are independent, and it is RSS: Root Sum Square is taken, it turns out that the eyeball angle estimation accuracy in the case of permitting rotation of a head is 1.988 degrees in a x direction at 1.821 degrees and a y direction.

If a look is presumed and rotation is permitted for a head in the above-mentioned restriction range from the face picture acquired from the camera which separated 150mm, the direction of a look can be presumed in the error of about 2 times. When an intersection with a look is put on the computer

display which left this 300mm, it is equivalent to about 10.472mm look and a display intersection position estimation error. When a with a pixel size (4 pixels / 10mm) computer display is assumed, this intersection position estimation error will be equivalent to about 4 pixels. Fig.16 sets up a target on 7 pixels from a center as an example of look stability, gets five subjects to gaze at the target concerned for 30 seconds, and shows what plotted the presumed intersection position. Therefore, by making distance between adjacent keys into 10 pixels or more showed that rotation of a head was permitted and the degree estimation method of eyeball rotation angle which does not need a calibration could be realized.

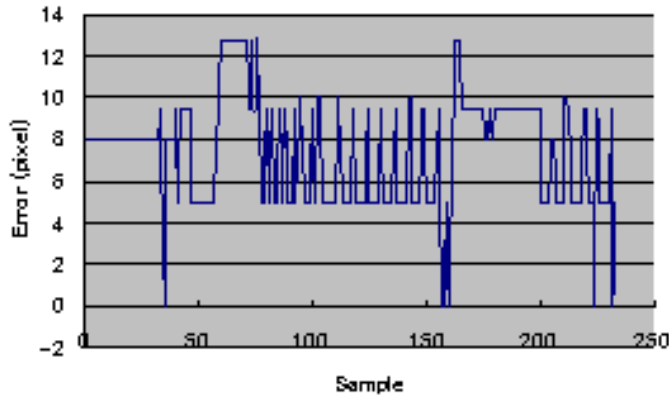


Fig. 16. Stability of the estimated location of fixed point

D. Error Analysis

In the experiment, eyeball angle estimation accuracy was checked by seeing five indices displayed on the display one by one, where a head is fixed simply. The presumed result of the eyeball angle detection from which a cornea curvature radius differs is shown in Fig.17. It is delta x and y when a cornea curvature radius is set to $R = 7.92 \text{ mm}$ at this time. $\Delta xy =$ it is 1.128. Near the measured cornea curvature radius has the highest degree detection accuracy of eyeball rotation angle. Therefore, it has checked that rather than led which uses the measured cornea curvature radius to improvement in the degree detection accuracy of eyeball rotation angle using the standard value of a cornea curvature radius.

Change of the look estimation result of survey by head parallel translation and rotation is shown in Fig.18. There are two sets of the error analysis results, delta x,y,z and mean of delta x,y,z. Fig.18 (a) and (b) show the two cases for cornea curvature radius estimation. On the other hand, the error analysis results for head angle estimation in directions of x,y,z are shown in Fig.18 (c), (d) and (e), respectively. Meanwhile, sensitivity analysis results for delta x,y,z and mean of delta x,y,z in directions of roll, pitch and yaw angles are shown in Fig.18 (f) to (i)

In measurement of a cornea curvature radius, it seems that the big accuracy fall has occurred when this is exceeded since it has measured in 3.0-5.0mm from the cornea center-of-curvature part. Moreover, in the influence on the presumed accuracy by the head rotation to the direction of a pitch, since the influence of eyelashes becomes large in downward rotation of a head, pupil detection becomes difficult (measurement is impossible), and since the influence of

upward rotation of a head of eyelashes decreases, its pupil detection accuracy improves. From this, the camera position at the time of measurement is understood that it is desirable to install by arrangement which looks up at a head.

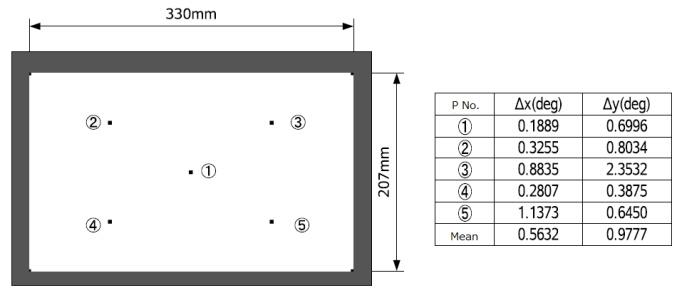
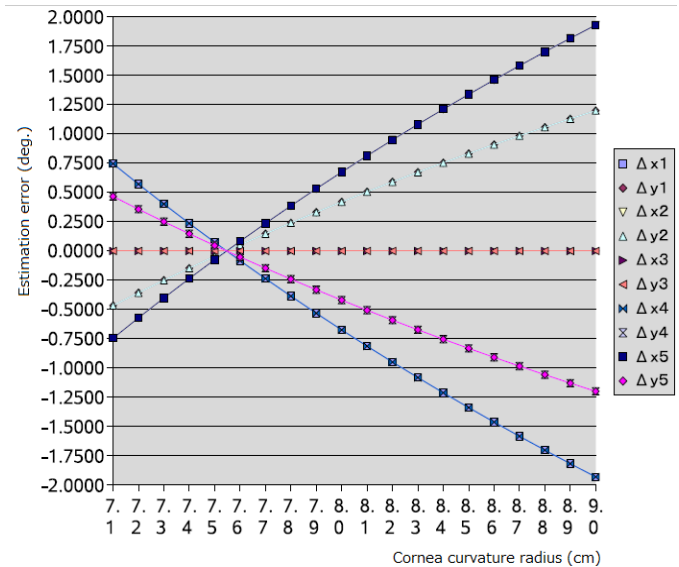
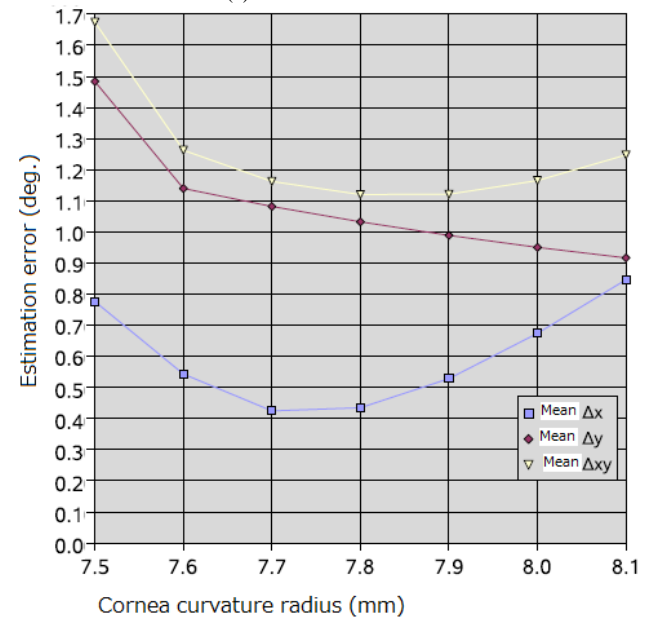


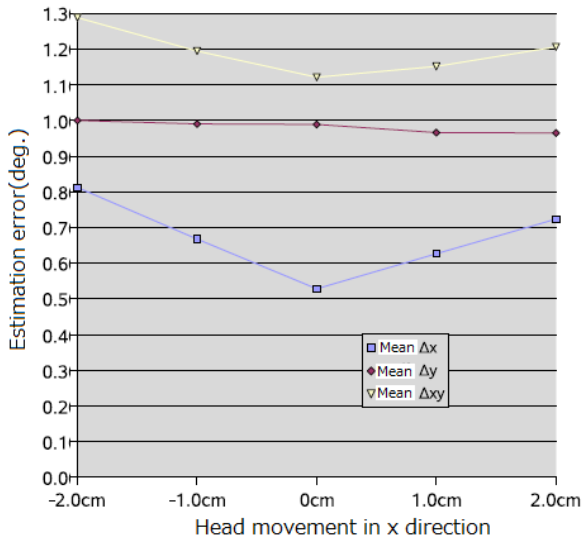
Fig. 17. presumed result of the eyeball angle detection from which a cornea curvature radius differs



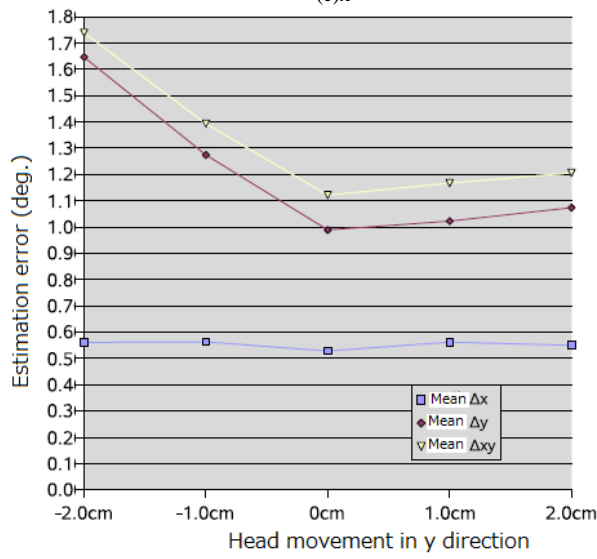
(a)Cornea curvature radius



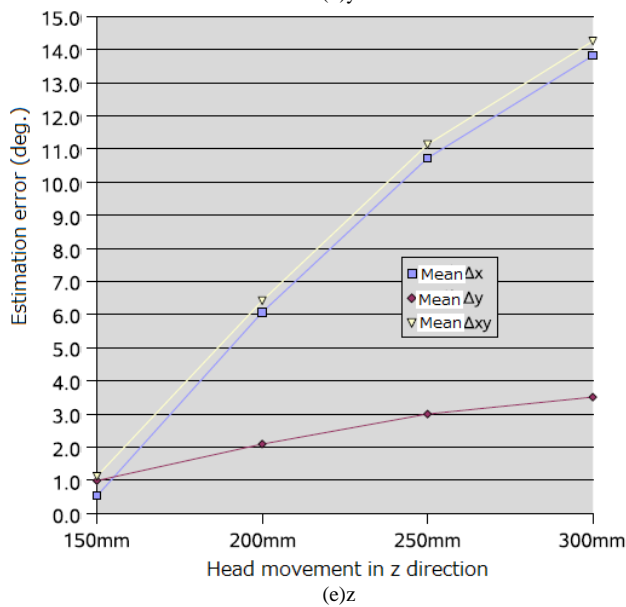
(b)Cornea curvature radius



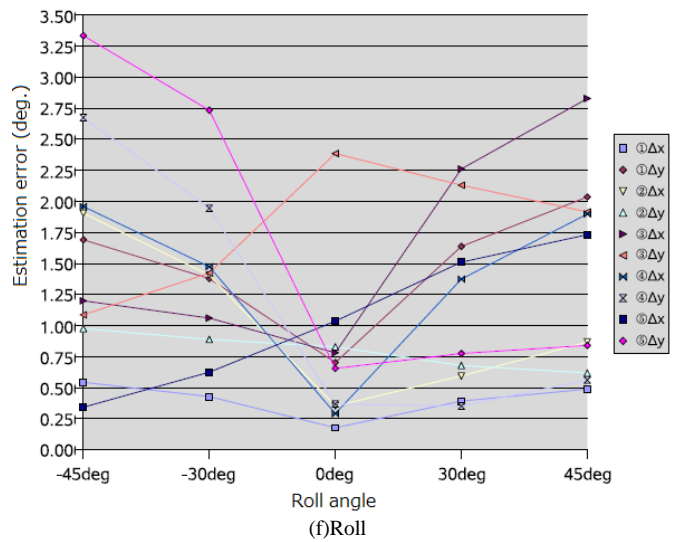
(c)x



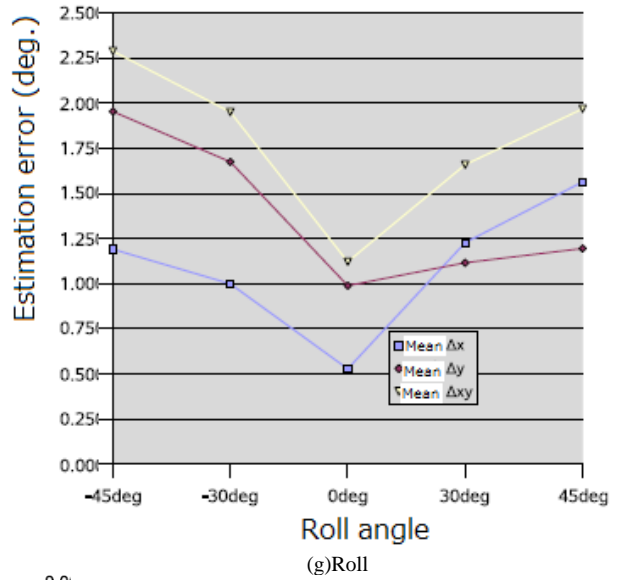
(d)y



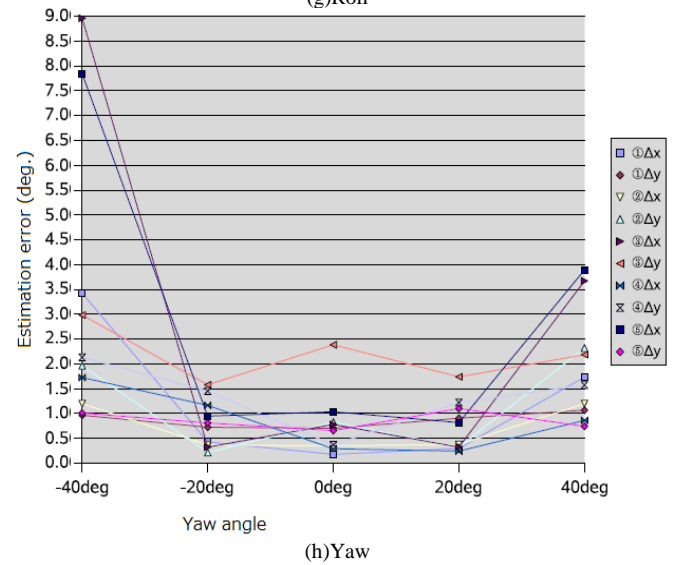
(e)z



(f)Roll



(g)Roll



(h)Yaw

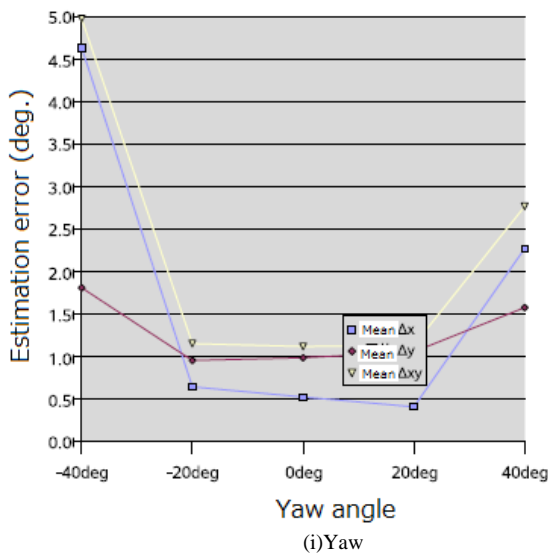


Fig. 18. Results from the Error Analysis

IV. CONCLUSION

Error analysis of line of sight estimation using Purkinje images for eye-based Human-Computer Interaction: HCI is conducted. Double Purkinje images which are obtained by two points of light sources are used in the proposed method for eye rotation angle estimation. It aimed at the improvement of the eyeball rotation angle accuracy by simply presuming the value of the curvature radius of the cornea. This technique is a cancellation of the time of the calibration that is the problem of past glance presumption. By presuming the size of the radius of curvature of the cornea. As a result, the eyeball rotation angle presumption accuracy of about 0.98deg was obtained 0.57deg and horizontally in the vertical direction without doing the calibration.

This paper proposed the estimation method of eyeball rotation angle which does not need the calibration for individual difference dissolution of cornea curvature by presuming a cornea curvature radius using the Purkinje image of two points obtained by using a two-point light source. As a result, in the state where the head was fixed in simple, they are 0.98deg(s) to 0.57deg(s) and the direction of y in the direction of x. The degree estimation accuracy of eyeball rotation angle was acquired with the error of a grade. Moreover, by the angle estimation method of the plane defined by the details of the face proposed since rotation of a head was permitted, when preparing restriction in each rotation of a roll, a pitch, and a yaw direction, it checked that the degree of rotation angle could be presumed with the error of about 0.5 degree. When it assumed that rotation of these heads and rotation of an eyeball were independent, it turned out that the eyeball angle estimation accuracy in the case of permitting rotation of a head is 1.988 degrees in a x direction at 1.821 degrees and a y direction. That is, since the degree of viewing angle beyond this error was detectable, when detaching and setting up the interval of a key rather than this, it turned out that it can guarantee that discernment of a key is possible.

ACKNOWLEDGEMENTS

Author would like to thank Mr. Makoto Yamaura of former student of Saga University for his efforts for conducting the experiments.

REFERENCES

- [1] K. Matsuda, T. Nagami and S. Yamane, Development of gaze measurement system, Technical Report of the Institute of Electronics, Information and Communication Engineers, TL2002-2, 2000.
- [2] T. Ohno, N. Takegawa, and A. Yoshikawa, Gaze estimation method based on eyeball shape model, Proc. of the 8th Image Sensing Symposium, pp.307-312, 2002.
- [3] Y. Ebisawa, 3D gaze measurement equipment, Japanese Patent No.2005-198743, 2005.
- [4] H. Tanaka, S. Hikita, K. Kasai, and A. Takeda, Gaze estimation method based on cornea curvature center estimation with two light sources, Journal of the Institute of Electronics, Information and Communication Engineers, 108, 479, MBE2008-128, 117-180, 2009.
- [5] Kohei Arai and Kenro Yajima, Communication Aid and Computer Input System with Human Eyes Only, Electronics and Communications in Japan, Volume 93, Number 12, 2010, pages 1-9, John Wiley and Sons, Inc., 2010.
- [6] Kohei Arai, Computer Input by Human Eyes Only and Its Applications, Intelligent Systems in Science and Information, 2014, Studies in Computer Intelligence, 591, 1-22, Springer Publishing Co. Ltd., 2015.
- [7] Kohei Arai, Makoto Yamaura, Blink detection accuracy improvement by means of morphologic filter in designated key selection and determination for computer input by human eyes only. Journal of Image Electronics Society of Japan, 37, 5, 601-609, 2008
- [8] Kohei Arai, Kenro Yajima, Communication aid system using computer input by human eyes only, Journal of Electric Society of Japan, Transaction C, 128-C,11,1679-1686, 2008
- [9] Kohei Arai, Kenro Yajima, Communication aid system using computer input by human eyes only, Journal of Electric Society of Japan, Transaction C, 128-C,11,1679-1686, 2008
- [10] Djoko Purwanto, Ronny Mardiyanto, Kohei Arai, Electric wheel chair control with gaze detection and eye blinking, Proceedings of the International Symposium on Artificial Life and Robotics, GS9-4, 2009
- [11] Djoko Purwanto, Ronny Mardiyanto and Kohei Arai, Electric wheel chair control with gaze detection and eye blinking, Artificial Life and Robotics, AROB Journal, 14, 694,397-400, 2009.
- [12] Kohei Arai, Ronny Mardiyanto, Computer input by human eyes only with blink detection using Gabor filter, Journal of Visualization Society of Japan, 29, Suppl.2, 87-90, 2009
- [13] Kohei Arai and Makoto Yamaura, Computer input with human eyes only using two Purkinje images which works in a real time basis without calibration, International Journal of Human Computer Interaction, 1, 3, 71-82, 2010
- [14] Kohei Arai, Ronny Mardiyanto, A prototype of electric wheel chair control by eye only for paralyzed user, Journal of Robotics and Mechatronics, 23, 1, 66-75, 2010.
- [15] Kohei Arai, Kenro Yajima, Robot arm utilized having meal support system based on computer input by human eyes only, International Journal of Human-Computer Interaction, 2, 1, 120-128, 2011
- [16] Kohei Arai, Ronny Mardiyanto, Autonomous control of eye based electric wheel chair with obstacle avoidance and shortest path finding based on Dijkstra algorithm, International Journal of Advanced Computer Science and Applications, 2, 12, 19-25, 2011.
- [17] Kohei Arai, Ronny Mardiyanto, Eye-based human-computer interaction allowing phoning, reading e-book/e-comic/e-learning, Internet browsing and TV information extraction, International Journal of Advanced Computer Science and Applications, 2, 12, 26-32, 2011
- [18] Kohei Arai, Ronny Mardiyanto, Eye based electric wheel chair control system-I(eye) can control EWC-, International Journal of Advanced Computer Science and Applications, 2, 12, 98-105, 2011.

- [19] Kohei Arai, Ronny Mardiyanto, Evaluation of users' impact for using the proposed eye based HCI with moving and fixed keyboard by using eeg signals, *International Journal of Research and Reviews on Computer Science*, 2, 6, 1228-1234, 2011.
- [20] Kohei Arai, Ronny Mardiyanto, Electric wheel chair controlled by human eyes only with obstacle avoidance, *International Journal of Research and Reviews on Computer Science*, 2, 6, 1235-1242, 2011.
- [21] K.Arai, R.Mardiyanto, Evaluation of users' impact for using the proposed eye based HCI with moving and fixed keyboard by using eeg signals, *International Journal of Research and review on Computer Science*, 2, 6, 1228-1234, 2012.
- [22] K.Arai, R.Mardiyanto, Electric wheel chair controlled by human eyes only with obstacle avoidance, *International Journal of Research and Review on Computer Science*, 2, 6, 1235-1242, 2012.
- [23] Kohei Arai, R.Mardiyanto, Robot arm control with human eyes only and its application to help having meal for patients, *Journal of Electrical Engineering Society of Japan*, Transaction C, C132, 3, 416-423, 2012.
- [24] Kohei Arai, Human-Computer Interaction with human eyes only and its applications, *Journal of Image Electronics Society of Japan*, 41, 3, 296-301, 2012.
- [25] R.Mardiyanto, K.Arai, Eye-based Human Computer Interaction (HCI) A new keyboard for improving accuracy and minimizing fatigue effect, *Scientific Journal Kursor*, (ISSN 0216-0544), 6, 3, 1-4, 2012.
- [26] K.Arai, R.Mardiyanto, Moving keyboard for eye-based Human Computer Interaction: HCI, *Journal of Image and Electronics Society of Japan*, 41, 4, 398-405, 2012.
- [27] Kohei Arai, R.Mardiyanto, Service robot which is controlled by human eyes only with voice communication capability, *Journal of Image Electronics Society of Japan*, 41, 5, 535-542, 2012.
- [28] Kohei Arai, Ronny Mardiyanto, Eye-based domestic robot allowing patient to be self-services and communications remotely, *International Journal of Advanced Research in Artificial Intelligence*, 2, 2, 29-33, 2013.
- [29] Kohei Arai, Ronny Mardiyanto, Method for psychological status estimation by gaze location monitoring using eye-based Human-Computer Interaction, *International Journal of Advanced Computer Science and Applications*, 4, 3, 199-206, 2013.
- [30] Kohei Arai, Kiyoshi Hasegawa, Method for psychological status monitoring with line of sight vector changes (Human eyes movements) detected with wearing glass, *International Journal of Advanced Research in Artificial Intelligence*, 2, 6, 65-70, 2013
- [31] Kohei Arai, Wearable computing system with input output devices based on eye-based Human Computer Interaction: HCI allowing location based web services, *International Journal of Advanced Research in Artificial Intelligence*, 2, 8, 34-39, 2013.
- [32] Kohei Arai Ronny Mardiyanto, Speed and vibration performance as well as obstacle avoidance performance of electric wheel chair controlled by human eyes only, *International Journal of Advanced Research in Artificial Intelligence*, 3, 1, 8-15, 2014.
- [33] Kohei Arai, Service robot with communicational aid together with routing controlled by human eyes, *Journal of Image Laboratory*, 25, 6, 24-29, 2014
- [34] Kohei Arai, Information collection service system by human eyes for disable persons, *Journal of Image Laboratory*, 25, 11, 1-7, 2014
- [35] Kohei Arai, Relations between psychological status and eye movements, *International Journal of Advanced Research on Artificial Intelligence*, 4, 6, 16-22, 2015.

AUTHORS PROFILE

Kohei Arai, He received BS, MS and PhD degrees in 1972, 1974 and 1982, respectively. He was with The Institute for Industrial Science and Technology of the University of Tokyo from April 1974 to December 1978 and also was with National Space Development Agency of Japan from January, 1979 to March, 1990. During from 1985 to 1987, he was with Canada Centre for Remote Sensing as a Post Doctoral Fellow of National Science and Engineering Research Council of Canada. He moved to Saga University as a Professor in Department of Information Science on April 1990. He was a councilor for the Aeronautics and Space related to the Technology Committee of the Ministry of Science and Technology during from 1998 to 2000. He was a councilor of Saga University for 2002 and 2003. He also was an executive councilor for the Remote Sensing Society of Japan for 2003 to 2005. He is an Adjunct Professor of University of Arizona, USA since 1998. He also is Vice Chairman of the Commission-A of ICSU/COSPAR since 2008. He received Science and Engineering Award of the year 2014 from the minister of the ministry of Science Education of Japan and also received the Bset Paper Award of the year 2012 of IJACSA from Science and Information Organization: SAI. In 2016, he also received Vikram Sarabhai Medal of ICSU/COSPAR and also received 20 awards. He wrote 34 books and published 520 journal papers. He is Editor-in-Chief of *International Journal of Advanced Computer Science and Applications* as well as *International Journal of Intelligent Systems and Applications*. <http://teagis.ip.is.saga-u.ac.jp/>

Method for Vigor Diagnosis of Tea Trees based on Nitrogen Content in Tealeaves Relating to NDVI

Kohei Arai ¹

¹ Graduate School of Science and Engineering
Saga University
Saga City, Japan

Abstract—Method for vigor diagnosis of tea trees based on nitrogen content in tealeaves relating to NDVI is proposed. In the proposed method, NIR camera images of tealeaves are used for estimation of nitrogen content in tealeaves. The nitrogen content is highly correlated to Theanine (amid acid) content in tealeaves. Theanine rich tealeaves taste good. Therefore, tealeaves quality can be estimated with NIR camera images. Also, leaf area of tealeaves is highly correlated to NIR reflectance of tealeaf surface. Therefore, not only tealeaf quality but also harvest amount can be estimated with NIR camera images. Experimental results shows the proposed method does work for estimation of appropriate tealeaves harvest timing with NIR camera images.

Keywords—Tealeaves; Nitrogen content; Amino acid; Leaf area; NDVI

I. INTRODUCTION

It is highly desired to monitor vitality of crops in agricultural areas automatically with appropriate measuring instruments in order to manage agricultural area in an efficient manner. It is also required to monitor not only quality but also quantity of vegetation in the farmlands. Vegetation monitoring is attempted with red and photographic cameras [1]. Grow rate monitoring is also attempted with spectral observation [2].

This paper deals with automatic monitoring of a quality of tealeaves with earth observation satellite, network cameras together with a method that allows estimation of total nitrogen and fiber contents in tealeaves as an example. Also this paper describes a method and system for estimation of quantity of crop products by using not only Vegetation Cover: VC and Normalized Difference Vegetation Index: NDVI but also Bi-directional Reflectance Distribution Function: BRDF because the VC and NDVI represent vegetated area while BRDF represents vegetation mass, or layered leaves.

Total nitrogen content corresponds to amid acid which is highly correlated to Theanine: 2-Amino-4-(ethylcarbamoyl) butyric acid for tealeaves so that total nitrogen is highly correlated to tea taste. Meanwhile fiber content in tealeaves has a negative correlation to tea taste. Near Infrared: NIR camera data shows a good correlation to total nitrogen and fiber contents in tealeaves so that tealeaves quality can be monitored with network NIR cameras. It is also possible to estimate total nitrogen and fiber contents in leaves with remote sensing satellite data, in particular, Visible and near infrared: VNIR radiometer data. Moreover, VC, NDVI, BRDF

of tealeaves have a good correlation to grow index of tealeaves so that it is possible to monitor expected harvest amount and quality of tealeaves with network cameras together with remote sensing satellite data. BRDF monitoring is well known as a method for vegetation growth [3],[4]. On the other hand, degree of polarization of vegetation is attempted to use for vegetation monitoring [5], in particular, Leaf Area Index: LAI together with new tealeaves growth monitoring with BRDF measurements [6].

It is obvious that nitrogen rich tealeaves tastes good while fiber rich tealeaves tastes bad. Theanine: 2-Amino-4-(ethylcarbamoyl) butyric acid that is highly correlated to nitrogen contents in new tealeaves are changed to catechin [7],[8],[9] due to sun light. In accordance with sunlight, new tealeaves grow up so that there is a most appropriate time for harvest in order to maximize amount and taste of new tealeaves simultaneously.

Optical properties of tealeaves and methods for estimation of tealeaves quality and harvest amount estimation accuracy are well reported [10]-[17].The method proposed here is to determine tealeaves harvest timing by using NIR camera images together with meteorological data. By using these relations between NDVI and nitrogen content in tealeaves as well as Theanine, it is possible to estimate vigor of tea trees. During the winter time, tea trees used to maintain their vigor. A good quality of remote sensing satellite data can be acquired during the winter season even if the revisit cycle is poor. Using such a good quality data derived from visible to near infrared radiometers onboard remote sensing satellites, it is capable to estimate vigor of tea trees.

The following section describes the proposed method together with some research background. Then experimental results are described followed by discussions. Finally, conclusions are described together with future research works.

II. PROPOSED METHOD AND SYSTEM

A. Proposed System

Fig.1 shows the proposed tea farm observation system for evaluation of tealeaf quality and harvest amount as well as vigor diagnosis. It is multi-layered observation system from space (remote sensing satellite), from the lower boundary layer (UAV, or drones), and ground based observation system (Near Infrared: NIR cameras).

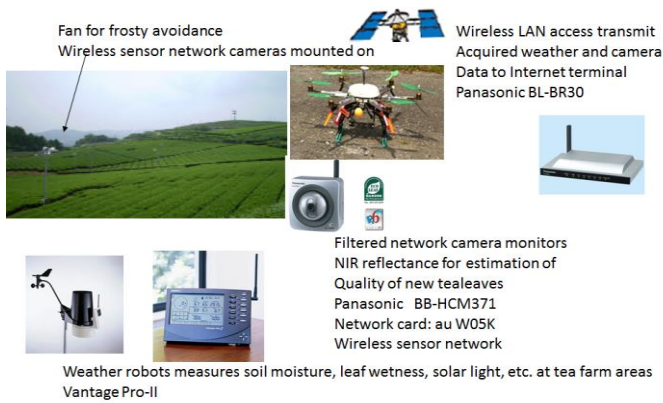


Fig. 1. Proposed tea farm observation system for evaluation of tealeaf quality and harvest amount as well as vigor diagnosis

B. Research Background

Due to the fact that revisit cycle of remote sensing satellites which carry visible to near infrared radiometer is too long, remote sensing satellite data cannot be used for monitoring the new tealeaf growing stage. Fig.2 shows annual cycle of tealeaf production. New tealeaves are borne in the begging of April. Then it is harvest timing in the begging of May. Therefore, the new tealeaves are used to be grown up within a month or so. Usually, revisit cycle of remote sensing satellites is more than 15 days. Therefore there are two chances to observe tea farm areas during the new tealeaves growing stage. It, however, cannot observe when it is cloudy, rainy with visible to near infrared radiometer onboard satellites. Therefore, it cannot be used for vigor diagnosis with remote sensing satellite data.

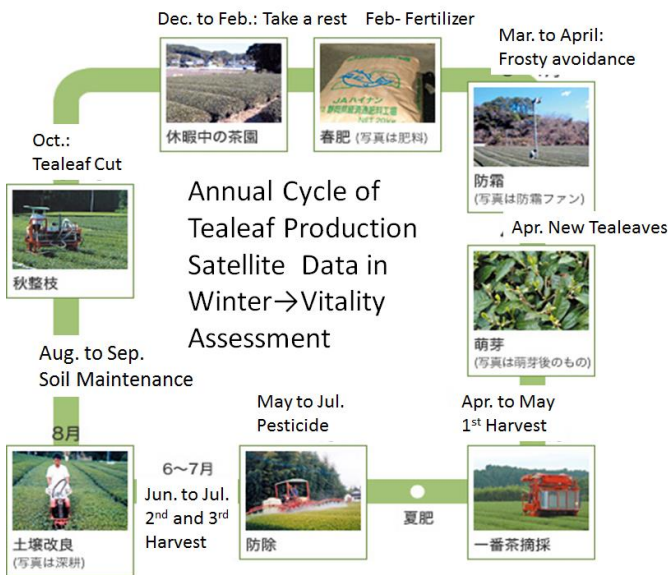


Fig. 2. Annual cycle of tealeaf production

Fig.3 shows annual cycle of nitrogen content in tealeaves. After the first harvest in the begging of May, pesticide and

fertilizer are put in tea farm areas during May to June. Then secondly grown tealeaves can be harvested in June. Then, the thirdly grown tealeaves can also be harvested in July. These three harvest timings are indicated in the Fig.3. Therefore, it is easily understand that the nitrogen content in tealeaves is repeated up and down annually.

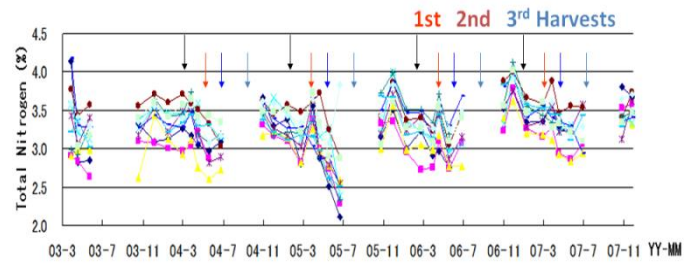
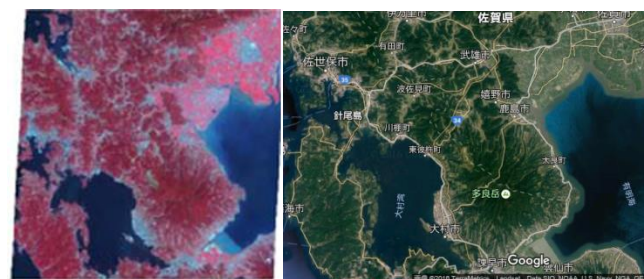


Fig. 3. Annual cycle of nitrogen content in tealeaves

During two months, August and September, soil maintenance has to be done for the future in order to maintain tea trees vitality. More than half of matured tealeaves are cut off in October (it is preparation for winter). Then tea trees take a rest during November to February in the next year. Fertilizer is put into tea farm areas in February. After that, fan is activated during March to April for forestry avoidance (tea trees are very week against forestry). Then new tealeaves are borne again in the latter in March or in the begging of April.

C. Remote Sensing Satellite Data

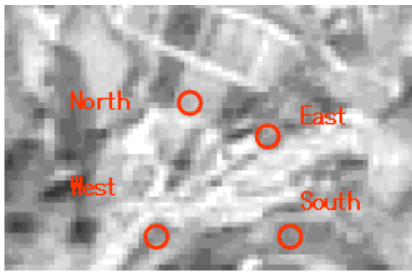
One of examples of visible to near infrared radiometer (ASTER/VNIR) imagery data (Instantaneous Field of View: IFOV is 15m) of remote sensing satellite (Terra) of Saga Prefectural Tea Research Institute (SPTRI): 33:07:3.9 (North), 129:59:47.0 (East), 95m (Elevation) which is acquired on February 2007 is shown in Fig.4 (a) on the right while the google map image is shown in Fig.4 (a) on the left. Also, pan-sharpened image with ALOS/PRISM is shown in Fig.4 (b) while Normalized Difference Vegetation Index: NDVI image of the pan-sharpened image is shown in Fig.4 (c).



(a)Scene of ASTER/VNIR image onboard Terra satellite



(b)Enlarged portion of pan-sharpened image



(c)NDVI of the four test sites in SPTRI

Fig. 4. Example of ALOS/AVNIR-2 image and Terra/ASTER/VNIR data of Saga Prefectural Tea Research Institute: SPTRI in Ureshino-city, Saga, Japan which are acquired on February 2007

Pan-sharpened image is derived from the following procedure,

- 1) ASTER/VNIR imagery data with three bands (Green, Red and Near infrared) is assumed to be color data (RGB).
- 2) RGB data is converted to Hue, Saturation and Intensity (HSI).
- 3) The Intensity image is replaced to pan-chromatic ALOS/PRISM imagery data with 2.5m of IFOV.
- 4) Then HSI is converted to RGB reversely.

Thus a high spatial resolution of ASTER/VNIR imagery data can be derived. Using the pan-sharpened imagery data, NDVI imagery data is generated by the following equation,

$$NDVI = \frac{NIR - VIS}{NIR + VIS} \quad (1)$$

As shown in Fig.4 (c), bright portion indicates vital vegetated areas while dark portion indicates poorly vegetated areas. It is well known that there is a strong relation between NDVI and nitrogen content in tealeaves (Total Nitrogen: TN) which are closely related to amino-acid, Theanine. Theanine rich tealeaves taste good. Therefore, tealeaf quality can be estimated with NDVI derived from ASTER/VNIR onboard Terra satellite of imagery data. Revisit cycle of Terra satellite is, however, so long, 16 days. Therefore, another monitoring system has to be prepared for growing up period. One of the solutions is ground based camera monitoring system. A single band of camera is much easier than two bands of camera, visible and near infrared to manufacture. Therefore, the relation between TN and reflectance of tealeaves at near infrared wavelength is investigated together with fiber content in tealeaves. Fiber content indicates tealeaf age. Namely, young tealeaves do not have much fiber (F-NIR: Fiber content measured with NIR radiometry while elder tealeaves are fiber rich. A good quality of tealeaves can be defined as good taste and young tealeaves resulting in TN rich and poor fiber.

D. Ground Based Camera Data

These can be measured with NIR camera. Using YubaFlex camera, the relation between NIR reflectance and TN as well as F-NIR is investigated. Essentially, YubaFlex is designed for NDVI camera. Therefore, visible to near infrared wavelength regions are covered with YubaFlex. The major specifications are as follows,

Cannon Power Shot S100: 1330pixels, 173g

Spectral response for Blue → Near Infrared

Spectral response of YubaFlex is shown in Fig.5. As shown in Fig.5, originally assigned spectral response of blue band is replaced to near infrared (Center wavelength of 870 nm). It is useful for NDVI data collections. It, however, does cost. Therefore, another NIR filter film attached camera is prepared for TN and F-NIR measurements.

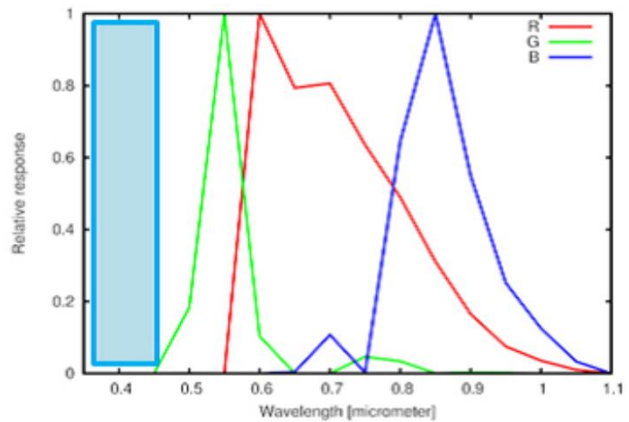


Fig. 5. Spectral of YubaFlex (NIR camera)

Reflectance measurements can be done with standard plaques such as Spectralon manufactured by LabSphere Co. Ltd. in USA. The Spectralon is not so cheap while photo print paper is very cheap. Therefore, photo print paper is used as a standard plaque. In order to compensate the difference between the Spectralon and the photo print paper used, the difference between reflectance of the Spectralon and the photo print paper used is measured. Fig.6 shows outlook of the Spectralon and a small portion of the photo print paper used while Fig.7 shows the difference between both reflectance of the Spectralon and the photo print paper used.



Fig. 6. Outlook of the Spectralon (left) and the photo print paper used (right)

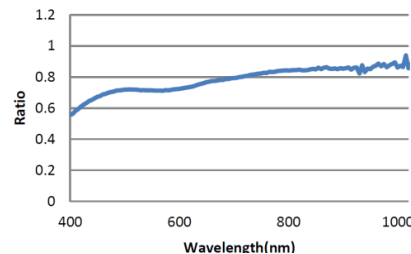


Fig. 7. Ratio of the Spectralon based NIR reflectance and the print sheet based NIR reflectance

E. Relation between Sensing Satellite Data and Tealeaf Quality

The relation between NIR reflectance of tealeaves measured at SPTRI on January 15 2008 and TN as well as F-NIR is shown in Fig.8. There are four test sites in the SPTRI, East (Yabukita), South (Oiwase), West (Benifuki), North (Okumidori), N (Yabukita-U), N (Yabukita-D). The names in the bracket denote the names of species while dash U and D denotes upper tea field and down tea field, respectively. Spectral reflectance of the typical tea farm areas in the SPTRI is shown in Fig.9.

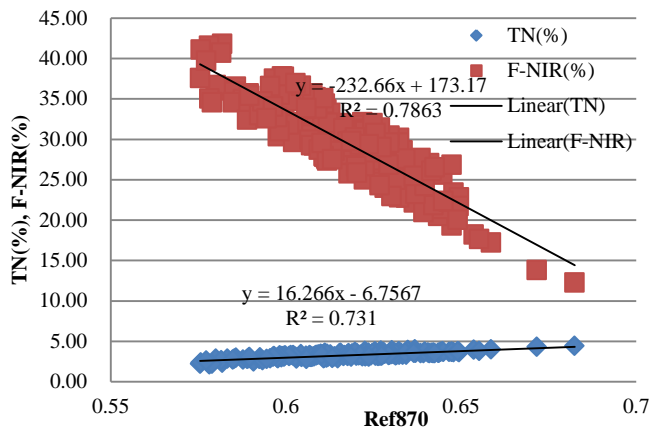


Fig. 8. Relation between NIR reflectance of tealeaves and TN as well as F-NIR

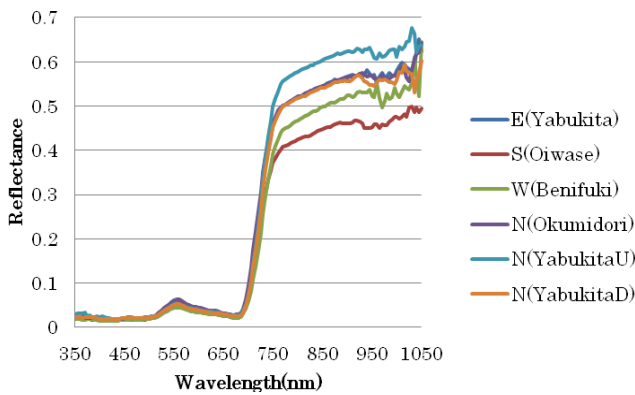


Fig. 9. Spectral reflectance of the typical tea farm areas in the SPTRI

The estimated TN and F-NIR as well as NDVI images can be superimposed on the corresponding geographical maps using Geographic Information System: GIS such as Fig.10. Thus the tea farmers can take a look at the tealeaf quality by field by field and then make fertilizer and pesticide plans as well as harvesting plan (find the best tealeaf quality) with the best weather condition appropriately.

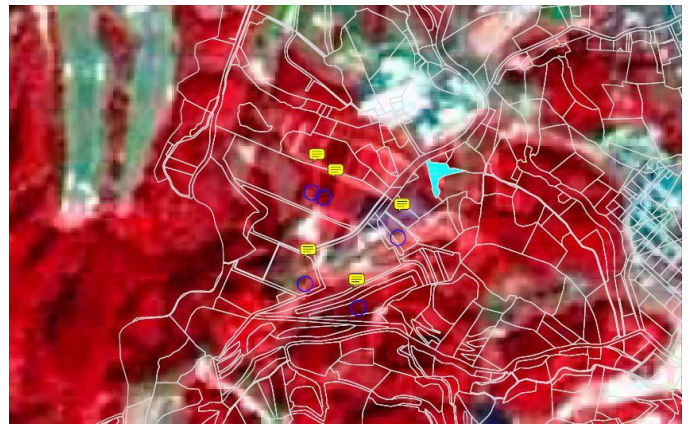
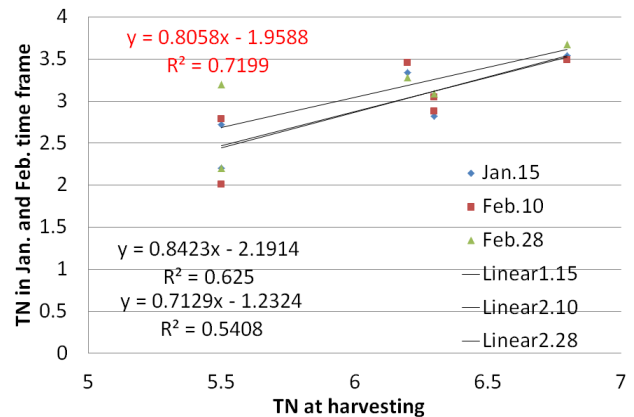


Fig. 10. GIS representation of pan-sharpened image on geographic map (also it is possible to superimpose NDVI, TN, F-NIR images on the same geographic maps)

F. Vigor Diagnosis with remote Sensing Satellite Data

As mentioned before, tea trees' vigor diagnosis can be done with visible to near infrared radiometer onboard remote sensing satellites. In order for that, a good quality of VNIR image has to be acquired in winter, during October and March next year. The vigor of tea trees is defined as TN content in tealeaves. Therefore, a relation between TN measured in winter and TN at harvest timing has to be investigated. Fig.11 shows the relation estimated with ASTER/VNIR imagery data as well as ground based camera data measured at SPTRI in 2009. R square values range from 0.541 to 0.720 depending on the data acquisition date. It is found that just before new tealeaves are borne (February 28 in this case) is the most appropriate timing for satellite data acquisition in order for tea tree vigor diagnosis.



Satellite data acquired in winter is useful for evaluation of Tea tree vitality which proportional to quality of new tealeaves

Fig. 11. Relation between TN measured in winter by using visible to near infrared reflectance derived from remote sensing satellite data and TN at harvest timing

Not only, can quality of tealeaves but also harvest amount be estimated with the remote sensing satellite data. Fig.12 shows the relation between TN and TN multiplied by weight of the harvested amount of tealeaves in unit of kg/a.

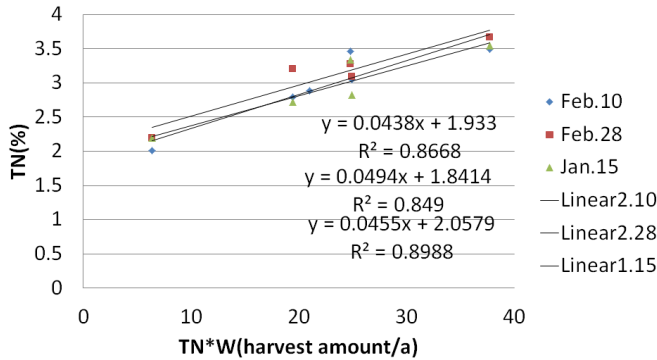


Fig. 12. Relation between TN and TN multiplied by weight of the harvested amount of tealeaves in unit of kg/a

III. EXPERIMENTS FOR VIGOR DIAGNOSIS

A. NDVI Derived from Remote Sensing Data

Remote sensing data acquisition is key issue for vigor diagnosis of tea trees. In order to check the availability of ASTER/VNIR data with less than 10% of cloud coverage of search condition, the following available data are retrieved,

- 2007: 7/2, 8/18, 10/23, 11/26, 12/24
- 2008: 1/4, 1/15, 2/10, 2/27, 2/28, 3/29, 4/14, 5/2, 5/16, 6/1,7/1, 7/2, 8/4, 8/20, 9/5, 10/8, 11/7, 12/10
- 2009: 1/11, 2/12, 2/28, 3/16, 4/17, 6/20, 7/6, 8/7, 8/23, 9/24, 10/10,10/14, 11/27, 12/29
- 2010: 1/30, 2/17, 3/3, 3/19, 4/4

On the other hand, ASTER/VNIR data acquired on the following dates are selected for vigor diagnosis

2010/3/19, 2011/12/19, 2012/11/3, 2013/12/8, 2014/10/24

One of the examples of NDVI image of Kyushu in Japan derived from the ASTER/VNIR data acquired on 2014/10/24 is shown in Fig.12.

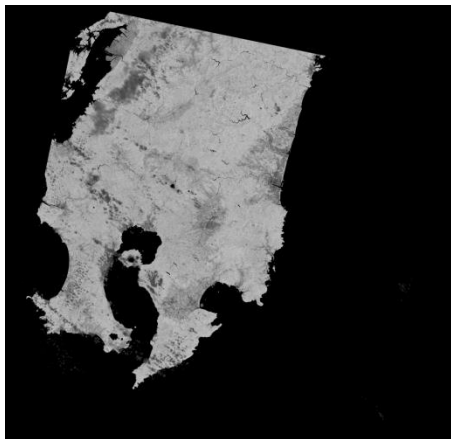


Fig. 13. One of the examples of NDVI image of Kyushu in Japan derived from the ASTER/VNIR data acquired on 2014/10/24

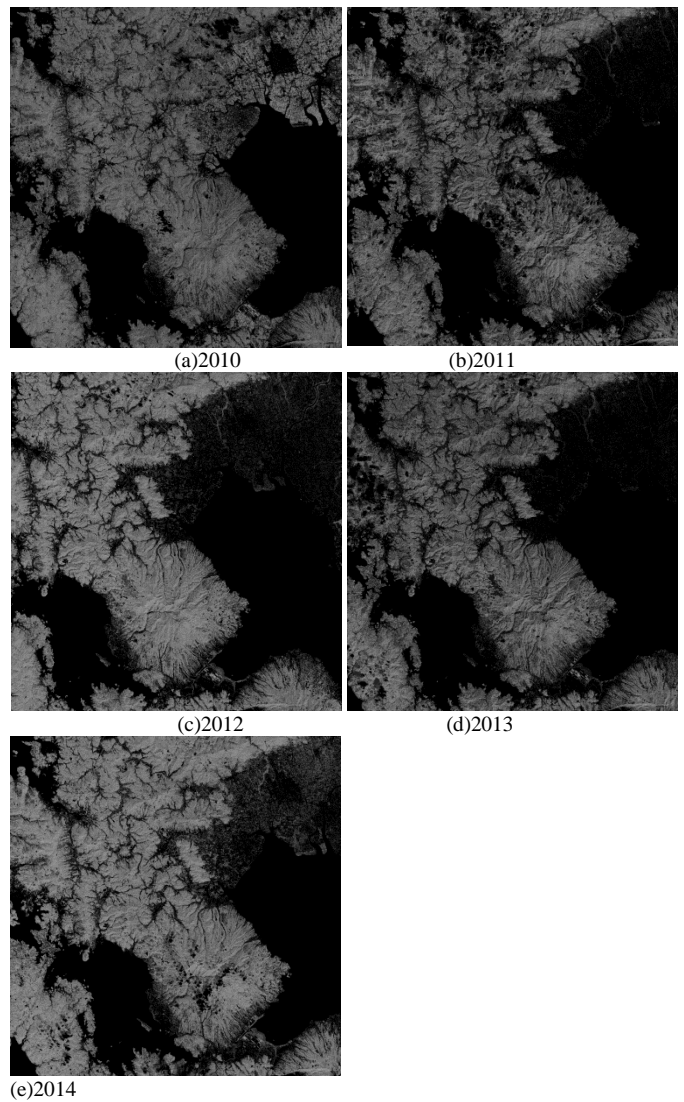


Fig. 14. NDVI images acquired in 2010 to 2014 for tea tree vigor diagnosis

From these NDVI, tea tree vigor diagnosis can be done based on the previously reduced regressive equations,

$$TN = 16.47 - 6.8672 \quad (2)$$

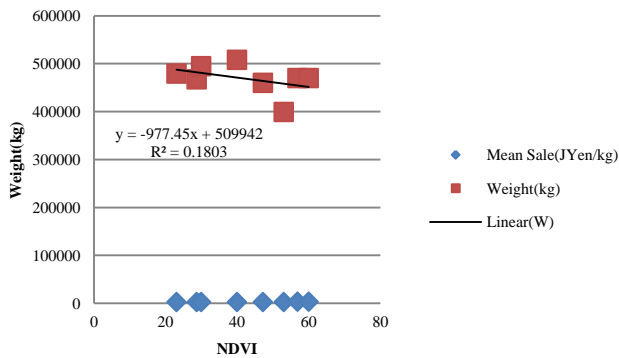
$$F-NIR = -236.18 + 175.58 \quad (3)$$

for TN and fiber content in tealeaves. Table 1 shows the averaged NDVI derived from ASTER/VNIR data and weight (tea product amount for the first harvest tealeaves), income of the tea product (sale), and averaged income per weight (mean sale) each year. The averaged income per weight indicates quality of tealeaves. Because the price of tea product depends on tealeaf quality, the averaged income per weight represents tealeaf quality. Therefore, if NDVI has a high correlation to the averaged income per weight, then it may be concluded that tealeaf quality at the harvest timing and tea tree vigor can be estimated remote sensing satellite data.

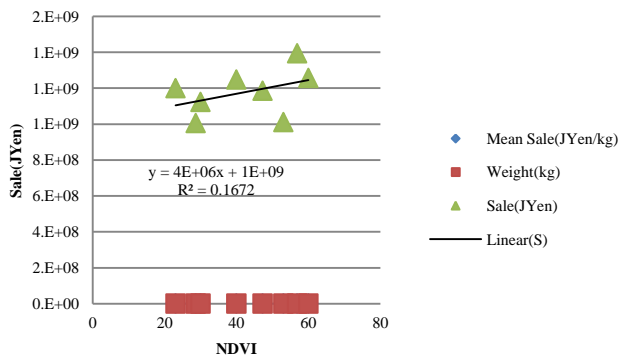
TABLE I. AVERAGED NDVI DERIVED FROM ASTER/VNIR DATA AND WEIGHT (TEA PRODUCT AMOUNT FOR THE FIRST HARVEST TEALEAVES), INCOME OF THE TEA PRODUCT, AND AVERAGED INCOME PER WEIGHT EACH YEAR

Year	Mean Sale(JYen/kg)	Weight(kg)	Sale(JYen)	NDVI
2016	2434	436815	1063099512	
2015	2533	398899	1010606868	53.042
2014	2150	467239	1004526406	28.692
2013	2577	459787	1185080949	47.276
2012	2503	479307	1199574944	23.066
2011	2572	471395	1212486871	
2010	2965	470176	1394118944	56.901
2009	2268	494784	1122402340	30
2008	2457	508127	1248218686	40
2007	2674	469883	1256342058	60

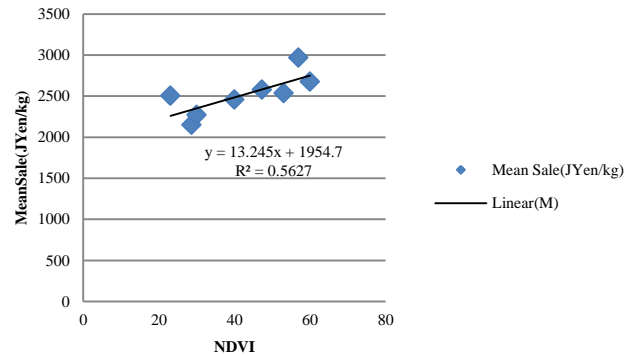
Although NDVI is neither related to the weight of sold amount of tea products, nor the total income per weight of sold amount of tea products, NDVI is related to the averaged income of sold tea products (tealeaf quality) with 0.5627 of R square value (determination coefficient) as shown in Fig.14 (a), (b) and (c).



(a)Weight of sold tea product



(b)Total income of sold tea products



(c)Averaged income of sold tea products

Fig. 15. Relation between NDVI and the averaged income of sold tea products, total income of sold tea products as well as total weight of sold tea products of the first harvested tealeaves

IV. CONCLUSION

Method for vigor diagnosis of tea trees based on nitrogen content in tealeaves relating to NDVI is proposed. In the proposed method, NIR camera images of tealeaves are used for estimation of nitrogen content in tealeaves. The nitrogen content is highly correlated to Theanine (amid acid) content in tealeaves. Theanine rich tealeaves taste good. Therefore, tealeaves quality can be estimated with NIR camera images. Also, leaf area of tealeaves is highly correlated to NIR reflectance of tealeaf surface. Therefore, not only tealeaf quality but also harvest mount can be estimated with NIR camera images.

Experimental results shows the proposed method does work for estimation of appropriate tealeaves harvest timing with NIR camera images. It is found that NDVI is neither related to the weight of sold amount of tea products, nor the total income per weight of sold amount of tea products. It is also found that NDVI is related to the averaged income of sold tea products (tealeaf quality) with 0.5627 of R square value (determination coefficient).

ACKNOWLEDGEMENTS

Author would like to thank Dr. Hideo Miyazaki of Saga Prefecture Tea Research Institute for his efforts for conducting the experiments.

REFERENCES

- [1] J.T.Compton, Red and photographic infrared linear combinations for monitoring vegetation, Journal of Remote Sensing of Environment, 8, 127-150, 1979.
- [2] C.Wiegand, M.Shibayama, and Y.Yamagata, Spectral observation for estimating the growth and yield of rice, Journal of Crop Science, 58, 4, 673-683, 1989.

- [3] S.Tsuchida, I.Sato, and S.Okada, BRDF measurement system for spatially unstable land surface-The measurement using spectroradiometer and digital camera- Journal of Remote Sensing, 19, 4, 49-59, 1999.
- [4] K.Arai, Lecture Note on Remote Sensing, Morikita-shuppan Co., Ltd., 2000.
- [5] K.Arai and Y.Nishimura, Degree of polarization model for leaves and discrimination between pea and rice types of leaves for estimation of leaf area index, Abstract, COSPAR 2008, A3.10010-08#991, 2008.
- [6] K.Arai and Long Lili, BRDF model for new tealeaves and new tealeaves monitoring through BRDF monitoring with web cameras, Abstract, COSPAR 2008, A3.10008-08#992, 2008.
- [7] Greivenkamp, John E., Field Guide to Geometrical Optics. SPIE Field Guides vol. FG01. SPIE. ISBN 0-8194-5294-7, 2004.
- [8] Seto R H. Nakamura, F. Nanjo, Y. Hara, Bioscience, Biotechnology, and Biochemistry, Vol.61 issue9 1434-1439 1997.
- [9] Sano M, Suzuki M ,Miyase T, Yoshino K, Maeda-Yamamoto, M.,J.Agric.Food Chem., 47 (5), 1906-1910 1999.
- [10] Kohei Arai, Method for estimation of grow index of tealeaves based on Bi-Directional reflectance function: BRDF measurements with ground based network cameras, International Journal of Applied Science, 2, 2, 52-62, 2011.
- [11] Kohei Arai, Wireless sensor network for tea estate monitoring in complementally usage with Earth observation satellite imagery data based on Geographic Information System(GIS), International Journal of Ubiquitous Computing, 1, 2, 12-21, 2011.
- [12] Kohei Arai, Method for estimation of total nitrogen and fiber contents in tealeaves with ground based network cameras, International Journal of Applied Science, 2, 2, 21-30, 2011.
- [13] Kohei Arai, Monte Carlo ray tracing simulation for bi-directional reflectance distribution function and grow index of tealeaves estimation, International Journal of Research and Reviews on Computer Science, 2, 6, 1313-1318, 2011.
- [14] K.Arai, Monte Carlo ray tracing simulation for bi-directional reflectance distribution function and grow index of tealeaves estimations, International Journal of Research and Review on Computer Science, 2, 6, 1313-1318, 2012.
- [15] K.Arai, Fractal model based tea tree and tealeaves model for estimation of well opened tealeaf ratio which is useful to determine tealeaf harvesting timing, International Journal of Research and Review on Computer Science, 3, 3, 1628-1632, 2012.
- [16] Kohei Arai, Method for tealeaves quality estimation through measurements of degree of polarization, leaf area index, photosynthesis available radiance and normalized difference vegetation index for characterization of tealeaves, International Journal of Advanced Research in Artificial Intelligence, 2, 11, 17-24, 2013.
- [17] K.Arai, Optimum band and band combination for retrieving total nitrogen, water, and fiber in tealeaves through remote sensing based on regressive analysis, International Journal of Advanced Research in Artificial Intelligence, 3, 3, 20-24, 2014.

AUTHORS PROFILE

Kohei Arai, He received BS, MS and PhD degrees in 1972, 1974 and 1982, respectively. He was with The Institute for Industrial Science and Technology of the University of Tokyo from April 1974 to December 1978 and also was with National Space Development Agency of Japan from January, 1979 to March, 1990. During from 1985 to 1987, he was with Canada Centre for Remote Sensing as a Post Doctoral Fellow of National Science and Engineering Research Council of Canada. He moved to Saga University as a Professor in Department of Information Science on April 1990. He was a councilor for the Aeronautics and Space related to the Technology Committee of the Ministry of Science and Technology during from 1998 to 2000. He was a councilor of Saga University for 2002 and 2003. He also was an executive councilor for the Remote Sensing Society of Japan for 2003 to 2005. He is an Adjunct Professor of University of Arizona, USA since 1998. He also is Vice Chairman of the Commission-A of ICSU/COSPAR since 2008. He received Science and Engineering Award of the year 2014 from the minister of the ministry of Science Education of Japan and also received the Bset Paper Award of the year 2012 of IJACSA from Science and Information Organization: SAI. In 2016, he also received Vikram Sarabhai Medal of ICSU/COSPAR and also received 20 awards. He wrote 34 books and published 520 journal papers. He is Editor-in-Chief of International Journal of Advanced Computer Science and Applications as well as International Journal of Intelligent Systems and Applications. <http://teagis.ip.is.saga-u.ac.jp/>

Flowcharting the Meaning of Logic Formulas

Sabah Al-Fedaghi

Computer Engineering Department
Kuwait University
Kuwait

Abstract—In logic, representation of a domain (e.g., physical reality) comprises the things its expressions (formulas) refer to and their relationships. Recent research has examined the realm of nonsymbolic representations, especially diagrams. It is claimed that, in general, diagrams have advantages over linguistic descriptions. Current diagrammatic representations of logic formulas do not completely depict their underlying semantics, and they lack a basic static structure that incorporates elementary dynamic features, creating a conceptual gap that can lead to misinterpretation. This paper demonstrates a methodology for mapping the sense of a logic formula and producing diagrams that integrate linguistic conception, truth-values, and meaning and can be used in teaching, communication, and understanding, especially with students specializing in logic representation and reasoning.

Keywords—*knowledge representation; logic formulas; diagrammatic representation; sense*

I. INTRODUCTION

In computer science, studies suggest that flowcharts have potential as tools in educational settings [1-3], despite the fact that complaints regarding their value in design and education [4-5] have led to their near-elimination since the mid-1970s. Currently (2016), flowcharts are “still very common in procedure documentation [and] some managers love them and use them for everything” [6]. They have also been revived in the form of UML activity diagrams. “Recently, many philosophers, psychologists, logicians, mathematicians, and computer scientists have become increasingly aware of the importance of multi-modal reasoning and, moreover, much research has been undertaken in the area of non-symbolic, especially diagrammatic, representation systems” [7]. Accordingly, any development of diagrammatic language is a contribution in this direction.

In computer science, flowcharting is useful as a form of program documentation, as a means of enhancing algorithm understanding and design, and as a tool for teaching programming [1]. In the field of traditional logic diagrams, studies of relationships between diagrammatic and linguistic representation systems have found advantages in diagrammatic representations over linguistic ones [8-9]. Venn diagrams, Euler circles, and Peirce's existential graphs are examples of these representations.

Certainly, in their proper form, flowcharts and diagrams can be used to represent a logic domain (e.g., physical reality, mathematics) that comprises the things its expressions (formulas) refer to and their relationships. The advantages in this context include the following:

- Teaching: Among the many applications of diagrams in an educational setting, they are especially useful for students specializing in logic representation and reasoning.

- Communication: Diagrams probably rank among the oldest forms of human communication [7]; they are basic, elementary, and require no spoken language.

- Understanding: Many scientific fields use diagrams to represent or depict knowledge and to assist in understanding of problems [10-13].

Diagrams are used to represent conceptualizations (e.g., underlying deep structures) of language expressions; however, while knowledge embedded in logic formulas can be shown in diagrams, dynamic features are conceptualized (e.g., deduction system, humans) in a way that fails to integrate structure and dynamic features. “It is a quite recent movement among philosophers, logicians, cognitive scientists and computer scientists to focus on different types of representation systems, and much research has been focused on diagrammatic representation systems in particular” [7].

A. Problem

Current diagrammatic representations of logic formulas do not completely depict their underlying semantics or provide a clear, basic, static structure with elementary dynamic features, creating a conceptual gap that sometimes causes misinterpretation. Structural correspondence between a diagrammatic representation and semantic content “plays a crucial role in both interpretation and inference processes with the representations” [14]

For example, as reported by Shin [15], Venn diagrams lack many features, such as representation of existential statements, but in Euler diagrams, such features as representation of existential statements not only obscure visual clarity but also raise serious interpretational problems. Peirce's diagrams are characterized by arbitrariness in conventions, making them confusing and inconsistent.

B. Proposed solution

This paper introduces a methodology for expressing the meaning (sense) of a logic formula in a diagram. The resultant schema connects the linguistic version of the formula, the formula's truth values, and its meaning in a diagrammatic apparatus called the Flowthing Model (FM), briefly described in the next section [16]. The example developed in the following sections is a new contribution.

II. DIAGRAMMATIC LANGUAGE

FM uses *flowthings* to represent a range of *things*, for example, a logic formula, its meaning, terms, truth values, and so on. *Flowthings* are defined as *what can be created, released, transferred, processed, and received* (see Fig. 1; flow is indicated by solid arrows). Hereafter, flowthings are referred to as *things*. Note that what we call a *thing* is, in general, not necessarily a substance in the philosophical sense; e.g., heat is a thing that is created, released, transferred, received, and processed.

FM also uses the notions of *spheres and subspheres*. These are the environments and relationships of the flow. FM also utilizes the notion of *triggering*, the activation of a flow, denoted in FM diagrams by a *dashed arrow*.

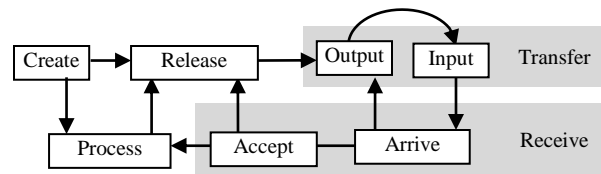


Fig. 1. Flow machine

Example: Borysowich [17] provides a flowchart (not shown here) that

... calculates customer discounts for a company that sells merchandise to wholesale and retail outlets. *Wholesale customers* receive a two percent *discount* on all orders. The company also encourages both wholesale and retail customers to pay cash on delivery by offering a two percent discount for this method of payment. Another two percent discount is given on orders of 50 or more units. [17] (Italics added)

Fig. 2 shows the corresponding FM representation of the sequence and flow of these processes.

The company (the global sphere) includes four things in its subspheres: value of the *Discount* (circle 10), *Customer type* (2), *Payment type* (3), and *No. of items*. Each has its own stream of flow. The procedure for calculating the discount is accomplished as follows.

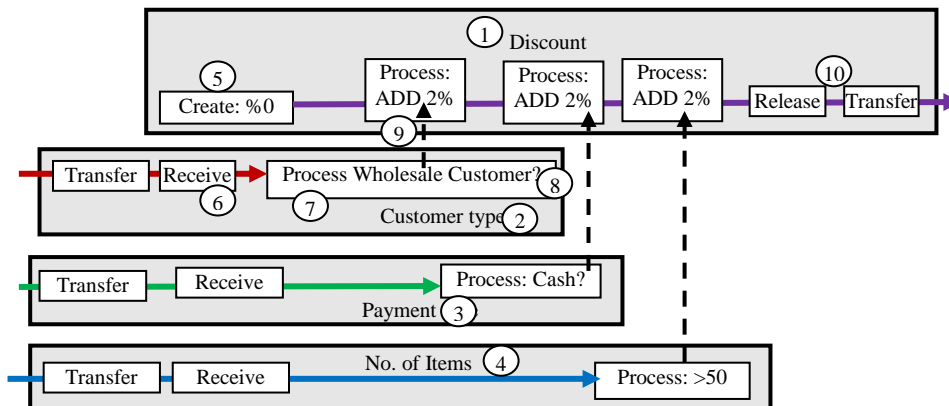


Fig. 2. FM representation of the example

1) The Discount is initiated at 0% (4). Its flow (movement through the sequence stages) is controlled by triggering from other flows. (This will become clearer later.)

2) The Customer type is received (6) and processed (7); if wholesale, then this triggers (8) adding 2% to the discount (9). The flow then proceeds along the stream without interruption.

3) A similar procedure is followed for Payment type and then for No. of items.

4) The value of the discount is released and output (10).

Note that, for clarity's sake, Process in Discount is represented by three boxes.

The diagram can be specified in a semiformal language as follows:

Discount.Create (%0)

Customer Type.Transfer, Receive, Process (If Wholesale Customer: **Discount.Process** (%2))

Payment Type.Transfer, Receive, Process (If Cash: **Discount.Process** (%2))

No of items.Transfer, Receive, Process (If >50: **Discount.Process** (%2))

Discount.Release, Transfer

The familiar dot notation is used to indicate stages inside subspheres. Assuming sequential execution, Fig. 3 shows the path of "control flow" by triggering. In such a sequential execution, it may be necessary to explicitly specify the interruption/resumption of flow inside the Discount sphere. One way to describe this is by storing the intermediate discount value in storage, as shown in Fig. 4. Thus, each internal triggering starts with fetching of the stored value.

It is clear that the FM representation is suitable for identifying parallel execution. For example, using classical function/parameters notation, a rough implementation can be specified as follows:

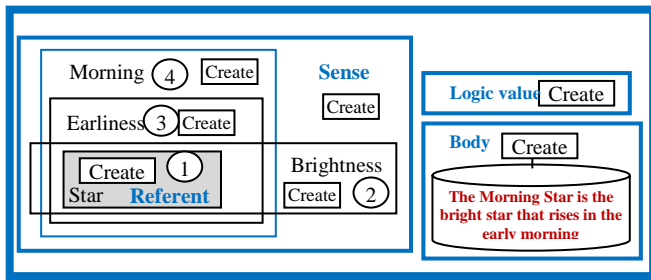


Fig. 6. (upper) The bright star that rises in the early morning, and (lower) The bright star that rises in the early evening

In the lower diagram, a similar method of representation describes *The bright star that rises in the early evening*. In Fig. 7, the two diagrams have been combined. In the online version of the paper, colors are used to indicate the boundaries of the individual diagrams. The diagrams reflect an alternative to written descriptions for illustrating logical language and its various aspects.

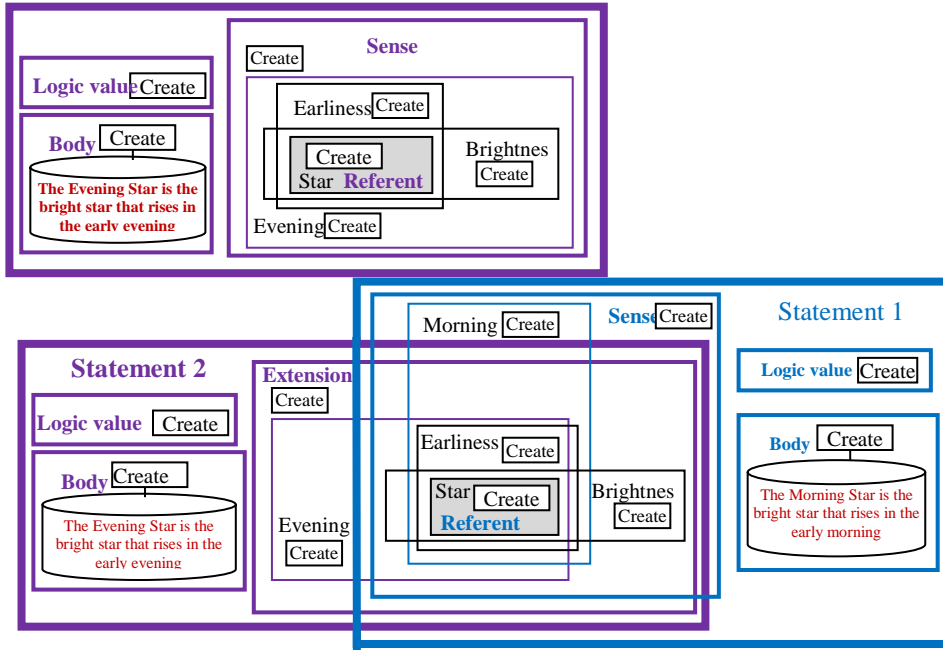


Fig. 7. The bright star that rises in the early morning and The bright star that rises in the early evening

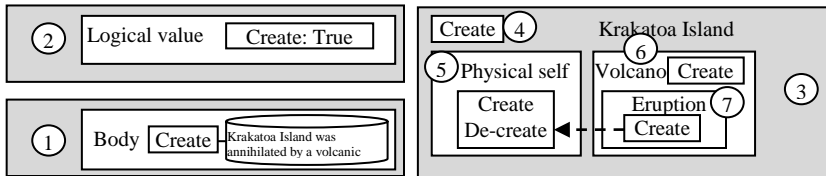


Fig. 8. It is true that Krakatoa Island was annihilated by a volcanic eruption if and only if Krakatoa Island was annihilated by a volcanic eruption

V. REPRESENTING POSSIBLE WORLDS

Bradley and Swartz [25] considered that, for any item and any attribute *a* and *F*, we can define “truth” and “falsity” as follows:

a) *It is true that a has F if, and only if, a has F*

For example, It is true that Krakatoa Island was annihilated by a volcanic eruption if and only if Krakatoa Island was annihilated by a volcanic eruption.

This can be represented by FM diagram as shown in Fig. 8. In such a *world*, there are three spheres: the *Proposition* (1), its truth value (2), and its meaning (3). The stage of *Create* in 1, 2, and 3 specifies *existence*. The meaning includes the Island sphere (4) in terms of its subspheres: its physical self (5) and the Volcano (6) that contains the sub-sphere, *Eruption* (7). *Create* and *De-create* express that at the beginning there exists,

physically, an island and because of the eruption, it no longer exists. Note that we do not differentiate between a proposition and a sentence in this example (see [25]).

Bradley and Swartz [25] describe the possible states of the elements as follows:

1) *Krakatoa Island exists but fails to have the attribute annihilated by a volcanic eruption*

In this case, the fragment *annihilated by a volcanic eruption* in the sentence is a fiction. Accordingly, we have the two worlds *Real* and *Fiction*, as shown in Fig. 9. The island exists in reality (circle 1), but the volcano (2) and the destruction (3) of the island exist in fiction. In reality, the body of symbols *Krakatoa Island was annihilated by a volcanic eruption* exists in reality (4). The whole proposition is *False* in reality (5), but it is true in fiction (6), e.g. a novel.

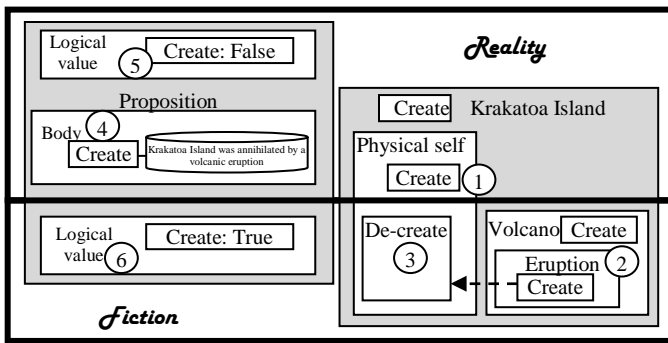


Fig. 9. Krakatoa Island exists but lacks the attribute annihilated by a volcanic eruption

2) Krakatoa Island does not exist. Since an attribute can be instanced by a logical item in a possible world only if that item exists in that possible world, the failure of an item to exist in a given possible world precludes it from having any attributes whatever in that world. [25]

Fig. 10 shows the corresponding FM representation. *Krakatoa Island was annihilated by a volcanic eruption* is just a sequence of symbols. It is False in reality; however, it has fictitious meaning and is True in the context of fiction, e.g., in a movie.

These notions are viewed as things that can be created, processed, released, transferred, and received. For example, the meaning of the words *Krakatoa Island was annihilated by a volcanic eruption* could be created in the sphere of the mind of a news correspondent who then processes this meaning, triggering creation of the news: *Krakatoa Island was annihilated by a volcanic eruption* in linguistic form (body); accordingly, the news is printed in a newspaper that is read by a person, thus creating a meaning in his/her mind with the truth value: True.

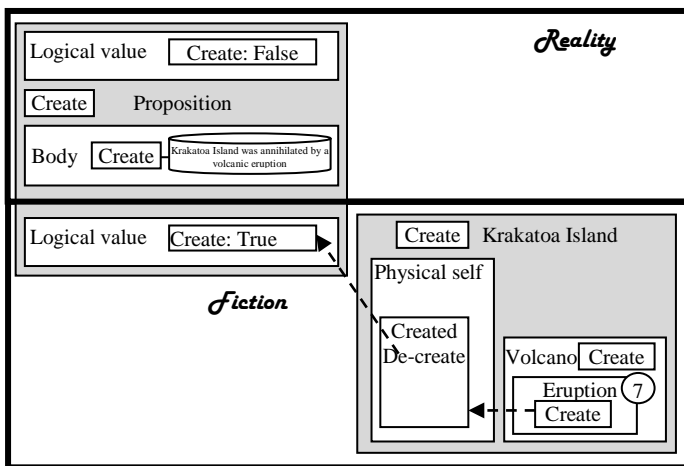


Fig. 10. Krakatoa Island does not exist

VI. CONCLUSION

This paper has proposed a methodology for mapping the sense of a logic formula through a schema that connects a linguistic conception, truth-values, and meaning in a unifying diagrammatic apparatus. Since diagrams have proven useful for enhancing understanding in design, and as a tool for

teaching, the description produced can be especially useful for students specializing in logic representation and reasoning.

It is important to note that this paper is not a contribution in the area of logic. Rather, it has utilized a diagrammatic methodology for flowcharting logic formulas, i.e., expressing them in terms of linguistic expression (body), truth-value, and sense. The diagrams are depictive illustrations that can be used to help students see the relationships among symbolic formulas, associated truth values, and meanings. The method is similar to drawing a flowchart of a computer program that represents the program but does not replace it. FM could potentially be applied in “diagrammatic thinking,” and in diagrammatic representations used in artificial intelligence.

The contribution of this paper is limited to proposing use of the diagramming methodology and demonstrating its viability for representing certain situations. A great deal of material has been left for future work, including quantifiers and adduction. Nevertheless, the FM representation is worth further discussion and investigation for its advantages in illustrating of formulas and their relationships. Furthermore, at this point, this proposed representation of logic formulas does not imply their use in any process such as proofs and reasoning.

Currently, the FM-based description is used as an aid in teaching a discrete structures course in computer engineering. Initial observations indicate mixed results in an academic setting; hence, the model is worth further discussion and investigation for portraying problems in such topics as logic and set theory.

REFERENCES

- [1] T. G. Gill, “Teaching flowcharting with FlowC,” *Journal of Information Systems Education*, vol. 15, no. 1, pp. 65-77, 2004.
- [2] D. A. Scanlan, “Structured flowcharts outperform pseudocode: an experimental comparison,” *IEEE Software*, pp. 28-35, Sept. 1989.
- [3] T. Crews and J. Butterfield, “Using technology to bring abstract concepts into focus: a programming case study,” *Journal of Computing in Higher Education*, vol. 13, no. 2, pp. 25-50, 2002.
- [4] T. Brooks, *The Mythical Man-Month: Essays on Software Engineering* Reading, MA: Addison Wesley, 1975.
- [5] B. Shneiderman, R. Mayer, D. McKay, and P. Heller, “Experimental investigations of the utility of detailed flowcharts in programming,” *Communications of the ACM*, vol. 20, no. 6, pp. 373-381, 1977.
- [6] G. Kesteven, “Flowcharts make bad documentation” [blog post], April 29, 2015. <http://phrontex.com/blog/?p=164>
- [7] S.-J. Shin, O. Lemon, and J. Mumma, “Diagrams,” *Stanford Encyclopedia of Philosophy*, 2013. <http://plato.stanford.edu/entries/diagrams/>
- [8] A. Shimojima, “The graphic linguistic distinction,” *Artificial Intelligence Review*, vol. 13, pp. 313-335, 2001.
- [9] K. Stenning, “Distinctions with differences: comparing criteria for distinguishing diagrammatic from sentential systems,” in *Diagrams 2000*, M. Anderson, P. Cheng, and V. Haarslev, Eds. LNCS (LNAI), vol. 1889, pp. 132-148, 2000.
- [10] R. Arnheim, *Visual Thinking*. Berkeley: University of California Press, 1980.
- [11] A. Barr and E. A. Feigenbaum, *The Handbook of Artificial Intelligence*, Vol. 1. Los Altos, CA: William Kaufmann, 1981, pp. 200-206.
- [12] A. Sloman, “Interactions between philosophy and A.I.: the role of intuition and non-logical reasoning in intelligence,” *Artificial Intelligence*, vol. 2, pp. 209-225, 1971.

- [13] A. Sloman, "Afterthoughts on analogical representations," in *Proceeding of the 1st Workshop on Theoretical Issues in Natural Language Processing (TINLAP-1)*, Cambridge, MA, 1975, pp. 164–168.
- [14] Y. Sato, K. Mineshima, and R. Takemura, "Interpreting logic diagrams: a comparison of two formulations of diagrammatic representations," in *Proceedings of the 33rd Annual Conference of the Cognitive Science Society*, C. Hoelscher, T. F. Shipley, and L. Carlson, Eds. Austin, TX: Cognitive Science Society, 2011, pp. 2182–2187.
- [15] S.-J. Shin, *The Logical Status of Diagrams*. Cambridge University Press, 1994.
- [16] S. Al-Fedaghi, "Anatomy of personal information processing: application to the EU privacy directive," *International Journal of Liability and Scientific Enquiry*, vol. 1, no. 7, 2007.
- [17] C. Borysowich, "Using logic flowcharts," *Toolbox.com*, Apr. 27, 2007. <http://it.toolbox.com/blogs/enterprise-solutions/using-logic-flowcharts-15950>
- [18] S. Al-Fedaghi, "Schematizing proofs based on flow of truth values in logic," *IEEE International Conference on Systems, Man, and Cybernetics (IEEE SMC 2013)*, Manchester, UK, 2013.
- [19] S. Al-Fedaghi, "Visualizing logical representation and reasoning," *15th International Conference on Artificial Intelligence (ICAI'13)*, Las Vegas, NV, USA, 2013.
- [20] S. Al-Fedaghi, "How to diagram your logical argument," *Intelligent Systems Conference 2015 (IntelliSys 2015)*, London, 2015.
- [21] S. Al-Fedaghi, "Schematizing formulas for logic students," *International Journal of Intelligent Information Processing*, vol. 4, no. 4, pp. 27-38, 2013.
- [22] S. Al-Fedaghi, "Function-behavior-structure model of design: an alternative approach," *International Journal of Advanced Computer Science and Applications*, vol. 7, no. 7, pp. 133-139, 2016.
- [23] A. Julien, "Frege was from Venus" [blog post], June 20, 2013. <https://welovephilosophy.com/tag/evening-star/>
- [24] *Stanford Encyclopedia of Philosophy*, "Gottlob Frege," Sep 13, 2016. <http://plato.stanford.edu/entries/frege/>
- [25] R. Bradley and N. Swartz, "Introduction: Possible Worlds," in *Logic and Its Philosophy*, Hackett, 2008.

Pursuit Reinforcement Competitive Learning: PRCL based Online Clustering with Learning Automata

- PRCL and its Application to Evacuation Simulation -

Kohei Arai¹

¹ Graduate School of Science and Engineering
Saga University
Saga City, Japan

Abstract—A new online clustering method based on not only reinforcement and competitive learning but also pursuit algorithm (Pursuit Reinforcement Competitive Learning: PRCL) as well as learning automata is proposed for reaching a relatively stable clustering solution in comparatively short time duration. UCI repository data which are widely used for evaluation of clustering performance in usual is used for a comparative study among the existing conventional online clustering methods of Reinforcement Guided Competitive Learning: RGCL, Sustained RGCL: SRGCL, Vector Quantization, and the proposed PRCL. The results show that the clustering accuracy of the proposed method is superior to the conventional methods. More importantly, it is found that the proposed PRCL is much faster than the conventional methods. The proposed method is then applied to the evacuation simulation study. It is found that the proposed method is much faster than the conventional method of vector quantization to find the most appropriate evacuation route. Due to the fact that the proposed PRCL method allows finding the most appropriate evacuation route, collisions among peoples who have to evacuate for the proposed method is much less than that of vector quantization.

Keywords—Pursuit Reinforcement Guided Competitive Learning; Reinforcement Guided Competitive Learning; Sustained Reinforcement Guided Competitive Learning Vector Quantization; Learning Automata

I. INTRODUCTION

Clustering is an exploratory data analysis tool that deals with the task of grouping objects that are similar to each other [1,2,3]. For many years, many clustering algorithms have been proposed and widely used. It is commonly used in many fields, such as data mining, pattern recognition, image classification, biological sciences, marketing, city-planning, document retrieval, etc.

Many cases of clustering commonly used the static data. It means that the clustering can be made after the entire data have been collected, then grouped into clusters whose members are similar in some way. In the data mining, there is a kind of data which comes every time so that we cannot stop it in a while in order to make clustering.

Online clustering is a kind of clustering that is used for dynamic data. It is not considering a number of data, but only focus on a new data and previous centroids. However, determining position of each centroid because of a new data attracted some approaches. Vector Quantization (VQ) was a

very simple approach to do online clustering. It is derived from concept of competitive learning network [4],[5]. Likas (1999) proposed Reinforcement Guided Competitive Learning (RGCL) [6] as an approach for on-line clustering based on reinforcement learning. It utilized the concept of reward in the reinforcement learning from winning unit in the Learning Vector Quantization. The Sustained RGCL (SRGCL) was modification of RGCL in considering a sustained exploration in reinforcement learning. On the other hand, other approaches such as modified ISODATA, k-means clustering, Self-Organization Mapping: SOM based clustering, spatial feature utilizing clustering, Fisher distance measure utilizing clustering, GA based clustering and so on are proposed in order to improve clustering performance [7]-[25].

A new approach for online clustering based on reinforcement learning, called Pursuit Reinforcement Guided Competitive Learning. PRCL which is derived from pursuit method in reinforcement learning that maintain both action-value and action preferences, with the preferences continually pursuing the action that is greedy according to the current action-value estimates together with learning automata is proposed. PRCL can be used as online clustering method. Image search application is discussed [26]. Another application is, then introduced for evacuation simulation.

The following section describes the proposed PRCL with learning automata together with the existing conventional online clustering methods of RGCL, SRGCL and VQ. Then preliminary experiments are described followed by its application of evacuation simulation. After all, conclusion is described with some discussions.

II. THEORETICAL BACKGROUND

Individuals appear and disappear in evacuation simulation. For instance, when a disaster occurs, individuals disappear if the individual evacuated in a safe area. Therefore, the number of individual varies for time being. The conventional cluster methods allow making clusters when the individuals are fixed. It is time consumable that conventional clustering is applied to the individuals each time of the number of individuals are changed. Therefore, online clustering is effective in such case. One of the problems of online clustering is computing performance. It has to be completed in a real time basis. Another problem of online clustering is clustering accuracy. In order to improve clustering accuracy, the proposed method

introduces reinforcement competitive learning with learning automata. Learning automata featured reinforcement competitive learning is new original idea.

A. Reinforcement Learning

Reinforcement Learning is learning what to do and how to map situations to actions so as to maximize a numerical reward signal [4]. The learner is not told which actions to take, as in most forms of machine learning, but instead must discover which actions yield the most reward by trying them. In the most interesting and challenging cases, actions may affect not only the immediate reward, but also the next situation and, through that, all subsequent rewards. These two characteristics (trial-and-error search and delayed reward) are the two most important distinguishing features of Reinforcement Learning.

Reinforcement Learning is defined not by characterizing learning algorithms, but by characterizing a learning problem. Any algorithm that is well suited to solving that problem we consider to be a Reinforcement Learning algorithm. Clearly such an agent must be able to sense the state of the environment to some extent and must be able to take actions that affect that state. The agent must also have a goal or goals relating to the state of the environment.

B. Competitive Learning

Competitive learning is defined as unsupervised learning method of which one of the output neurons firing through competition among the neurons without training sample. It has both of the features of supervised and unsupervised learning methods. It can be applicable for clustering. In such case, inputs are the data in concern while outputs are clusters. The following cost function is usually used.

$$J = \sum_{i=1}^n m_r d(x_i, w_r) \quad (1)$$

In the clustering based on competitive learning, J implies the minimum distance $\min.d(x,w)$ between input data x_i and cluster center w_r . Therefore, J is sum of dissimilarity within cluster.

C. Simple Competitive Learning

SCL (Simple Competitive Learning) is the simplest competitive learning. The basic idea of the SCL is WTA (Winner Take All). Namely, winner of the neuron gets all. The winner of the neuron is determined with the following equation,

$$W_m^T x = \max_i (W_i^T x) \quad (2)$$

$$\Delta W_m^T = \alpha (x - W_i^T x)$$

Where W_i denotes weight of the neuron i while x denotes input data, and α is the coefficient for determine its convergence speed.

D. Reinforcement Competitive Learning

The following reinforcement competitive learning based online clustering is typical.,

VQ (Vector Quantization),

RGCL (Reinforcement Guided Competitive Learning),

SRGCL (Sustained Reinforcement Guided Competitive Learning).

VQ (Vector Quantization)

Process flow of the VQ is as follows,

- 1) weighting vector is defined as the selected sample vector of each cluster.
- 2) input data belongs the sample vector of cluster i^* which shows the shortest distance between input data and the sample vector.
- 3) sample vector is updated based on the following equation,

$$\Delta w_{ij}^{t+1} = \begin{cases} \alpha(x_j - w_{ij}^t) & \text{if } i = i^* \\ 0 & \text{if } i \neq i^* \end{cases} \quad (3)$$

Where t denotes leaning number of which the number is incremented for each input data. The weight is increased with Δw_i when the input data x_j is matched with t -th sample vector. Meanwhile, weight is not changed when the input data does not match to any sample vector. Repeating these process, representative vector is updated and then most appropriate clusters are formed.

RGCL (Reinforcement Guided Competitive Learning)

All the clusters of output neurons are represented with Bernoulli units where the weight is assumed to be vector. The distance between input data and weighting vector is calculated with the following equation,

$$s_i = d(x, w_i) \quad (4)$$

Then probability p_i is calculated with the equation (5),

$$p_i = h(s_i) = 2(1 - f(s_i)) \quad (5)$$

where

$$f(x) = \frac{1}{1 + e^{-x}} \quad (6)$$

The probability is increased in accordance with input data is getting close to weighting vector. Therefore, it is probable that the distance between input data and the neuron of which the output is 1. Then the input data belongs the cluster representing the neuron of which the output is 1.

The process flow of RGCL is as follows,

- 1) a data is selected from the samples randomly
- 2) determine a winner neuron i^*
- 3) reward r_i of input data x_j is updated as follows,

$$r_i = \begin{cases} 1 & \text{if } i = i^* \text{ and } y_i = 1 \\ -1 & \text{if } i = i^* \text{ and } y_i = 0 \\ 0 & \text{if } i \neq i^* \end{cases} \quad (7)$$

Then weight vector is updated as follows,

$$\Delta w_{ij}^{t+1} = \alpha r_i (y_i - p_i)(x_j - w_{ij}^t) \quad (8)$$

SRGCL (Sustained Reinforcement Guided Competitive Learning)

SRGCL is the method which allows control the convergence speed with the parameter η which is added to the RGCL as follows,

$$\Delta w_{ij}^{t+1} = \alpha r_i (y_i - p_i)(x_j - w_{ij}^t) - \eta w_{ij}^t \quad (9)$$

It is not always true that SRGCL is superior to RGCL. The convergence performance depends on the relation between input data and the control parameter. Therefore, the most appropriate control parameter has to be determined.

Learning Automata

N arm bandit problem is defined as the machine learning problem which allows analyzes a most appropriate strategy for getting the maximum prize from a slot machine with at least one lever. Learning automata is one of the N arm bandit problem solving methods in an efficient manner.

The action of “draw one the specific lever” is represented as a , while play is defined with t , together with the probability of the prize is expressed with $\pi_t(a)$, $(n + 1)$ -th play of total prize depends on the accumulated prize at n -th play and the current prize. In case of the total prize is increased, the probability is expressed as follows,

$$\pi_{t+1}(a) = \pi_t(a_{t+1}^*) + \beta[1 - \pi_t(a_{t+1}^*)] \quad (10)$$

Also, the probability is represented as follows, in case of the total prize is decreased,

$$\pi_{t+1}(a) = \pi_t(a) + \beta[0 - \pi_t(a)] \quad (11)$$

Where β is the convergence speed control parameter. If the appreciable actions are always selected, then the total prize is getting close to the maximum prize. This method is one of the learning automata. Namely, reward is provided when it is predicted to win while punishment is given when it is predicted to loose. Through these processes with actions, the total prize is getting closer to the maximum prize.

E. Proposed Clustering Method

In the convergence process of RGCL, it is sometime happened that the convergence speed is decreased and or unstable due to the weight is too large or too small. The method proposed here uses learning automata for adjustment of the weight. Namely, most appropriate prediction of win/loose probability can be done with learning automata. Thus the most appropriate reward and punishment can be given.

Online clustering method based on competitive and reinforcement learning as well as learning automata is proposed here. Namely, winner of the neuron is determined with WTA at first based on competitive neural network of basic learning method, a reward is calculated with the result of the winner neuron based on learning automata. Then the final winner neuron is determined through agent action which has

the maximum reward based on reinforcement learning method. Therefore, the proposed method is called PRCL: Pursuit Reinforcement Guided Competitive Learning.

The procedure of the proposed PRCL is as follows,

1) Initializing the reward r for each data as follows,

$$r(x, u_i^0) = \frac{1}{n} \quad (12)$$

Where n denotes the desirable number of cluster, while u_i^0 denotes initial cluster center.

2) data is selected from the samples randomly

3) winner neuron i^* is determined with equation (13)

$$d_{i^*} = \mathop{\text{arg}} \min_i d(\mathbf{x}, w_i) \quad (13)$$

4) the reward of each output neuron corresponding to input data is updated based on equation (14)

$$r(x, u_i^{t+1}) = \begin{cases} r(x, u_i^t) + \beta(1 - r(x, u_i^t)) & i \neq i^* \\ r(x, u_i^t) + \beta(1 - r(x, u_i^t)) & i = i^* \end{cases} \quad (14)$$

where $r(x, u^t)$ denote the current reward while $r(x, u^{t+1})$ denotes that for the next learning number, respectively.

5) The neuron i^* which has the maximum reward is selected by equation (15)

$$u_{i^*} = \mathop{\text{arg}} \min_i d(\mathbf{x}, w_i) \quad (15)$$

6) weight is updated with the followed equation,

$$\Delta w_{ij}^{t+1} = \begin{cases} \alpha(x_j - w_{ij}^t) & i = i^* \\ 0 & i \neq i^* \end{cases} \quad (16)$$

III. EXPERIMENTS

A. Preliminary Experiments

Comparative study on online clustering performance is conducted with Iris, Wine, New thyroid, Ruspini, Chernoff and Fossil datasets form the well-known UCI repository. One of the examples of learning process and convergence speed for Iris dataset is shown in Fig.1. In this case, the maximum learning number is set at 15000 while the parameters for each method is set as follows,

$$\begin{aligned} \text{VQ } \alpha &= 0.1 \\ \text{RGCL1 } \alpha &= 0.1 \\ \text{RGCL2 } \alpha &= 0.5(t \leq 500), \alpha = 0.1(t > 500) \\ \text{SRGCL1 } \alpha &= 0.1, \eta = 0.0001 \\ \text{SRGCL2 } \alpha &= 0.5(t \leq 500), \alpha = 0.1(t > 500), \eta = 0.0001 \\ \text{PRCL } \alpha &= 0.1, \beta = 0.1 \end{aligned}$$

Fig.1 shows convergence processes of the proposed online clustering method (Pursuit Reinforcement guided Competitive Learning: PRCL) and the other conventional methods with a variety of parameters for UCI repository data. Meanwhile, Fig.2 shows relation between cost function J and computation time required for reach J to the designated values.

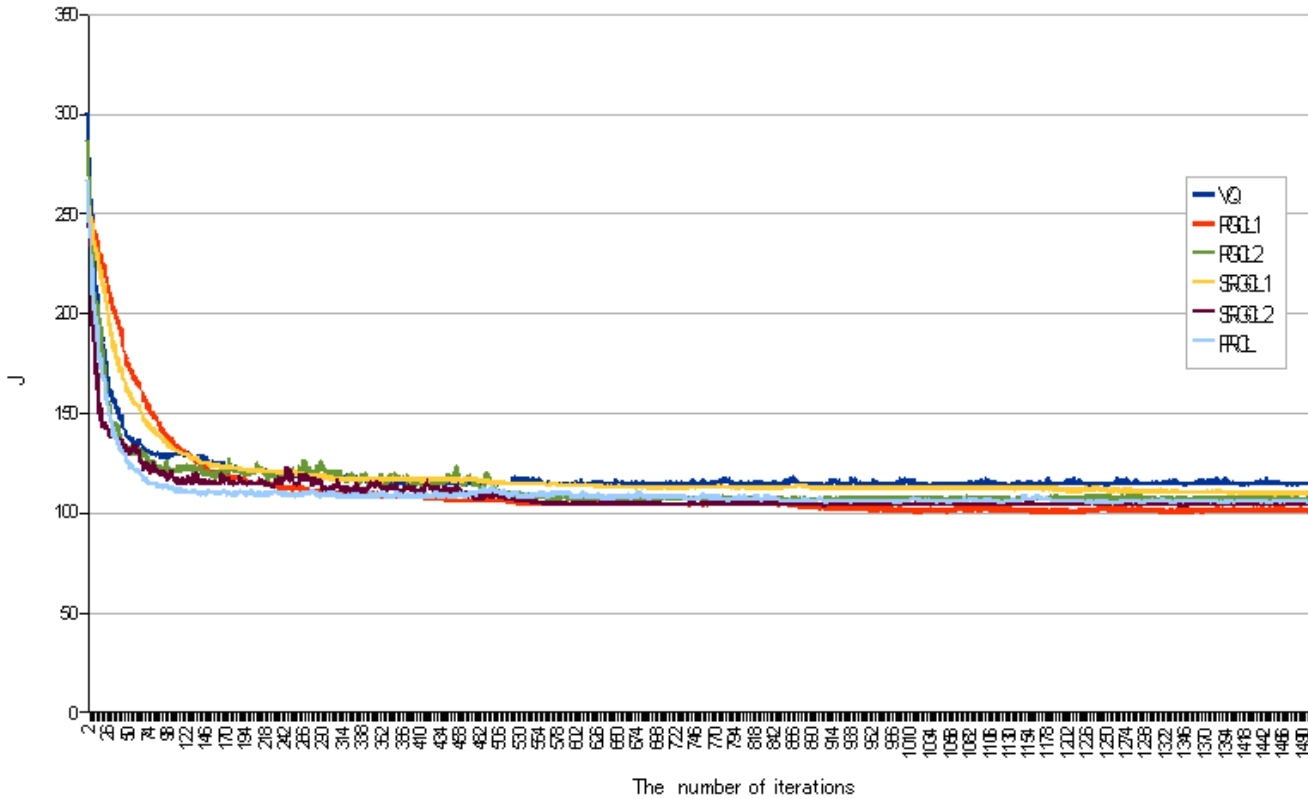


Fig. 1. Convergence processes of the proposed online clustering method (Pursuit Reinforcement guided Competitive Learning: PRCL) and the other conventional methods with a variety of parameters for UCI repository data

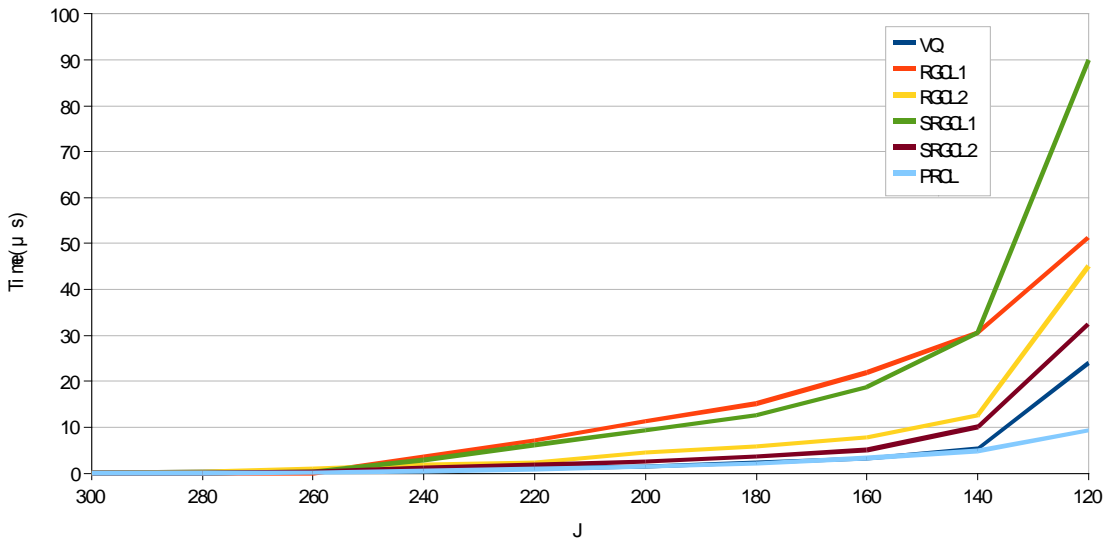


Fig. 2. Relation between cost function J and computation time required for reach J to the designated values

It is found from Fig.1 that the convergence performance of RGCL and SRGCL has influenced by the parameter α . The averaged processing time over 100 times of 4000 of learning number (which is defined as 1 set) is evaluated. Table 1 shows just one of the examples of evaluation results for Iris dataset.

TABLE I. AVERAGED COMPUTATION TIME REQUIRED FOR CONVERGENCE OF THE PROPOSED AND THE OTHER CONVENTIONAL METHODS FOR IRIS DATA IN THE UCI REPOSITORY DATA

	PRCL	VQ	RGCL	SRGCL
Time (s)	0.057	0.043	0.129	0.144

From Table 1, it is found that the proposed method is second fastest method. The proposed method, however, shows the highest convergence performance in terms of convergence speed and stability as shown in Fig.1.

Table 2 shows clustering errors of the proposed and the other conventional methods for each UCI repository data. All the parameters are set as follows,

$$\begin{aligned} \text{VQ } \alpha &= 0.1 \\ \text{RGCL } \alpha &= 0.1 \\ \text{SRGCL } \alpha &= 0.1, \eta = 0.0001 \\ \text{PRCL } \alpha &= 0.1, \beta = 0.1 \end{aligned}$$

TABLE II. CLUSTERING ERRORS OF THE PROPOSED AND THE OTHER CONVENTIONAL METHODS FOR EACH UCI REPOSITORY DATA

Error (%)	PRCL	VQ	RGCL	SRGCL
Iris	19.09	14.99	17.01	14.09
Wine	32.51	31.72	29.41	28.94
Ruspini	8.77	9.15	7.39	5.87
Fossil	21.45	27.24	26.44	26.44
New thyroid	22.69	26.15	31.33	40.82

From Table 2, it is found that all of online clustering methods show almost same (within 5%) clustering performance for relatively simple dataset of Iris, Ruspini, while the clustering performance are different for comparatively complicated dataset, Fossil, New thyroid. In such case, the proposed PRCL shows the highest performance. In particular, clustering performance of PRCL for New thyroid is 3.54% better than VQ, and 8.64% better than RGCL as well as 18.13% better than SRGL. It is because that the PRCL is functioning for adjustment of the complexity of the input data by the learning automata.

B. Evacuation Simulations

It is assumed that the peoples in the disaster occurred area evacuate to safe areas such as shelters. Online clustering is considerably effective because the peoples who could evacuate

to the shelter has to be disappeared from the input nodes. Furthermore, convergence performance and stability of the convergence status is much more important. Therefore, it is expected that the proposed PRCL does work such cases.

Simulation condition is as follows,

1) 256 by 256 mesh size of the simulation cells are assumed to be disaster occurred area. The shelters are situated at the top right corner and the top middle. Then 100 peoples are distributed randomly in the simulation cells.

2) The peoples move toward one of the nearby shelters by one cell by one cell at once of learning number.

3) The simulation is stopped when all the people is reached to the shelter.

4) There are two evacuation conditions, with and without consideration of the queuing at shelter entrance.

Three methods, Minimum Distance: MD, the proposed PRCL, and the VQ are taken into account. Therefore, there are six methods, MD1 and MD2 with and without que, PRCL1 and PRCL2 with and without que, and VQ1 and VQ2 with and without que.

The action strategy is as follows,

1) if there is no people in the target cell, then the people may forward one step further.

2) if there is people in the target cell, then the people searches an empty nearby cell in clock wise direction

3) when the cell surrounding to the shelters are occupied by the other peoples, the people wait for the next learning number, or next simulation number.

Convergence process of the proposed PRCL with the different parameters of α and β are shown in Fig.3. It is found that the parameter α is not so effective while the parameter β is relatively effective for residual error expressed with equation (1).

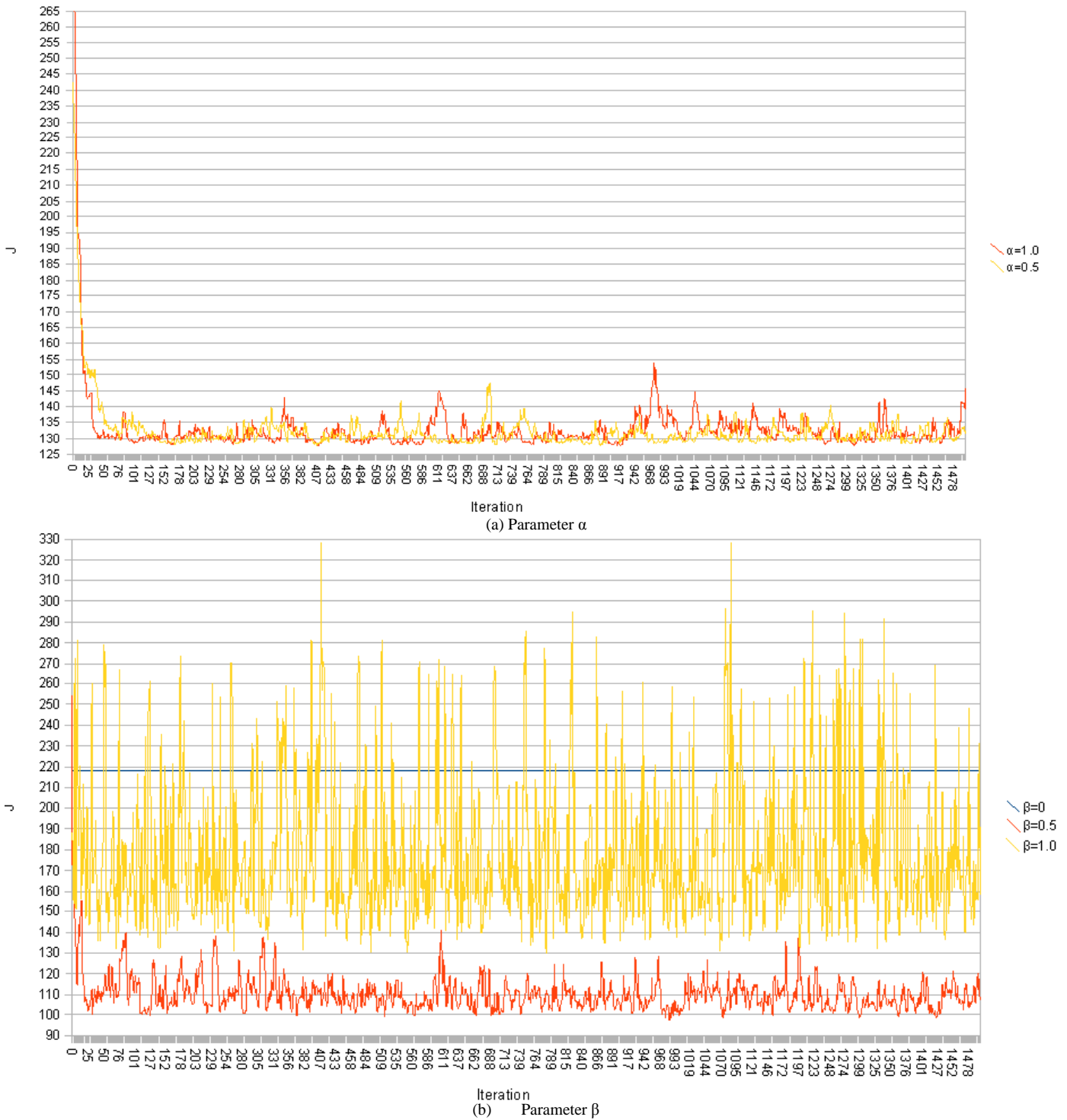


Fig. 3. Relation between parameters α, β and convergence performance

Fig.4 shows the distribution of peoples who have to evacuate (Left: The learning number of turn is 50 while Right: the learning number of turn is 200). As shown in Fig.3, the number of evacuated peoples for the right and the middle

shelters are almost equivalent for both. On the other hand, VQ does not have such capability essentially. Therefore, the number of evacuation peoples for both is not equivalent.

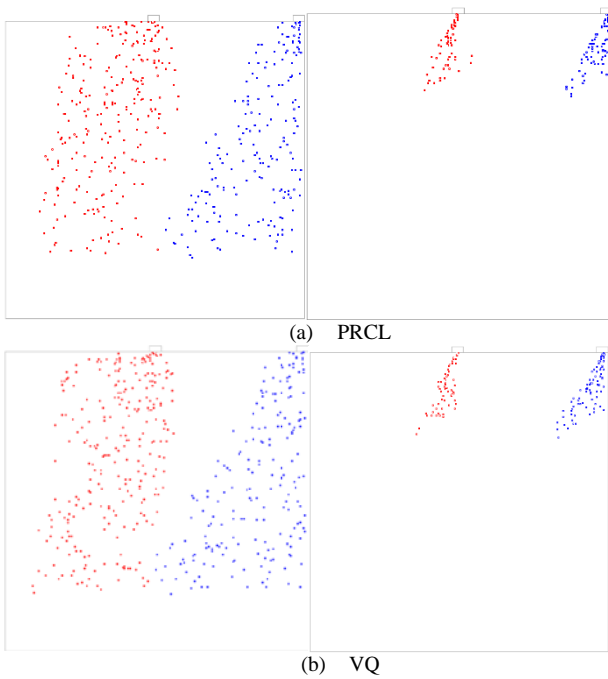


Fig. 4. Distribution of peoples who have to evacuate (Left: The number of turn is 50 while Right: the number of turn is 200)

Table 3 shows the summarized evacuation simulation results. No turn in Table 3 shows the required number of learning for all the people is evacuated. Meanwhile, Rout 1 and Rout 2 denotes the number of peoples who evacuated through the top right and the top middle shelters respectively. No collision denotes the number of which the people could not

step due to the cell intended to move is occupied by the other people already.

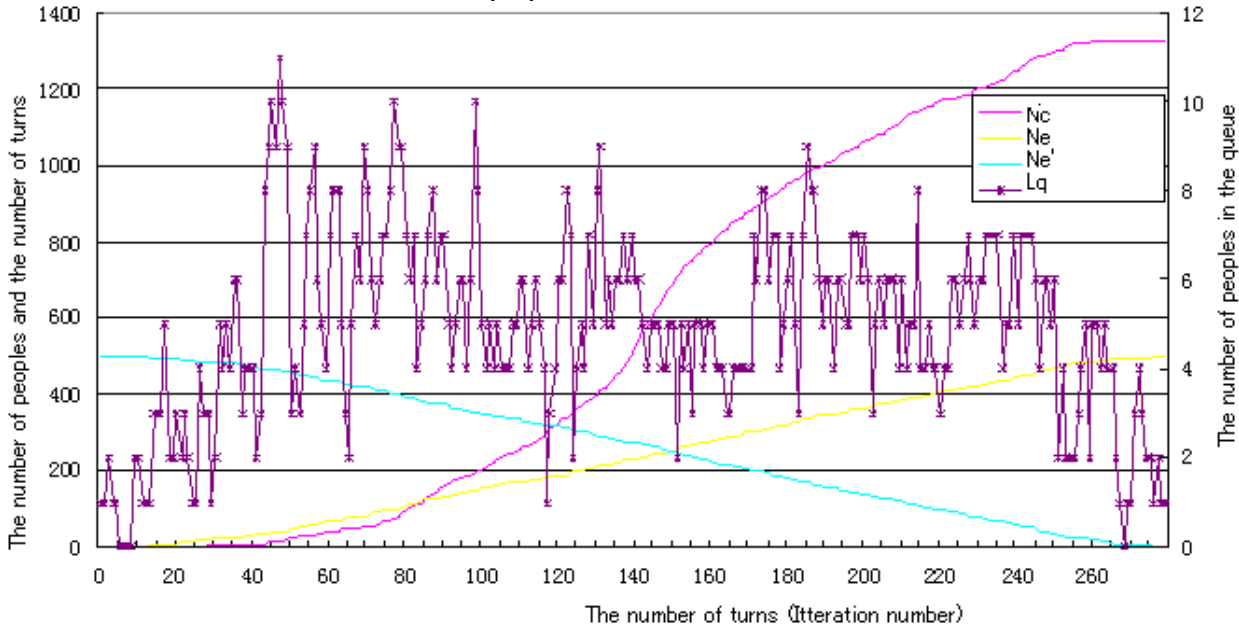
TABLE III. EVACUATION SIMULATIONS SUMMERY

	No.Turn	Route 1	Route 2	No.Collision
Mini.dist. 1	323	382	118	2472
Mini.dist.2	280	321	179	2231
PRCL1	278	294	206	1525
PRCL2	280	285	215	1509
VQ 1	299	317	183	1988
VQ 2	291	299	201	1974

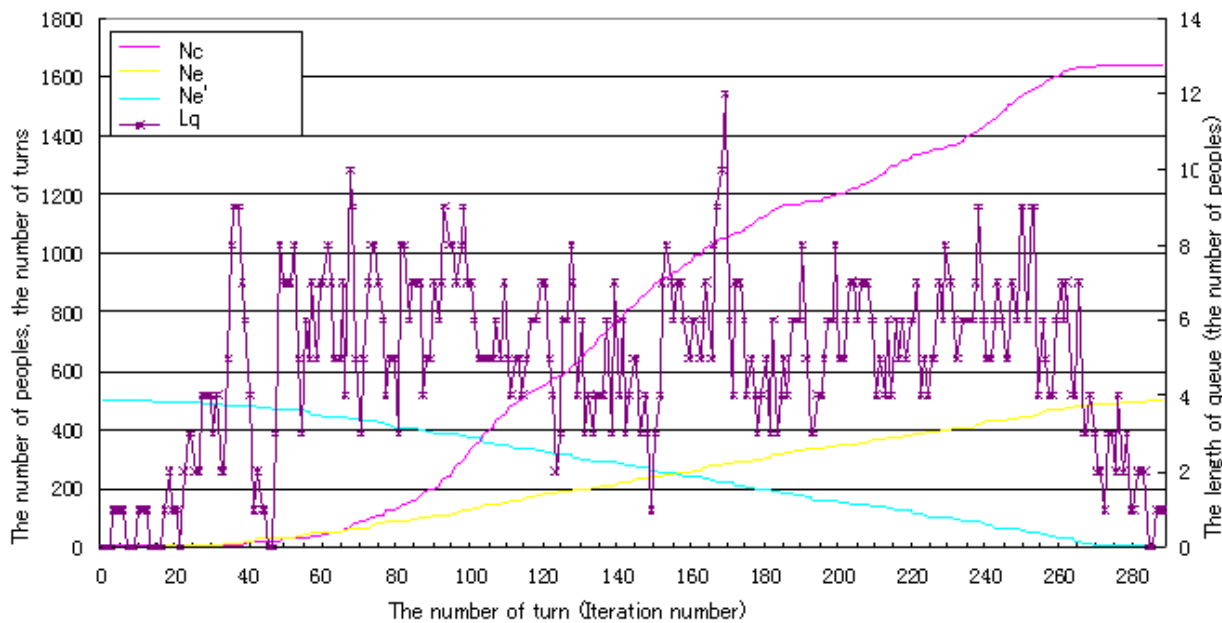
From Table 3, the evacuation time of PRCL is shortest in comparison to the other methods. Furthermore, the number of evacuated peoples from two shelters are almost equal for PRCL comparing to the other methods. The number of collisions, also, shows minimum for PRCL in comparison to the other methods.

Therefore, it is concluded that the proposed PRCL is superior to the other typical online clustering methods. Meanwhile, the evacuation performance for the methods of which que is taken into account shows better than those of which que is not taken into account.

Fig.5 (a) shows the number of peoples who have to evacuate, who have evacuated, collision and the queue length (waiting peoples at the evacuation route) for the proposed PRCL (Nc: No. of collision, Ne: No. of peoples who have evacuated, Ne': No. of peoples who have to evacuate, Lq: Length of queue



(a) PRCL(Nc: No. of collision, Ne: No. of peoples who have evacuated, Ne': No. of peoples who have to evacuate, Lq: Length of queue



(b) VQ(Nc: No. of collision, Ne: No. of peoples who have evacuated, Ne': No. of peoples who have to evacuate, Lq: Length of queue)

Fig. 5. The number of peoples who have to evacuate, who have evacuated, collision and the queue length (waiting peoples at the evacuation route) for the proposed and the conventional method of vector quatization

Meanwhile, Fig.4 (b) shows the number of peoples who have to evacuate, who have evacuated, collision and the queue length (waiting peoples at the evacuation route) for the VQ.

IV. CONCLUSION

A new online clustering method based on not only reinforcement and competitive learning but also pursuit algorithm (Pursuit Reinforcement Guided Competitive Learning: PRCL) as well as learning automata is proposed for reaching a relatively stable clustering solution in comparatively short time duration. UCI repository data which are widely used for evaluation of clustering performance in usual is used for a comparative study among the existing conventional online clustering methods of Reinforcement Guided Competitive Learning: RGCL, Sustained RGCL: SRGCL, Vector Quantization, and the proposed PRCL.

The results show that the clustering accuracy of the proposed method is superior to the conventional methods. More importantly, it is found that the proposed PRCL is much faster than the conventional methods. The proposed method is then applied to the evacuation simulation study. It is found that the proposed method is much faster than the conventional method of vector quatization to find the most appropriate evacuation route. Due to the fact that the proposed PRCL method allows finding the most appropriate evacuation route, collisions among peoples who have to evacuate for the proposed method is much less than that of vector quatization.

ACKNOWLEDGEMENTS

Author would like to thank Dr. Ali Ridoh Barakbah of EEPIS, Indonesia and Dr. Bu Kenkyo of former student of Saga University for their efforts for conducting the experiments.

REFERENCES

- [1] G. Karypis, E.H. Han, V. Kumar, Chameleon: a hierarchical clustering algorithm using dynamic modeling, *IEEE Computer: Special Issue on Data Analysis and Mining*, 32(8):68W5, 1999.
- [2] M. Halkidi, Y. Batistakis, M. Vazirgiannis, Clustering algorithms and validity measures, *Proceedings of the 13th International Conference on Scientific and Statistical Database Management*, July 18–20, IEEE Computer Society, George Mason University, Fairfax, Virginia, USA, 2001.
- [3] W.H. Ming and C.J. Hou, Cluster analysis and visualization, *Workshop on Statistics and Machine Learning*, Institute of Statistical Science, Academia Sinica, 2004.
- [4] R.S. Sutton, A.G. Barto, Reinforcement learning: an introduction, The MIT Press, 1998.
- [5] Genevieve B. Orr, Simple competitive learning, *Neural networks course*, <http://www.willamette.edu/~gorr/classes/cs449/Unsupervised/competitive.html>.
- [6] A. Likas, A reinforcement learning approach to on-line clustering, *Neural Computation*, 11:1915- 32, 1999.
- [7] Ali Ridho Barakbah and Kohei Arai, Pursuit reinforcement competitive learning: An approach for on-line clustering, *Proceedings of the IEEE Indonesian Chapter of the 2nd Information and Communication Technique Seminar*, ISSN1858-1633, 45-48, 2006.
- [8] Akira Yoshizawa, Kohei Arai, Clustering Method Based on Genetic Algorithm Using Spectral and Spatial Context Information, *Journal of Image Electronics Society of Japan*, Vol.31, No.2, 202-209, 2003
- [9] Akira Yoshizawa, Kohei Arai, Clustering Method Based on Genetic Algorithm Using Spectral and Spatial Context Information, *Journal of Image Electronics Society of Japan*, Vol.31, No.2, 202-209, 2003.
- [10] Kohei Arai, Akira Yoshizawa, Koichi Tateno, Application of Messy Genetic Algorithm for Satellite Image Clustering, *Journal of Japan Society of Photogrammetry and Remote Sensing*, Vol.41, No.5, 34–41, 2003.
- [11] Kohei Arai, Learning processes of image clustering method with density maps derived from Self-Organizing Mapping(SOM), *Journal of Japan Society of Photogrammetry and Remote Sensing*, 43,5,62-67 (2004)
- [12] Kohei Arai, Non-linear merge and split method for image clustering, *Journal of Japan Society of Photogrammetry and Remote Sensing*, 43, 5, 68-73 (2004)

- [13] Ali Ridho Barakbah and Kohei Arai, Revised pattern of moving variance for acceleration of automatic clustering, *Electric and Electronics Polytechnics in Surabaya EEPIS Journal*, 9, 7, 15-21 (2004)
- [14] Kohei Arai, Bu Quang Quong, ISODATA clustering with parameter estimation based on genetic algorithm, taking into account concave characteristics of probability density function, *Journal of Japan Society of Photogrammetry and Remote Sensing*, 47, 1, 17-25, 2008
- [15] Kohei Arai, Bu Quang Quong, Image portion retrievals in large scale imagery data by using online clustering taking into account psuite algorithm based Reinforcement learning and competitive learning, *Journal of Image Electronics Society of Japan*, 39, 3, 301-309, 2010
- [16] Kohei Arai, Bu Quang Quong, Convergence performance improvement of online clustering with reinforcement and competitive learning with learning automaton, *Journal of Image Electronics Society of Japan*, 40, 2, 361-168, 2011.
- [17] Kohei.Arai, Bu Quang Quong, Comparative study between the proposed GA based ISODATA clustering and the conventional clustering methods, *International Journal of Advanced Computer Science and Applications*, 3, 7, 125-131, 2012.
- [18] Kohei.Arai, Image clustering method based on density maps derived from Self Organizing Mapping: SOM, *International Journal of Advanced Computer Science and Applications*, 3, 7, 102-107, 2012.
- [19] Kohei.Arai, Clustering method based on Messy Genetic Algorithm: GA for remote sensing satellite image clustering, *International Journal of Advanced Research in Artificial Intelligence*, 1, 8, 6-11, 2012.
- [20] Kohei Arai, Visualization of learning process for back propagation Neural Network clustering, *International Journal of Advanced Computer Science and Applications*, 4, 2, 234-238, 2013.
- [21] Kohei Arai, Image clustering method based on Self-Organization Mapping: SOM derived density maps and its application for Landsat Thematic Mapper image clustering, *International Journal of Advanced Research in Artificial Intelligence*, 2, 5, 22-31, 2013.
- [22] Kohei Arai, Cahya Rahmad, Comparative study between the proposed shape independent clustering method and the conventional method (k-means and the others), *International Journal of Advanced Research in Artificial Intelligence*, 2, 7, 1-5, 2013.
- [23] Kohei Arai, Genetic Algorithm utilizing image clustering with merge and split processes which allows minimizing Fisher distance between clusters, *International Journal of Advanced Research in Artificial Intelligence*, 2, 9, 7-13, 2013.
- [24] Kohei Arai, Fisher distance based GA clustering taking into account overlapped space among probability density functions of clusters in feature space, *International Journal of Advanced Research in Artificial Intelligence*, 2, 11, 32-37, 2013.
- [25] Ali Ridho Barakbah, K.Arai, Centronit: Initial Centroid Designation Algorithm for K-Means Clustering, *EMITTER: International Journal of Engineering Technology*, 2, 1, 50-62, 2014.
- [26] Kohei Arai, Pursui reinforcement competitive learning: PRCL based on online clustering with tracking algorithm and its application to image retrieval, *IJARAI*, 5, 9, 9-16, 2016.

AUTHORS PROFILE

Kohei Arai, He received BS, MS and PhD degrees in 1972, 1974 and 1982, respectively. He was with The Institute for Industrial Science and Technology of the University of Tokyo from April 1974 to December 1978 and also was with National Space Development Agency of Japan from January, 1979 to March, 1990. During from 1985 to 1987, he was with Canada Centre for Remote Sensing as a Post-Doctoral Fellow of National Science and Engineering Research Council of Canada. He moved to Saga University as a Professor in Department of Information Science on April 1990. He was a counselor for the Aeronautics and Space related to the Technology Committee of the Ministry of Science and Technology during from 1998 to 2000. He was a councilor of Saga University for 2002 and 2003. He also was an executive councilor for the Remote Sensing Society of Japan for 2003 to 2005. He is an Adjunct Professor of University of Arizona, USA since 1998. He also is Vice Chairman of the Commission-A of ICSU/COSPAR since 2008. He received Science and Engineering Award of the year 2014 from the minister of the ministry of Science Education of Japan and also received the Bset Paper Award of the year 2012 of IJACSA from Science and Information Organization: SAI. In 2016, he also received Vikram Sarabhai Medal of ICSU/COSPAR and also received 20 awards. He wrote 34 books and published 520 journal papers. He is Editor-in-Chief of International Journal of Advanced Computer Science and Applications as well as International Journal of Intelligent Systems and Applications. <http://teagis.ip.is.saga-u.ac.jp/>